

**SYNTHESIS AND EVALUATION OF NOVEL REAGENTS FOR
SEPARATION OF PALLADIUM FROM HIGH LEVEL LIQUID
WASTE**

By

RITESH RUHELA

CHEM 012008040013

Bhabha Atomic Research Centre, Mumbai, INDIA

A thesis submitted to the

Board of Studies in Chemical Sciences

In partial fulfillment of requirements

For the Degree of

DOCTOR OF PHILOSOPHY

Of

HOMI BHABHA NATIONAL INSTITUTE



October, 2012

Homi Bhabha National Institute

Recommendations of the Viva Voce Board

As members of the Viva Voce Board, we certify that we have read the dissertation prepared by Ritesh Ruhela entitled “**SYNTHESIS AND EVALUATION OF NOVEL REAGENTS FOR SEPARATION OF PALLADIUM FROM HIGH LEVEL LIQUID WASTE**” and recommend that it may be accepted as fulfilling the dissertation requirement for the Degree of Doctor of Philosophy.

_____ **Date:**

Chairman - Prof. K.L. Ramakumar

_____ **Date:**

External Examiner - Prof. A.K. Singh

_____ **Date:**

Guide / Convener - Prof. B.S. Tomar

_____ **Date:**

Member 1- Prof. A. Goswami

_____ **Date:**

Member 2 – Prof. P.K. Mohapatra

Final approval and acceptance of this dissertation is contingent upon the candidate's submission of the final copies of the dissertation to HBNI.

I hereby certify that I have read this dissertation prepared under my direction and recommend that it may be accepted as fulfilling the dissertation requirement.

Date:

Place:

STATEMENT BY AUTHOR

This dissertation has been submitted in partial fulfillment of requirements for an advanced degree at Homi Bhabha National Institute (HBNI) and is deposited in the library to be made available to borrowers under rules of the HBNI.

Brief quotations from this dissertation are allowable without special permission, provided that accurate acknowledgement of source is made. Requests for permission for extended quotation from or reproduction of this manuscript in whole or in part may be granted by the Competent Authority of HBNI when in his or her judgment the proposed use of the material is in the interests of scholarship. In all other instances, however, permission must be obtained from the author.

Ritesh Ruhela

DECLARATION

I, hereby declare that the investigation presented in the thesis has been carried out by me. The work is original and has not been submitted earlier as a whole or in part for a degree/diploma at this or any other institution/University.

Ritesh Ruhela

Dedicated to

**My Parents
&
Wife**

Acknowledgements

This thesis owes its existence to the help, support, encouragement and inspiration of many people. It is indeed a pleasure to express my deep gratitude to my guide Dr. B. S. Tomar, Head, Radioanalytical Chemistry Division, BARC for his invaluable guidance and constant support and encouragement during the entire course of this study. I take this opportunity to state that his keen interest and valuable suggestions were of immense help in improving the quality of work as well as enriching my knowledge.

Sincere thanks are to Shri J. N. Sharma who introduced me to the field of solvent synthesis and metal extraction relevant to back end of nuclear fuel cycle.

I sincerely acknowledge the support and encouragement rendered to my research work by Dr. A. K. Suri, Director, Materials Group, Dr. R. C. Hubli, Head, Material Processing Division and Shri A. K. Singh, Head, Hydrometallurgy Section.

Chairman (Dr. K. L. Ramakumar) and members (Dr. A. Goswami, Dr. P. K. Mohapatra) of the doctoral committee are gratefully acknowledged for their critical review and valued suggestions during progress review and pre-synopsis viva-voce. I also wish to thank Dr. M. S. Murali, Dr. T. K. Ghanty, Dr. D. Bhattacharya, Dr. Neetika Rawat, Mr. Sumit Kumar, Mr. Krishankant, Mr. T. Gadly, Mr. Raghunath Choudhary, Dr. T. K. Shesagiri and Dr. V. C. Adya, for their co-operation during the course of this study. My batch mates from 48th batch of OCES chemistry discipline have been like real friends supporting me during all the difficult periods and I wish to thank all of them.

Nothing is going to complete without saying thank you to my parents, my brother and sister, and my in-laws without whose support and blessings I would not have completed the research work.

Last but not the least, my family-my son and wife have been like pillars of strength for me and I take this opportunity to express my profound love to my family.

Ritesh Ruhela

Contents

Synopsis	i
List of Figures	x
List of Tables	xviii
Chapter 1	1
Introduction	
1.1. Occurrence of palladium in nature	2
1.2. Applications of palladium	3
1.3. Waste from spent fuel reprocessing	6
1.4. Platinum group metals - resources and production in the reactor	8
1.5. Nuclear Technology	11
1.5.1. Structural and Special Materials	11
1.5.2. Hydrogen isotope separation	12
1.5.3. Waste Management	13
1.7. Recovery of palladium from High Level Solid Waste (HLSW) arising from dissolution of spent nuclear fuel	15
1.8. Recovery of palladium from High Level Liquid Waste (HLW) solution arising from PUREX process raffinate	16
1.8.1. Precipitation	17
1.8.2. Electrochemical Reduction	18
1.8.3. Ion Exchange and Sorption	19
1.8.4. Solvent Extraction	22
1.8.4.1. Hard donor extractants	23
1.8.4.2. Soft donor extractants	27

1.9. Motivation for the present work	32
Chapter 2	34
Synthesis & Characterization of Novel Reagents and Experimental Methodologies	
2.1. Synthesis and Characterization of ligands and grafted polymeric resins	34
2.1.1. <i>N, N, N', N'</i> -tetra-(2-ethylhexyl)-thiodiglycolamide (T(2EH)TDGA)	34
2.1.2. <i>N, N, N', N'</i> -tetra-(2-ethylhexyl)-dithiodiglycolamide (DTDGA)	37
2.1.3. <i>2-Acetyl pyridine group functionalized Amberlite XAD-16 resin</i>	39
2.2.4. <i>2-Acetyl amide group functionalized Amberlite XAD-16 resin</i>	42
2.3. Feed solutions	44
2.4. Experimental methodologies	47
2.4.1. Solvent extraction studies	47
2.4.2. Acid Uptake Studies	47
2.4.3. Gamma Radiolysis Experiments	49
2.4.4. Hydrolysis Experiments	51
2.4.5. Sorption Studies	51
2.4.6. Structural investigation studies	53
2.4.6.1. EXAFS Studies	54
2.4.6.2 DFT Calculations	57
CHAPTER 3	58
Evaluation of T(2EH)TDGA for separation of Pd(II) from high level liquid waste	
3. Evaluation of the extractant	59
3.1. Extraction of nitric acid	59
3.2. Extraction equilibrium studies	61

3.3. Effect of nitric acid concentration	62
3.4. Effect of nitrate ion concentration	64
3.5. Effect of concentration of T(2EH)TDGA	64
3.6. Effect of diluents	66
3.7. Loading studies	67
3.8. Back extraction studies	67
3.9. Recovery of palladium from stripping solution	68
3.10. Thermodynamic studies	68
3.11. FTIR and FT-Raman Studies	72
3.12. Extraction studies with SHLW Solution	74
3.13. Extraction behavior of HLLW elements	75
3.14. Reusability of the Extractant	76
3.15. Hydrolytic and radiolytic stability studies	77
3.15.1. Hydrolysis of T(2EH)TDGA solvent system	77
3.15.2. Qualitative analysis of radiolytic degradation products	79
3.15.3. Radiolytic stability of T(2EH)TDGA solvent system	83
3.15.4. Effect of radiolysis of solvent on extraction behavior of SHLW	86
Elements	
3.16. Extractive Spectrophotometric Determination of Palladium	89
Conclusions	97
CHAPTER IV	99
Evaluation of <i>N,N,N',N'</i>-tetra-(2-ethylhexyl)-dithiodiglycolamide (DTDGA) for separation of Pd(II) from HLLW	
4.0. Evaluation of the Extractant	99
4.1. Extraction equilibrium studies	100

4.2. Effect of nitric acid concentration on palladium extraction	100
4.3. Nitric acid uptake	102
4.4. Effect of diluents	104
4.5. Loading Studies	105
4.6. Back extraction and subsequent recovery of palladium from strip solution	105
4.7. Determination of Pd-DTDGA complex stoichiometry	107
4.8. Comparison of ligands	108
4.9. Extraction Studies with SHLW Solution	109
4.10. Extraction Studies with tracer spiked HLLW Solution	110
4.11. Reusability of the Extractant	111
4.12. McCabe-Thiele Diagram	112
4.13. Flow sheet for separation and recovery of palladium from SHLW	113
4.13. Stability Studies of <i>N,N,N',N'</i> -tetra-(2-ethylhexyl) dithiodiglycol amide (DTDGA)	114
4.14. Structural investigation studies of Pd-ligand complex	123
Conclusions	132
CHAPTER V	134
Evaluation of Ligand Grafted Polymeric Resins	
5.0. Evaluation of AP-XAD 16 and ACAM-XAD 16	136
5.1. Sorption kinetics	136
5.2. Effect of Acidity	140
5.3. FTIR studies	142
5. 4. Sorption studies	143
5.5. Maximum loading capacity	147

5.6. Back extraction studies	147
5.7. Sorption studies with simulated high level waste solution (SHLW)	147
Conclusions	150
Chapter VI	151
Summary and conclusions	
List of Publications	158
References	160

Synopsis

Since the first successful demonstration of nuclear fission process and its subsequent application in energy production, the share of nuclear power has been increasing steadily owing to both the fast dwindling of the non renewable (fossil) energy resources as well as the various environmental concern associated with their use. Nuclear energy, therefore, has an important role to play in the long term as a sustainable source of energy produced through controlled fission reaction of heavy elements like uranium and plutonium [1, 2]. Worldwide there are 450 nuclear power reactors in operation with natural or enriched uranium as fuel with ^{235}U as the fissile material. Unlike conventional fuels, nuclear fuels cannot be burnt totally due to the accumulation of the fission products, many of which are neutron poison leading to neutron economy loss and also the loss of valuable fissile material. Therefore, irradiated fuels are to be reprocessed for the recovery of fissile materials like uranium and plutonium in order to make them available for recycling.

Among the various methods, the solvent extraction method, Plutonium Uranium Reduction Extraction (PUREX) process is being followed world over [3, 4] for reprocessing of spent nuclear fuel. In this process, the spent fuel after sufficient cooling is decladed and dissolved in nitric acid. Uranium and plutonium are extracted in 30% Tri-n-butyl phosphate (TBP) in n-dodecane leaving behind fission products in the aqueous phase. Further separation of plutonium from uranium is termed as partitioning which is achieved by selective reduction of plutonium either chemically or electrolytically.

Like any other industrial activity, spent nuclear fuel reprocessing also leads to generation of waste streams diverse in nature with respect to their physical, chemical and radiochemical characteristics. Depending upon their radioactivity levels, they are categorized as high level liquid waste (HLLW), intermediate level waste (ILW) and low

level waste (LLW). Among these wastes, HLLW is found to be the most hazardous as it contains more than 99% of the total nonvolatile fission products generated in the entire nuclear fuel cycle. The extreme radiotoxicity of HLLW makes its safe disposal a matter of serious attention. Consequently, the management of HLLW forms an important task in the back-end of the nuclear fuel cycle [5]. The composition of HLLW depends on several factors like type of reactor, nature of fuel, its burn-up, cooling period, chemicals added during reprocessing, efficiency of the reprocessing plant, etc.

The HLLW contains small quantity of actinide elements like uranium, neptunium, plutonium, americium, curium, etc. along with many fission products, such as, strontium, yttrium, zirconium, niobium, molybdenum, technetium, ruthenium, rhodium, palladium, cesium, barium and lanthanides in appreciable quantities. Some of the proposed strategies for management of HLLW involve (i) Immobilization in suitable matrix, (ii) Partitioning of long lived actinides and long lived fission products from HLLW followed by their transmutation to either short lived or stable products, (iii) Separation of heat producing radionuclides, like, ^{137}Cs , ^{90}Sr , etc. as well as other valuable radionuclides for their use in various possible applications.

Platinum group metals, namely, Ru, Rh and Pd are found in appreciable quantities in HLLW, and usually interfere during vitrification of HLLW by formation of separate phases in the vitrified glass, thereby destabilizing the latter [6]. This necessitates the efficient separation and recovery of these elements from HLLW prior to its vitrification. Fission palladium comprises of stable isotopes ^{104}Pd (17 wt %), ^{105}Pd (29 wt%), ^{106}Pd (21 wt%), ^{108}Pd (12 wt%), ^{110}Pd (4 wt%) and a radioactive isotope ^{107}Pd (17 wt%) with a half life of 6.5×10^6 years. The intrinsic radioactivity of ^{107}Pd (soft β -emitter with E_{max} of 35 keV) is quite less and hence can be tolerated for many industrial applications [7]. However, the public acceptance would be a major challenge and will have to be taken

care by selective separation of its constituent radioactive isotope by enrichment techniques. Also, there are various applications in nuclear field where the associated radioactivity of ^{107}Pd will be insignificant compared to the inherent radioactivity of the major components. Thus, the separation of palladium from spent nuclear fuel is an attractive route to alleviate its growing scarcity in distant future. Separation of Pd from HLLW will provide an additional advantage of mitigating various problems associated with the presence of palladium during vitrification.

Depending upon the burn-up of the fuel, reactor type and reprocessing flow sheet, the expected amount of palladium in HLLW is in the range of 100-500 ppm. Palladium being a soft metal can be effectively complexed with ligands having soft donor atoms like 'S' and 'N'. Accordingly several separation methods have been suggested in literature for the recovery of palladium from HLLW. Among them, the most promising one is the liquid-liquid extraction of palladium from HLLW. Various ligands namely, tertiary and quaternary amines (tri-n-octylamine, and tri-n-octylmethylammonium nitrate) [8], α -benzoinoxime (ABO) [9], dioctyl sulfides (DOS), dioctyl sulfoxides (DOSO), Triisobutyl phosphinesulfide (TIPS) [10] and benzoylmethylene triphenylphosphorane (BMTTP) [11], have been evaluated for this purpose during the last two decades. However, these ligands suffer from various limitations such as slow kinetics, poor decontamination factor, pH sensitivity, solubility and instability in acidic medium. In order to overcome some of the limitations of liquid-liquid extraction process, another method which involves the solid phase extraction of Pd from HLLW has also been explored in detail. For instance several anion exchangers like 4-(*N,N*-dimethylbenzimidazole)phenyl (AR-01), tertiary Amberlite IRA-93ZU and quaternary Amberlite IRA-900, Amberlite IRN-78 [12], Dowex 1X8-400 and Dowex 2X8-400 as well as cation exchangers, namely, sulfonic acid resin KU-2X8 and phosphoric acid resin KRF-20t-60 [13] have been studied

for Pd separation from HLLW. In addition to this several other class of sorbents like bis-(2,4,4-trimethylpentyl)-monothiosphonic acid (Cyanex-302) encapsulated in microcapsules of Ca alginate gel [14], tri-isobutyl phosphine sulphide (Cyanex-471X) impregnated on chromosorb-102 [15], imidazolium nitrate immobilized on polystyrene-divinylbenzene resin matrix [16], have also been explored. However, there are some limitations associated with these resins like slow kinetics, low uptake of Pd, poor decontamination factor, etc. In view of growing concern for separation and recovery of Pd from HLLW, it becomes essential to develop simple and effective methods for its recovery in pure form.

As a part of this thesis, novel ligands, namely, *N,N,N',N'*-tetra(2-ethylhexyl)thiodiglycolamide (T(2EH)TDGA) and *N,N,N',N'*-tetra(2-ethylhexyl)dithiodiglycolamide (DTDGA) have been synthesized, characterized and evaluated in detail for liquid-liquid extraction of Pd from HLLW. Also, novel ligand grafted resins, namely, 2-acetyl pyridine grafted XAD-16 (AP-XAD16) and 2-acetyl amide grafted XAD-16 (ACAM-XAD16) have been synthesized, characterized and evaluated for the same purpose. The results of these studies are reported in the thesis. The work reported in this thesis is divided in to six chapters as described below:

The first Chapter is an introductory chapter. In this chapter a brief introduction to nuclear fuel cycle, reprocessing of spent nuclear fuel and classification of various radioactive waste are given. The fission yield and the corresponding concentration of palladium that may occur in HLLW are given. The various problems posed by the presence of Pd in waste management have been discussed. The various methods available for separation and purification of Pd from spent nuclear fuel and especially from HLLW have been discussed in great detail. The extensive literature available on Pd recovery from HLLW has been reviewed. Further, the possible applications of recovered Pd in nuclear and non

nuclear fields have also been mentioned. Lastly the motivation for the work carried out as a part of this thesis has been explained.

The second chapter provides details of the various instrumental techniques being used for the characterization of novel ligands as well as ligand grafted resins. The synthesis and characterization of the ligands and grafted resin has been provided in this chapter. Experimental details for liquid-liquid as well as solid phase extraction are discussed. Also the details of the experimental techniques to study the hydrolytic and radiolytic stability are included in this chapter. Various techniques which are used for quantification of metal ions present in the aqueous feed solution have also been discussed. Finally the details of extended X-ray absorption fine structure spectroscopy (EXAFS) as well as computational methods (DFT Calculations) used for structural elucidation of Pd-ligand complex have been given.

In the third chapter, the details of evaluation of novel ligand namely *N,N,N',N'*-tetra-(2-ethylhexyl)thiodiglycolamide (T(2EH)TDGA) have been described. Detailed extraction studies with Pd and various metal ions present in simulated high level waste (SHLW) as well as actual high level liquid waste (HLLW) have been carried out. The kinetics of extraction is found to be fast with almost quantitative uptake achieved within five minutes. The ligand has shown very high extractability and selectivity for Pd over other elements present in high level waste. Back extraction of Pd as well as its further recovery as palladium sulphide has also been established. The composition of the extracted complex as determined by log-log plot is found to be $\text{Pd}(\text{NO}_3)_2 \cdot 2\text{T}(2\text{EH})\text{TDGA}$. The FTIR and Raman studies have confirmed the ligation of Pd with both the thioetheric 'S' and the carbonyl oxygen of the amidic moiety. Also, the ligand is found to be fairly stable in nitric acid as well radiation environment and thus is quite promising for use at plant

scale. Moreover, using this ligand an extractive spectrophotometric method has been developed for the determination of Pd in SHLW.

The efficacy of T(2EH)TDGA can be further improved by incorporating another thioetheric 'S' atom appropriately spaced by the ethylene bridge to offer more stable chelation toward metal ion. The conceptualization of the novel ligand, namely, *N,N,N',N'*-tetra-(2-ethylhexyl)dithiodiglycolamide (DTDGA) and its evaluation are discussed in chapter 4. The stoichiometry of Pd-ligand complex using mole ratio plot and ESI-MS was determined to be 1:1. This conforms to our assumption that both the sulphur atoms and the carbonyl oxygen will be involved in complex formation thereby forming a stable chelate. This ligand was found to be the most effective among the ligands reported in the literature for Pd separation from HLLW. Kinetics of extraction of Pd was determined to be fast, the equilibrium being attained within five minutes. The ligand can be used for recovery of Pd from nitric acid medium of wide range of concentration. Very high extractability and selectivity are obtained for Pd over other metal ions. The ligand was found to be hydrolytically as well as radiolytically stable and therefore have proven to be most promising for Pd separation from HLLW. Detailed extraction studies with SHLW have been carried out and subsequently a flow sheet has been developed to recover Pd from HLLW. Further the structure of the extraction complexes of palladium (II) with novel ligands, namely, *N,N,N',N'*-tetra-(2-ethylhexyl) thiodiglycolamide (T(2EH)TDGA) and *N,N,N',N'*-tetra-(2-ethylhexyl) dithiodiglycolamide (DTDGA), have been determined by EXAFS as well as computational methods. The structures of the extraction complexes of Pd(II)-T(2EH)TDGA and Pd(II)-DTDGA have been found to be square planar with slight distortion owing to the bulkier alkyl groups of the amidic moieties. DFT calculations for the Pd-ligand complexes show that Pd(II)-DTDGA complex with 1:1

stoichiometry is more energetically stable than Pd(II)-T(2EH)TDGA complex with 1:2 stoichiometry.

The evaluation of two novel ligand grafted resins, namely, AP-XAD16 and ACAM-XAD16 have been described in chapter 5. These two resins differ in the nature of primary donor atoms. While AP-XAD 16 contains 'N' and carbonyl oxygen as donor atoms, ACAM-XAD16 has two carbonyl oxygen atoms as donor atoms. This is also reflected in their uptake behavior towards Pd in nitric acid medium. Hence, with AP-XAD16 uptake of Pd (D_{Pd}) decreases with increase in acidity of aqueous feed solution whereas with ACAM-XAD16 the D_{Pd} increases with increase in acidity. The significant decrease in D_{Pd} in the case of AP-XAD16 is attributed to protonation of 'N' atom of pyridine moiety at higher acidity. Maximum Pd loading capacity of the resin was determined to be approximately 8 to 9 mg/g. Sorption studies revealed that both the resins follow pseudo second order sorption kinetics. Also, in both the cases the sorption data could be fitted well by Langmuir as well as Freundlich isotherms. Back extraction of Pd from the loaded resin is comfortably achieved by acidic thiourea solution. FTIR studies have been used to understand the mode of ligation of the polymeric resin to palladium. Sorption studies with SHLW elements showed that AP-XAD16 can be used directly for separation of Pd from HLLW since other metal ions are hardly sorbed, whereas ACAM-XAD16 can be used only after actinide partitioning since it tends to sorb palladium along with trivalent lanthanides and actinides in appreciable quantities.

In the concluding chapter 6 a summary of the results and important conclusions drawn from all the above studies have been discussed along with the recommended flow sheet for the recovery of palladium from HLLW.

References

1. G. Friedlander, J.W. Kennedy, E.S. Macias, J.M. Miller, Nuclear and Radiochemistry, 3rd Edition, 1981.
2. S. Glasstone, Source book of Atomic Energy, US Atomic Energy Commission, 1967.
3. E.R. Iresh, W.H. Rheas, USAEC Report TID-7534 (BK-1) (1953).
4. E.R. Iresh, USAEC Report HW-60116 (1959).
5. W.E. Kastenber, L.J. Gratton, Physics Today, 50 (1997) 41.
6. S.K. Sundaram, J.M. Perez Jr., PNNL-13347, Pacific Northwest National Laboratory, Richland, WA (2000).
7. H.J. Ache, L.H. Baetsle, R.P. Bush, A.F. Nechaev, U.P. Popik, Yu. Ying, IAEA Technical Report Series (1989).
8. E.A. Mezhov, A.V. Kuchmunov, V.V. Druzhnikov, Radiochemistry, 44(2) (2002) 135.
9. A. Dakshinamoorthy, P.S. Dhami, P.W. Naik, S.K. Dudwadkar, S.K. Munshi, P.K. Dey, V. Venugopal, Desalination, 232 (2008) 26.
10. G.H. Rizvi, J.N. Mathur, M.S. Murali, R.H. Iyer, Sep. Sci. Tech., 31 (1996) 1805.
11. M. Mohan Raj, A.D. Panchanatheswaran, K.A. Venkatesan, T.G. Srinivasan, P.R. Vasudeva Rao, Hydrometallurgy, 84(2006) 118.
12. S.H. Lee, H. Chung, J. Nucl. Sci. Technol., 37, 3 (2000) 281.

13. V.V. Milyutin, S.B. Peshkishev and V.M. Gelis, Radiokhimiya, 36 (1994) 25;
Sov. Radiochem., 36 (1994) 26.
14. H. Mimura, H. Ohta, K. Akiba, Y. Onodera, Jour. of Nucl. Sci. Tech., 38(5)
(2001) 342.
15. A. Dakshinamoorthy, T. Kumar, K.K. Nandy, R.H. Iyer, J.N. Mathur, S.B.
Manohar, Jour. of Radioanal. & Nucl. Chem., 245(3) (2000) 595.
16. A.K. Venkatesan, B. Robert Selvan, M.P. Antony, T.G. Srinivasan, P.R.
Vasudeva Rao, Hydrometallurgy, 86 (3-4) (2007) 221.

List of Figures

- Fig. 1.1. Applications of palladium.
- Fig. 1.2. Composition of irradiated fuel.
- Fig. 1.3. Nuclear waste management.
- Fig. 1.4. Temporal profile of left over radioactivity.
- Fig. 1.5. Mass yield distribution in thermal (T) neutron fission of ^{235}U and fast (F) neutron induced fission of ^{239}Pu .
- Fig. 2.1. Reaction scheme for T(2EH)TDGA.
- Fig. 2.2. Reaction scheme for DTDGA.
- Fig. 2.3. Reaction scheme for 2-Acetyl pyridine group functionalized Amberlite XAD-16 resin.
- Fig. 2.4. TGA of AP-XAD16.
- Fig. 2.5. Reaction Scheme for ACAM-XAD16.
- Fig. 2.6. TGA of ACAM-XAD16.
- Fig. 3.1. Extraction of HNO_3 from aqueous solution by 0.1M T(2EH)TDGA/n-dodecane at different initial nitric acid concentrations.
- Fig. 3.2. Extraction of nitric acid form aqueous solution by 0.1 M T(2EH)TDGA/n-dodecane.
- Fig. 3.3. Variation of % E of palladium as a function of contact time. Organic phase: 0.01 M T(2EH)TDGA/n-dodecane, Aqueous phase: 10^{-3} M palladium in 4.0 M nitric acid.
- Fig. 3.4. Dependency of D_{Pd} on HNO_3 concentration. Aqueous phase: 10^{-3} M Pd in 0.5 M to 6.0M HNO_3 . Organic

phase: 0.005 M T(2EH)TDGA/n-dodecane.

Fig. 3.5. Extraction dependency of D_{Pd} in 4.0 M(H, Na)NO₃.

Org. phase: 0.005 M T(2EH)TDGA /n-dodecane,

Aqueous phase: 4M(H, Na) NO₃.

Fig. 3.6. Extraction dependency of palladium on initial nitrate

ion concentration. Organic phase: 0.005M

T(2EH)TDGA/n-dodecane, Aqueous Phase: 10⁻³M

palladium in (0.5H+Na)NO₃.

Fig. 3.7. Dependency of the distribution ratio of Pd on

T(2EH)TDGA concentration. Aqueous phase: 10⁻³M Pd

in 0.5M HNO₃. Organic phase: 0.001 to 0.005M

T(2EH)TDGA in n-dodecane.

Fig. 3.8. Dependence of D_{Pd} on T(2EH)TDGA concentration.

Aqueous phase: 2.5x10⁻⁴M Pd in 0.2M HNO₃. Organic

phase: 0.002 M to 0.005 M T(2EH)TDGA in n-

dodecane.

Fig. 3.9. Dependence of D_{Pd} on temperature. Aqueous phase:

2.5x10⁻⁴M Pd in 0.2 M HNO₃. Organic phase: 0.003 M

T(2EH)TDGA /n-dodecane.

Fig.3.10. Dependence of conditional extraction constant (K'_{ex}) on

temperature.

Fig. 3.11. FT-IR spectra of T(2EH)TDGA and Pd(II)-

T(2EH)TDGA.

Fig. 3.12. FT-Raman spectra of T(2EH)TDGA and Pd(II)-

T(2EH)TDGA.

- Fig. 3.13. FT-IR spectra of 0.05M T(2EH)TDGA/n-dodecane kept in 3.0M Nitric acid.
- Fig. 3.14. GC-MS of pure T(2EH)TDGA.
- Fig. 3.15. GC-MS of neat T(2EH)TDGA after an absorbed dose of 0.5 MGy.
- Fig. 3.16. GC-MS of 0.05M T(2EH)TDGA/n-dodecane in contact with 3.0 M nitric acid after an absorbed dose of 0.5MGy.
- Fig. 3.17. Radiolytic degradation paths of T(2EH)TDGA.
- Fig. 3.18. Degradation curve of T(2EH)TDGA as a function of absorbed dose.
- Fig. 3.19. Plot of $\log C/C_0$ vs. Dose (MGy) for neat T(2EH)TDGA.
- Fig. 3.20. Extraction of Pd as a function of absorbed dose. Aq. phase: 1×10^{-3} M Pd in 3.0 M HNO₃.
- Fig. 3.21. Comparison of D_{Pd} and % Extraction of palladium as a function of absorbed dose. Aq. phase: 1×10^{-3} M Pd in 3.0 M HNO₃.
- Fig.3.22. Absorption spectrum of T(2EH)TDGA/n-dodecane and Pd-T(2EH)TDGA/n-dodecane complex. Concentration of Pd= 1.0×10^{-4} M in 1.0M nitric acid. Concentration of T(2EH)TDGA= 2.0×10^{-3} M.
- Fig. 3.23. Effect of diluents. Concentration of Pd = 1.0×10^{-4} M in 1.0 M nitric acid. Concentration of T(2EH)TDGA = 2.0×10^{-3} M.

- Fig. 3.24. Effect of acid. Concentration of Pd = 1.0×10^{-4} M, concentration of T(2EH)TDGA = 2.0×10^{-3} M.
- Fig. 3.25. Calibration plot. Concentration of Pd = 1.0 μ g/ml to 20 μ g/ml, concentration of T(2EH)TDGA = 2.0×10^{-3} M.
- Fig. 3.26. Job's plot. Concentration of Pd = 1.0×10^{-4} M in 0.5 M HNO₃, concentration of T(2EH)TDGA = 1.0×10^{-4} M.
- Fig. 4.1. Variation of % E of palladium as a function of contact time. Organic phase: 0.0015 M DTDGA/n-dodecane, Aqueous phase: 10^{-3} M palladium in 3.0 M nitric acid.
- Fig. 4.2. Effect of nitric acid concentration on distribution ratio of palladium (D_{Pd}). Org. phase: 0.0015 M DTDGA/n-dodecane, aqueous phase: 10^{-3} M Pd at different initial nitric acid concentrations.
- Fig. 4.3. Variation of D_{Pd} with [HNO₃] at fixed ionic strength. Org. phase: 0.0015 M DTDGA/n-dodecane, aqueous phase: 3 M (H, Na)NO₃.
- Fig. 4.4. Extraction of HNO₃ from aqueous solutions by 0.1 M DTDGA/n-dodecane at different initial nitric acid concentrations.
- Fig. 4.5. Determination of Acid uptake constant (K_H). Org. phase: 0.1 M DTDGA/n-dodecane, Aq. phase: nitric acid at different concentrations.
- Fig. 4.6. Mole Ratio Plot, Org.: DTDGA/n-dodecane, Aq.: 0.98×10^{-3} M Pd in 3.0M HNO₃.
- Fig. 4.7. ESI-MS (% abundance vs m/z) of 10^{-4} M DTDGA/n-

hexane after contacting with 10^{-4} M Pd in 3.0 M nitric acid medium.

- Fig. 4.8. Comparison of extraction efficiency of various extractants (L).
- Fig. 4.9. γ -spectra of HLW stock solution and organic phase after contacting with HLW stock solution.
- Fig. 4.10. Distribution ratio of various metal ions present in SHLW. Aqueous phase: SHLW feed solution, Organic Phase: 0.025 M DTDGA/n-dodecane.
- Fig. 4.11. McCabe-Thiele plot for extraction of palladium from 3.0 M nitric acid solution. Organic: 0.0025 M DTDGA/n-dodecane, aqueous phase: 200 mg/L Pd in 3.0 M nitric acid (O/A varied from 8:2 to 2:8).
- Fig. 4.12. Flow sheet for extraction and recovery of palladium from HLW solution.
- Fig. 4.13. GC-MS of pure DTDGA.
- Fig. 4.14. GC-MS of neat DTDGA after an absorbed dose of 0.5 MGy.
- Fig. 4.15. GC-MS of 0.05M DTDGA/n-dodecane in contact with 3.0M nitric acid after an absorbed dose of 0.5MGy.
- Fig. 4.16. Radiolytic degradation paths of DTDGA.
- Fig. 4.17. Degradation curve of DTDGA as a function of absorbed dose.
- Fig. 4.18. Plot of $\log C/C_0$ vs. Dose (MGy).
- Fig. 4.19. Extraction of Pd as a function of absorbed dose. Aq.

phase: 1×10^{-3} M Pd in 3.0 M HNO_3 .

- Fig. 4.20. k^2 -weighted EXAFS spectra of Pd(II) aqua ion and comparison of the corresponding Fourier transforms of the experimental data (solid line) with those of the theoretical signal (circles).
- Fig. 4.21. Optimized geometry of tetra aqua Pd(II).
- Fig. 4.22. k^2 -weighted EXAFS spectra of the extraction complexes (Pd(II)-T(2EH)TDGA)) and comparison of the corresponding Fourier transforms of the experimental data (solid line) with those of the theoretical signal (circles).
- Fig.4.23.A. Optimized geometry of Pd(II)-TIBTDGA complex (Diagonally placed 'S' and 'O' donor atoms) (DPDA).
- Fig.4.23.B. Optimized geometry of Pd(II)-TIBTDGA complex (Symmetrically placed 'S' and 'O' donor atoms) (SPDA).
- Fig. 4.24. k^2 -weighted EXAFS spectra of the extraction complexes (Pd(II)-DTDGA)) and comparison of the corresponding Fourier transforms of the experimental data (solid line) with those of the theoretical signal (circles).
- Fig. 4.25. Optimized geometry of Pd(II)-TIBDTDGA complex.
- Fig. 5.1. Kinetics of Sorption of palladium on AP-XAD 16 resin as a function of time.
- Fig. 5.2. Kinetics of sorption of palladium on ACAM-XAD16 resin.

- Fig. 5.3. Pseudo-first-order plot of palladium sorption onto AP-XAD16.
- Fig. 5.4. Pseudo-second-order plot of palladium sorption onto AP-XAD16.
- Fig. 5.5. Pseudo-first-order plot of palladium sorption onto ACAM- XAD16.
- Fig. 5.6. Pseudo-second-order plot of palladium sorption onto ACAM-XAD16.
- Fig. 5.7. Sorption of palladium on AP-XAD 16 resin as a function of initial nitric acid concentration.
- Fig. 5.8. Sorption of palladium on ACAM-XAD 16 resin as a function of initial nitric acid concentration.
- Fig. 5.9. FT-IR spectra of AP-XAD 16 resin.
- Fig. 5.10. Equilibrium adsorption isotherms for palladium on AP-XAD16.
- Fig. 5.11. Equilibrium adsorption isotherms for palladium on ACAM-XAD 16.
- Fig. 5.12. Langmuir plot for the sorption of palladium onto AP-XAD16 resin.
- Fig. 5.13. Freundlich plot for the sorption of palladium onto AP-XAD16 resin.
- Fig.5.14. Langmuir plot for the sorption of palladium onto ACAM-XAD 16 resin.
- Fig. 5.15. Freundlich plot for the sorption of palladium onto ACAM-XAD 16 resin.

Fig. 5.16. Distribution ratio and % sorption of SHLW elements for AP-XAD 16 resin.

Fig. 5.17. Distribution ratio of SHLW elements for ACAM-XAD 16 resin.

List of Tables

- Table 1.1. Physical properties of palladium.
- Table 1.2. World resources of Platinum group metals.
- Table 1.3. Global projections of Platinum group metals from nuclear power programmes.
- Table 1.4. Isotope composition of palladium from nuclear and natural sources.
- Table 2.1. Elemental analysis of T(2EH)TDGA.
- Table 2.2. GC-MS of T(2EH)TDGA.
- Table 2.3. ¹H-NMR of T(2EH)TDGA.
- Table 2.4. Elemental analysis of DTDGA.
- Table 2.5. GC-MS of DTDGA.
- Table 2.6. ¹H-NMR of DTDGA.
- Table 2.7. FT-IR of AP-XAD16.
- Table 2.8. Elemental analysis of AP-XAD16.
- Table 2.9. FT-IR of ACAM-XAD16.
- Table 2.10. Elemental analysis of ACAM-XAD16.
- Table 2.11. Composition of simulated high level waste (SHLW) for pressurized heavy water reactor (PHWR), 6700MWD/te; Acidity: 3.0 M HNO₃.
- Table 2.12. Nuclear data of actinides and long lived fission products present in the HLLW.
- Table 3.1. Distribution ratios of various metal ions present in SHLW.

- Table 3.2 Distribution ratios of HLLW elements. Organic phase: T(2EH)TDGA/*n*-dodecane, aqueous phase: HLLW feed solution.
- Table 3.3 Distribution data of Pd in five successive cycles of extraction and stripping; Aqueous phase: SHLW feed solution. Organic phase: 0.025M T(2EH)TDGA/*n*-dodecane.
- Table 3.4. Distribution ratio of various metal ions present in SHLW. Aqueous phase: SHLW feed solution, Organic Phase: T(2EH)TDGA/*n*-dodecane kept in contact with 3.0 M nitric acid for two weeks.
- Table 3.5. EI-MS of degradation products found in T(2EH)TDGA after an absorbed dose of 0.5MGy.
- Table 3.6. Determination of concentration of palladium using Spectrophotometric method.
- Table 3.7. Determination of concentration of palladium using ICP-AES and Spectrophotometric method. Organic phase: 2.0×10^{-3} M in *n*-dodecane, Aqueous phase: SHLW diluted 20 times (Final acidity 1.0 M HNO₃).
- Table 3.8. Comparison of the present method with the other spectrophotometric methods for the determination of palladium(II).
- Table 4.1. Back extraction (% E) of palladium from loaded organic phase (0.0015 M DTDGA/*n*-dodecane).
- Table 4.2. Extraction of HLW elements, Org.: 0.0025M

DTDGA/n-dodecane, Aq.: 3.0 M HNO₃ solutions spiked with genuine HLW and other 'γ' tracers.

Table 4.3. Distribution data of Pd in five successive cycles of extraction and stripping; Aqueous phase: SHLW feed solution. Organic phase: 0.0015 M DTDGA/n-dodecane.

Table 4.4. EI-MS of degradation products found in DTDGA after an absorbed dose of 0.5 MGy.

Table 4.5. Summary of curve fitting and DFT optimized results for Pd(H₂O)₄²⁺.

Table 4.6. Summary of EXAFS curve fitting and DFT optimization results for Pd(II)-T(2EH)TDGA.

Table 4.7. Summary of EXAFS curve fitting and DFT optimization results for Pd(II)-DTDGA complex.

Table 4.8. Thermodynamic parameters for Pd(II) thiodiglycolamide complexes.

CHAPTER 1

Introduction

Palladium is a rare and lustrous silvery-white metal that was discovered in 1803 by William Hyde Wollaston [1], who named it palladium after the asteroid Pallas, which in turn, was named after the epithet of the Greek goddess Athena, who is said to have acquired it after staring the giant Pallas.



The main physical properties of palladium metal [2] as reported in literature are given in Table 1.1.

Description	Value
Atomic number	46
Atomic weight	106.4
Valences	2,3 and 4
Thermal neutron cross section for ^{108}Pd (in barns= 10^{-24} cm^2)	8.5 ± 1.0
Density (g/cc) at 25°C	3.8898
Melting point	1552°C
Boiling point	2870°C
Thermal conductivity ($\text{Cals}^{-1} \text{ m}^{-1} \text{ }^\circ\text{C}^{-1}$ at 100°C)	0.184
Specific heat (Cal/g mol at 25°C)	0.058

1.1. Occurrence of palladium in nature

Palladium, one of the rarest elements in earth's crust, belongs to platinum group metals (PGMs). The group consists of the two triads: (I) ruthenium, rhodium, palladium and (II) osmium, iridium, and platinum. The occurrence of PGMs in nature in primary and secondary ores is in the range of 0.7 to 7 ppm [3]. Palladium constitutes only 0.85% of the total naturally available PGMs. The concentrations of lighter triads of ruthenium, rhodium and palladium in the earth's crust are 5×10^{-7} %, 10^{-7} % and 10^{-6} % respectively [4]. Table 1.2 shows the world resources of these metals individually and as a whole.

Table 1.2

World resources of Platinum group metals

Country	Resources (10^3 t)			
	Pt	Pd	Rh	PGM
Canada	0.12	0.12	0.03	0.28
Columbia	0.03	NA	NA	0.03
South Africa	10.90	4.7	0.62	18.04
USSR (Old)	1.9	3.7	0.12	4.2
USA	NA	NA	NA	0.03
World total	12.95	8.52	0.77	24.58

*NA=Not available

It is seen from the table that the world resources of PGM are mainly in South Africa and USSR (erstwhile).

1.2. Applications of palladium

Palladium has been found to exhibit extraordinary catalytic and corrosion resistance properties, both as a metal and as an alloy, which have led to its widespread applications [5]. Over half of the supply of palladium and its congener platinum goes into catalytic converters, which convert up to 90% of harmful gases from auto exhaust (hydrocarbons, carbon monoxide and nitrogen dioxide) into less harmful substances (nitrogen, carbon dioxide and water vapor). Palladium is also used in electronics, dentistry, medicine, hydrogen purification, chemical applications and groundwater treatment. Palladium plays a key role in the technology used for fuel cells, which combine hydrogen and oxygen to produce electricity, heat and water. Further, palladium can adsorb 800 times its volume of gaseous hydrogen to give material useful as a reducing agent which makes this metal, a suitable storage material for hydrogen [6].

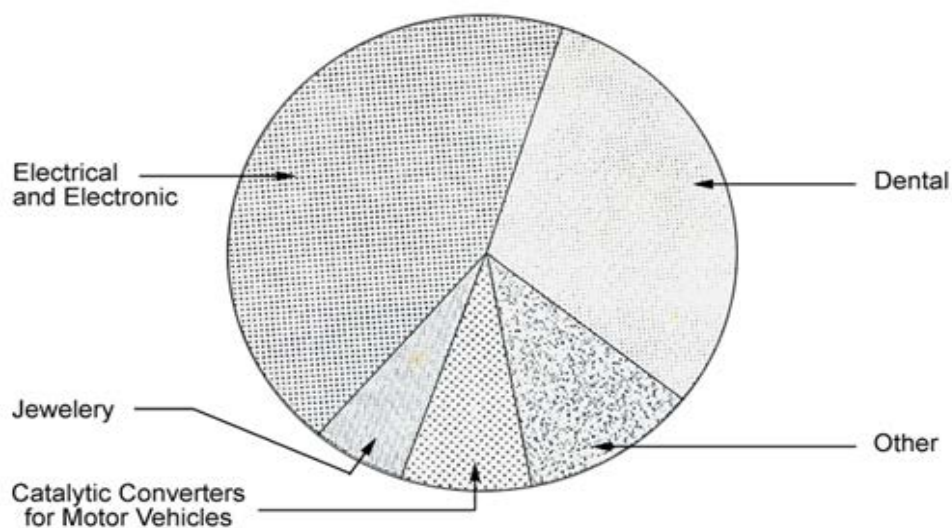


Figure 1.1 Applications of palladium

In recent years, various newer properties of palladium compounds have been explored, offering promise of major widening of the scope of the possible Pd applications. Some of the noteworthy applications are as follows

- (i) Compounds of Pd with organometallic compounds of transition metals can be used in organic synthesis [7], and Pd/SiO₂ catalyst, in synthesis of methanol from CO [8].
- (ii) Palladium based catalyst can be used for removing (by exhaustive oxidation) toxic organic compounds from water [9]. Such catalysts efficiently remove compounds comprising the P-C and S-C bonds.
- (iii) Pd can be used in making of gas sensors and devices for controlling the environmental pollution and the composition of gases in processes. Sensors made from Pd doped SnO₂ are sensitive to CO [10]. Peroxopolytungestic acid films prepared by sol-gel technique with Pd additives exhibit a gasochrome effect when treated with hydrogen or H/Ar mixture in air. Also, sensors sensitive to H₂S are manufactured from Pd-coated porous and amorphous Si [11].
- (iv) Pd finds applications in metallic glass formulations in the Pd-Ni-P systems. It was found that, among many of the metallic glass formulations, the largest glass formation power is exhibited by alloy with the composition Pd₄₀Ni₄₀P₂₀ [12, 13].
- (v) Palladium can be extensively used in solar batteries where it has been found to increase the efficiency via improving the conductivity of the metal/semiconductor contacts in the Si/Ti/Pd/Ag/SnO₂ system [14].
- (vi) Some Pd-based materials exhibit excellent thermoelectric properties. For example, CePd₃ exhibit an unusually high thermoelectric power at 100 – 300K [15].
- (vii) Compounds of palladium hold promise for manufacturing instruments for measuring ultra low temperatures e.g. PdMn and PdFe [16].

(viii) Palladium and its alloys are used for making highly conducting contacts in integrated circuits and various connections, and substantially decrease the losses in these contacts [17].

(ix) Palladium sulphide thin films can be used as photovoltaic material [18]. PdS thin films present high absorption coefficient in the range of the solar energy spectrum ($\alpha \sim 10^5 \text{ cm}^{-1}$ at $h\nu > 2.0 \text{ eV}$).

Owing to widespread applications of palladium in modern civilization there has been a steady growth in the demand for palladium over the years. Since the resources are limited, there is a need to look out for alternative sources of platinum group metals.

One such source can be spent nuclear fuel arising from nuclear power reactors. The production of power from nuclear fuels is gaining importance and its power share in total electricity generation is increasing because of depletion in the resources of conventional fuels like coal, oil and gas. Nuclear energy therefore has an important role to play in long range as a source of energy obtained through the controlled fission of heavy elements [19, 20] namely, uranium, plutonium etc. Commercial reactors are operating on natural uranium or enriched uranium with ^{235}U as the fissile isotope.

Unlike conventional fuels, nuclear fuels cannot be burnt totally due to the accumulation of the fission product isotopes upsetting the neutron balance and also due to loss of fissile material by fission and activation (^{239}Pu is converted into higher isotopes). Hence irradiated fuels (Fig. 1.2) are to be reprocessed for the separation and purification of uranium and plutonium from the highly radioactive fission products.

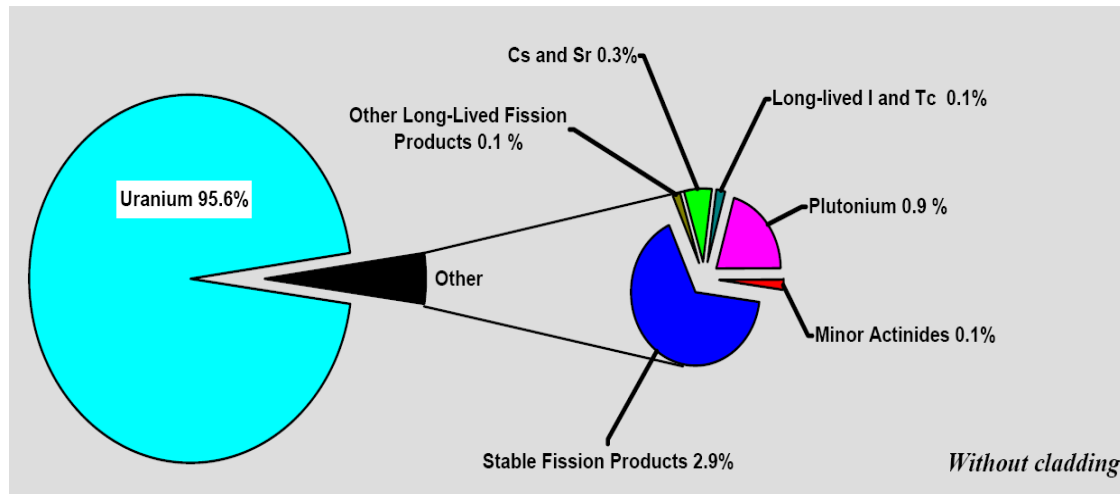


Fig. 1.2 Composition of irradiated fuel

1.3. Waste from spent fuel reprocessing

Like any other industrial activity, spent fuel reprocessing also generates waste streams which are diverse in nature with respect to their physical, chemical and radiochemical characteristics. Depending upon their radioactivity levels, they are categorized as high level, intermediate level and low level radioactive wastes [21]. Different types of wastes are generated at various stages of fuel reprocessing. High level solid waste (HLSW) after dissolution of chopped fuel, high level liquid waste (HLLW) after the first cycle of separation of uranium & plutonium from fission products, intermediate level liquid wastes (ILW) as concentrates from waste cycle evaporators and low level liquid waste (LLW) as condensate waste of the waste evaporators of the plant. The type of waste generated during reprocessing and the process followed for waste management are shown schematically in Figure 1.3.

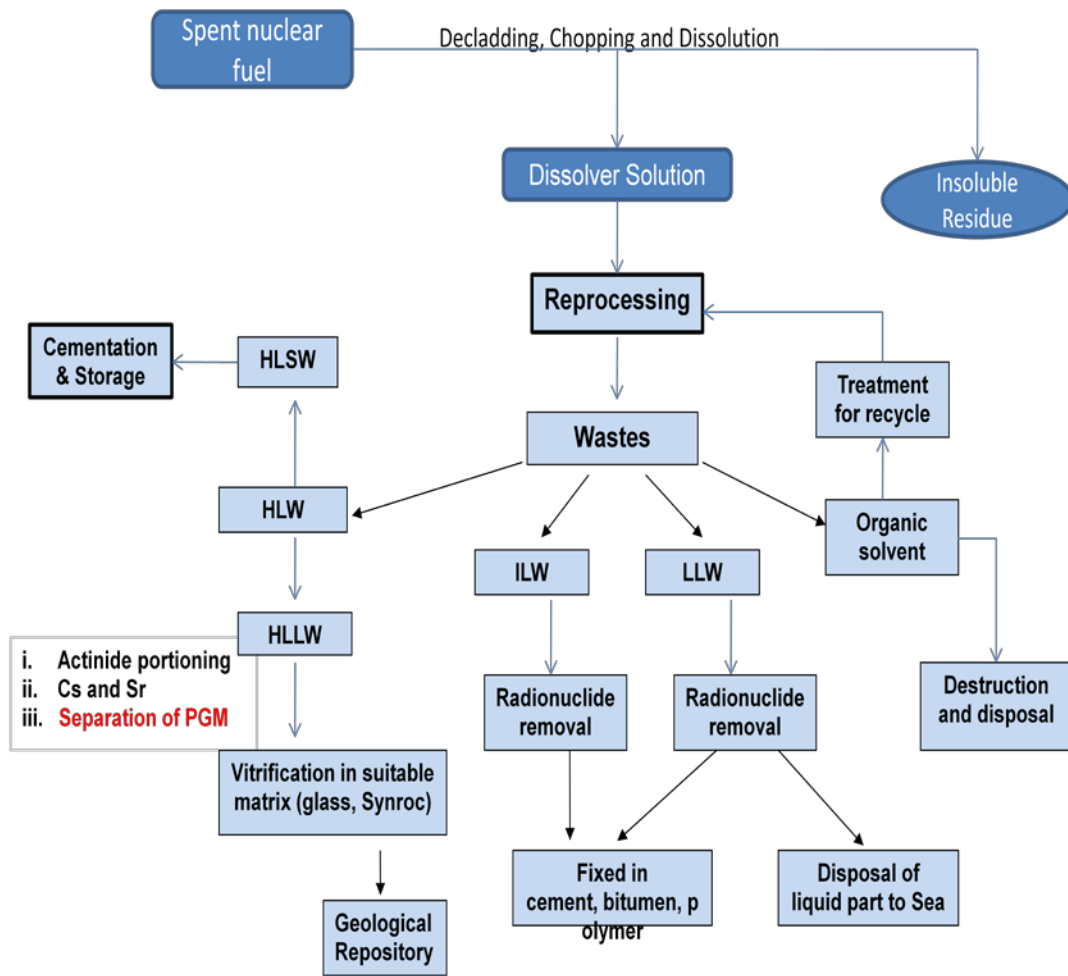


Figure 1.3: Nuclear Waste management

The objective of waste management is to keep the impact of the waste disposal on the environment as low as reasonably achievable [22]. In the case of HLLW, it is achieved by reducing the waste volume and immobilizing the radio nuclides in suitable matrices and storage under surveillance. Research and development efforts in nuclear waste management are continued for [23],

- (1) Immobilization in suitable matrix.
- (2) Partitioning of long lived actinides and fission products and their transmutation to either short lived or stable products.

- (3) Separation of heat producing radionuclides like ^{137}Cs , ^{90}Sr , etc. and,
- (4) Separation and recovery of valuable radionuclides for their use in various possible applications.

The above four steps of waste management will ensure that the valuable fission products as well as actinides can be recovered and the solid waste formed after various steps of processing will eventually have intrinsic radioactivity below that of natural uranium (Fig. 1.4) and, therefore, can be stored in near surface repositories [24].

The concept of recovery and utilization of by product from spent fuel reprocessing is attractive due to the following reasons:

- (i) Some of the radioactive fission products like ^{137}Cs , ^{90}Sr , etc. may find large scale application in medical fields and processing industries. Removal of these fission products could reduce the waste management cost.
- (ii) Some of the end products are useful and important material like platinum group metals (PGM) (Pd, Ru, and Rh). Their supply is limited. They are present in the waste in substantial quantities. Hence, their recovery from the nuclear waste prior to disposal by vitrification is attractive.

1.4. Platinum group metals - resources and production in the reactor

The noble metals (Pd, Ru & Rh) are produced by fission of ^{235}U and ^{239}Pu with yields of a few percent as shown in Figure 1.5 [25]. About 4 kg and 19 kg of PGM per ton of heavy metal are produced in light water reactors and fast breeder reactors [25] respectively.

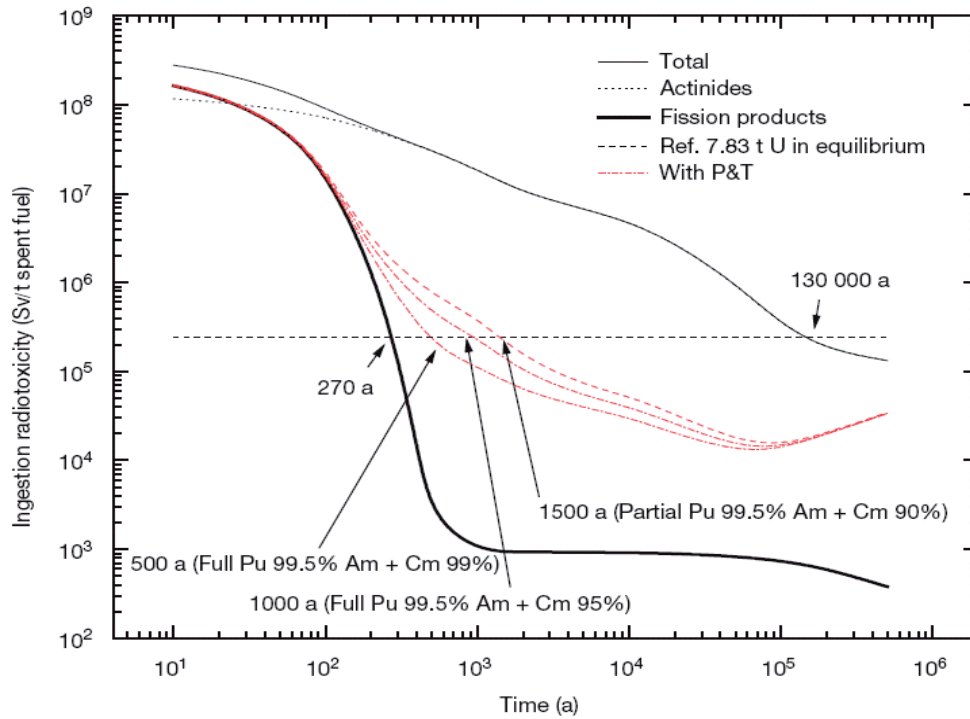


Fig. 1.4. Temporal profile of left over radioactivity.

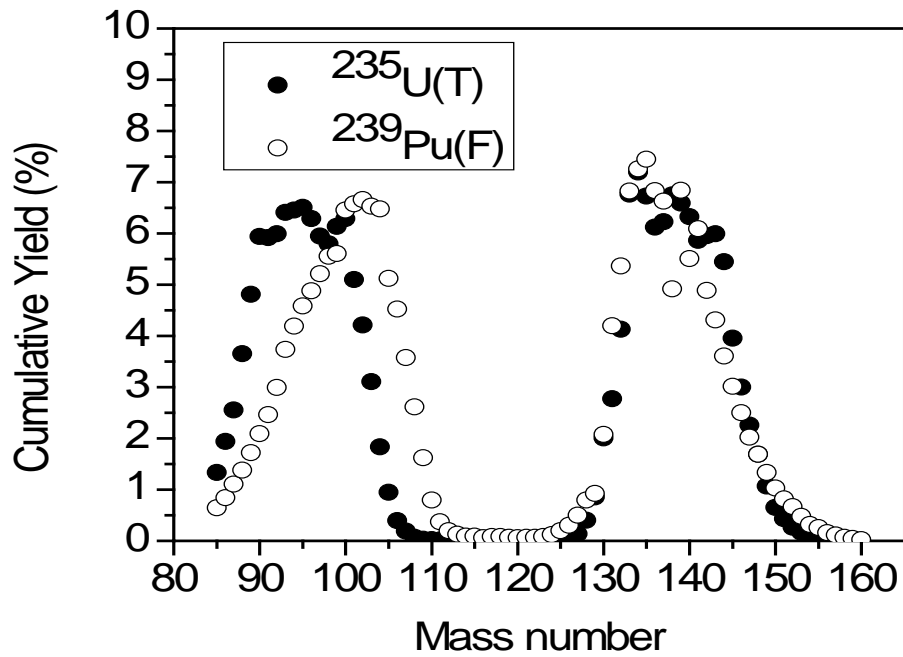


Fig. 1.5. Mass yield distribution in thermal (T) neutron fission of ^{235}U and fast (F) neutron induced fission of ^{239}Pu .

Table 1.3. gives the projected production of platinum group metals from nuclear power programs.

Table1.3. Global projections of platinum group metals from nuclear programs.

Specific Platinum group metal	In 2030 (t)
Ruthenium	1588
Rhodium	312
Palladium	950

It can be seen that significant quantities of resources of platinum group metals are present in the spent fuels arising from nuclear programs. Hence spent fuel forms a major source of platinum group metals [26]. Table 1.4 compares the isotopic composition of palladium produced from the reactors and the natural source. It can be seen that palladium of nuclear waste origin will have ^{107}Pd in addition to the stable isotopes. ^{107}Pd has half life of 7×10^6 years and emits low energy β (0.035 MeV). The specific activity of fission product palladium is $8.0 \mu\text{Ci/g}$ [26, 27]. F.P. Roberts and J.C. Shippard studied the stopping power of thin metal foils towards the beta rays from ^{107}Pd [27-28] and concluded that the biological damage if any, to the human beings will be confined to surface of the skin only. These studies indicate that even though ^{107}Pd is radioactive, owing to (i) low energy of beta particle (ii) absence of any gamma radiation and (iii) low range and low specific activity, palladium separated from spent fuel waste causes insignificant dose rate and has no biological adsorption. Thus fission palladium can be used with minimum biological effect and it may be compatible with uses other than dental and jewelry. However, this

aspect needs further careful study. It may be necessary to have control on its use avoiding contamination of palladium obtained from natural sources during recycling of palladium.

Table 1.4. Isotope composition of palladium from nuclear and natural sources

Isotope	Half life	Natural source %	Spent fuel source (after discharge) %	
			1 year	30 years
102	Stable	1.02		
104	Stable	11.14	16.9	15.8
105	Stable	22.33	29.3	27.4
106	Stable	27.33	21.3	26.4
107	6.5 x 10 ⁶ years (0.035 MeV, β)	-	17.0	15.9
108	Stable	26.46	11.7	10.9
110	Stable	11.72	3.8	3.6

This implies the need for segregation of the fission product palladium from natural palladium at all points in the utilization cycle. Some of the important and upcoming applications of palladium where the associated radioactivity can do no harm or at least be in a controlled manner are described as:

1.5. Nuclear Technology

1.5.1. Structural and Special Materials

Areas where palladium would improve the properties of structural materials:

- (i) To inhibit hydrogen embrittlement of pressure tubes (Zr-Nb alloy) in Canadian deuterium-uranium reactor (CANDU) [29, 30].
- (ii) To lower the corrosion potential of Ni/Co based alloy or stainless steel used in pressurized nuclear reactor [31].
- (iii) To prevent the embrittlement of Zircaloy cladding of oxide fuel by fission cadmium [32].
- (iv) To increase the oxidation resistance of Zircaloy-4 cladding of fuel elements [33].
- (v) To reduce the ^{60}Co embedded oxide scales on surface of stainless steel in boiling water reactor [34].
- (vi) To make shape memory alloys which find application in passive safety systems, thermo coupling for pipes and electric devices, thermo mechanical dampers and flow rate regulators etc. [35, 36].

1.5.2. Hydrogen isotope separation

Some of the noteworthy applications can be:

- (i) Tritium can be removed from the off gas stream of a fission reactor by conversion to tritiated water using palladium deposited on alumina or silica [37].
- (ii) Tritium can be removed from the aqueous effluents of nuclear plant and directed into an aqueous concentrate in combining the electrolysis of tritiated water with catalytic isotopic exchange using palladium deposited on styrene divinyl benzene copolymer [38, 39].
- (iii) Hydrogen in the primary cooling circuit of gas cooled nuclear power plant can be separated from radioactive impurities by passing through a Pd-alloy film [40].
- (iv) Palladium on a ceramic granular material is incorporated in nuclear reactor for hydrogen mitigation (hydrogen oxygen recombination) during core-melt accident [41, 42].

- (v) Tritium can be separated from liquid Li in a thermonuclear power plant by transfer through a niobium “window” into a helium stream at 980⁰C. The window is protected from oxygen attack on the He side by an electrolytically deposited Pd layer (0.001cm) [43, 44].
- (vi) Hydrogen isotopes can be removed from fission and fusion liquid coolants by “pumping” against a partial pressure drop. A gas containing hydrogen isotopes as impurities is kept in a vacuum (10⁻⁸ Pa) or a reducing atmosphere on the lower concentration side and hydrogen isotope are permeated through a Pd or Pd-Ag diaphragm [45] or a Pd-coated Zr membrane [46] into an oxidizing atmosphere on the higher concentration side.
- (vii) For separation of hydrogen isotopes in thermonuclear devices, Pd-Pt (8 at. % Pt) alloy on some adsorbent like Kieselguhr or alumina have been used at pilot plant scale [47, 48].
- (viii) Palladium- coated Ta was tested for removal of hydrogen for reactor casing [49]. Such type of apparatus can be used in hydrogen handling and protection against excessive pressure in boiling water reactor casings.

1.5.3. Waste Management

Some of the applications where palladium can be used in solidification of waste are:

- (i) Ti-0.2Pd alloy can be a prospective material for the construction of containers for solid high level radioactive wastes, which are to be disposed in a rock salt depository. The passive layers of the material are adequately resistant to gamma radiation when it is in contact with salt brine [50].
- (ii) Palladium can be used for immobilization of long lived fission products like ¹²⁹I and trivalent actinides [51]. Such matrices have shown very high stabilities and have the

added advantage that these will require simple processing after irradiation (transmutation).

From above discussion it is clear that palladium recovered from nuclear spent fuel could readily find applications in nuclear technology. It is worthwhile to mention that the associated radioactivity of one its isotope, namely, ^{107}Pd tends to restrict its use in public domain. However, the possible separation of the radioactive isotope by laser enrichment technique would enable us to reconsider its use. Moreover, since platinum group metals tend to form separate phases during vitrification of HLLW, their presence in it will tend to destabilize the latter thereby causing concern among waste management practices [52]. Thus, it becomes desirable to separate palladium prior to vitrification. The separation and recovery of palladium from spent nuclear fuel is therefore an attractive option in terms of effective waste management and future applications as evidenced by various reviews [53-55]. These reviews have not only broadened the understanding of various problems associated with palladium recovery from spent nuclear fuel but also elaborated the various applications where the recovered palladium will find its use. In fact, these reviews have provided the much needed impetus to again look upon the problem of separation and recovery of palladium from spent nuclear fuel.

Designing the scheme for palladium separation from spent nuclear fuel necessitates the knowledge of the states in which palladium can exist during fuel irradiation as well as various stages of spent fuel reprocessing. Though, it is difficult to perform the chemical analysis of the irradiated fuel, various reports containing the detailed examination of irradiated fuel from different types of power reactors at the micro level have shown that platinum group metals generally form part of intermetallic inclusions, forming an independent phase in irradiated fuel [56, 57], wherein the compounds of Rh and Pd with actinides, $(\text{U}_{1-x}\text{Pu}_x)$ $(\text{Rh}_{1-y}\text{Pd}_y)$ and $(\text{U}_x\text{Pu}_{1-x})$ $(\text{Rh}_y\text{Pd}_{1-y})$, with AuCu_3 structure were

detected. Palladium was also detected in compounds of Pd-Ag-Cd and Pd-Sn-Sb-Te, with the latter containing two phases with the following fixed composition (wt %): Pd-81, Sn-9, Sb-2, Te-8 and Pd-69, Sn-3, Sb-4, Te-24. The central cavity of the fuel elements and the core surface has been found to contain compounds of type $\text{Pu}(\text{Pd}, \text{In}, \text{Sn}, \text{Te})_{3-x}$.

During reprocessing, the irradiated (spent) fuel undergoes decladding, chopping and dissolution in nitric acid medium, wherein, palladium along with other fission products was found to be distributed between two streams, namely, the dissolver solution and the undissolved residue, known as high level solid waste (HLSW). The exact proportion of palladium in the above two streams, of course, is dictated by its physico-chemical state in the fuel (metal, alloy, or oxide) and the various conditions followed during the dissolution. The dissolver solution, after acidity adjustment, is reprocessed to obtain pure uranium and plutonium (PUREX Process), wherein, palladium along with other fission products and actinides goes into the raffinate, known as high level liquid waste (HLLW). Various methods have been proposed to recover palladium from above two streams. Some of the most prominent ones are discussed below.

1.7. Recovery of palladium from High Level Solid Waste (HLSW) arising from dissolution of spent nuclear fuel

Platinum group metals (PGMs) occur in the fuel as metal alloys with actinide or fuel elements. Depending upon the nature of alloy, these are either insoluble or partly soluble in nitric acid medium. Among the PGMs, palladium appears in insoluble residue with lowest proportion. Palladium enters into the composition of a Ru-based alloy (ϵ phase) which is poorly soluble in nitric acid [36]. Recovery of palladium from insoluble residues (HLSW) is normally carried out by non-aqueous processing methods. The process involves separation by liquid-liquid partitioning of PGM between two immiscible liquid metals [58-61]. Several liquid metal extraction and partitioning systems have been

reported which give the required separation of ruthenium, rhodium and palladium [62, 63]. The dissolver residue is treated with liquid magnesium at temperature up to 950°C. Liquid magnesium extracts Ru, Rh, Pd as well as Cd. Separation of Ru and Pd can be carried out by contacting magnesium melt with U-Cr eutectic which extracts Ru. Another non-aqueous process [64] using lead oxide, graphite and sodium carbonate at 1050°C has been reported. The resultant lead metal extracts more than 94% palladium, 88% technetium and 48% rhodium. The lead extraction method has been tried for the recovery of Ru-Rh from the waste [65]. Another process using liquid lead as scavenger for noble metals has been reported [66] for the recovery of noble metals from insoluble residue of spent fuel, prior to vitrification.

These methods have the following advantages;

- (i) Liquid metal systems display higher radiation stability than aqueous solutions or organic compounds during extraction process.
- (ii) Since the process streams have smaller volume than in hydrometallurgy, the operations can be performed in compact equipment.

However, the non-aqueous processes have the disadvantages, such as,

- (i) Requirement of high temperature, which can cause volatilization of metal and thereby putting constrains on the container material.
- (ii) Discontinuous nature of many of the operations and the difficulty in achieving continuous operations.

1.8. Recovery of palladium from High Level Liquid Waste (HLLW) solution arising from PUREX process raffinate

It has been established that during spent fuel dissolution, majority of fission palladium goes into the nitric acid solution along with other fission products and actinides. Generally, Palladium occurs in divalent state as Pd(II) in PUREX process raffinate.

However, the exact composition of various palladium species that may occur will depend upon the redox conditions as well as the acidity of the PUREX process raffinate. Various strategies have been followed exploiting different properties of palladium to recover it from HLW. Some of the prominent ones are described below:

1.8.1. Precipitation

Precipitation procedures require simple equipment and can yield high-purity palladium. However, since this is a discontinuous process, its applicability on large scale poses some difficulties especially increase of amorphous precipitates like hydroxides are to be encountered. Such separation is much less complete than conventional ion exchange and liquid-liquid extraction. A considerable amount of the liquid phase may be occluded by the precipitate, and this makes it difficult to wash out solutes that are required to remain in the supernatant. Judicial use of highly selective precipitation reactions may overcome some of the above disadvantages. Some of the most important precipitants are as under:

- (i) Formic acid used for denitration of HLLW can precipitate platinum group elements in the metallic forms as Pd, Rh and Ru, the purity achieved during this precipitation is reported to be high [67].
- (ii) Palladium is also precipitated as $\text{Pd}_{1.1}\text{C}_{2.1}\text{H}_{4.1}\text{N}_2\text{O}$ in the partial denitration of the HLLW by sucrose at reflux temperature of 50°C [68].
- (iii) Trichlorostannate can be used to precipitate palladium from HLLW. The complex formed is $[\text{PdCl}(\text{SnCl}_3)_3]^{2-}$ which can be precipitated from the solution with CsCl and Et_3NHCl . The recovery is almost 100 %. However, this method is now considered unacceptable [69].
- (iv) Sodium salt of dimethylglyoxime (Na_2DMG) can be used to precipitate palladium from HLLW. Thus, 0.1% of Na_2DMG has been used to recover palladium, the precipitation being almost quantitative below 2.0 M nitric acid [70]. The precipitation

decreases with increasing acidity. High decontamination factor was achieved with respect to some of the metal ions present in HLLW. However, the addition of sodium salt would inevitably increase the solid waste volume which is most undesirable from the view point of waste management.

(v) Palladium can be precipitated from nitric acid medium using hydrazine or CO [71].

Reaction of palladium with hydrazine yields a white precipitate of $[\text{Pd}(\text{N}_2\text{H}_4)_2](\text{NO}_3)_2 \cdot x\text{H}_2\text{O}$, which decomposes to form Pd metal. From 0.9 to 3.0 M HNO_3 , 50 to 90% of palladium was precipitated at room temperature. Although palladium is efficiently recovered by this method, the presence of excess hydrazine and its oxidation products prevents the use of this method in industrial processing of HLLW.

(vi) At low concentration of HNO_3 , CO reduces palladium to the metal. However, it does not precipitate palladium from 2-4 M nitric acid because of high solubility of Pd in HNO_3 . This problem can be circumvented by adding H_2O_2 , KMnO_4 , N_2H_4 or sulfamic acid, which can decompose HNO_2 present in equilibrium with HNO_3 , the former being responsible for oxidation of palladium metal back to solution [72]. The decontamination factors achieved with this method are high for rare earth elements and other fission products except Ru and Sb.

1.8.2. Electrochemical Reduction

Electrochemical method for the separation and recovery of palladium is one of the easy and promising techniques due to its simplicity and accessibility of reduction potential of palladium in nitric acid medium. Pd was deposited from a simulated HLW onto a Pt electrode at a potential of -0.2 to 0.1 V (vs. SCE) and a current density of 8-70 mA cm^{-2} [73]. However, the deposition rates are found to decrease with increase in feed acidity [74]. Several other complications occurred in the presence of interfering elements of

HLLW such as Ag, Fe, NO_3^- , etc. during electrolysis [75]. Due to this, the recovery and Faraday efficiency was found to be below 40%. Thus, this method can only be applied in combination with an efficient separation method for selective recovery of palladium. For example, electrodeposition of palladium from aliquat-336, after extraction from nitric acid medium has shown effective recoveries [76].

1.8.3. Ion Exchange and Sorption

Ion exchange has been frequently applied in radiochemical process for treating highly radioactive solutions. However, it is less useful than liquid-liquid extraction owing to its discontinuous nature and limited throughput, despite the possibility of a quasi-continuous operation mode. However, unlike liquid – liquid extraction there are no problems of third phase formation and compatibility issues with the diluent. Conventionally the distribution ratio (D_M) is defined as:

$$D_M = \frac{[M]_r \cdot V}{[M]_{aq} \cdot W} \quad (1)$$

Here, $[M]_r$ is the metal ion concentration loaded on the resin and $[M]_{aq}$ is the metal ion concentration left in the aqueous phase, V is the volume (in ml) of the solution and W is the mass (in g) of ion exchanger.

The most prominent ion exchangers and sorbents studied for palladium recovery from HLW are as under:

(i) Anion exchangers: Most of the sorbents proposed for palladium recovery from HLLW are based on the fact that at higher nitric acid/nitrate ion concentrations (≥ 3.0 M), palladium generally exists as $\text{Pd}(\text{NO}_3)_3^-$ or $\text{Pd}(\text{NO}_3)_4^{2-}$ [77] and therefore, anion exchanger can be used for this purpose. In view of the acidity of HLLW between 1.0 to 4.0 M HNO_3 , the, discussion is made only at those acidities. Thus, with 4-(*N,N*-dimethyl benzimidazole) phenyl (AR-01), very high distribution ratio of palladium was achieved at

lower HNO_3 concentrations. [78]. However, the exchange is so slow that equilibrium is attained only after 20 hours of contact at 60°C . For other anion exchangers like tertiary Amberlite IRA-93ZU and quaternary Amberlite IRA-900, Amberlite IRN-78, Dowex 1X8-400 and Dowex 2X8-400, sorption of palladium is less effective with the disadvantage that equilibrium is achieved after 1 hour at 60°C [78]. It was observed that thiourea can back extract palladium from loaded resin and therefore ensure the re-use of the resin. The strongly basic resin AV-17X8 gives distribution ratio of 64, 56 and 200 for Pd(II) at acidities of 0.5, 3.0 and 8.0 M HNO_3 respectively [78]. Similarly, a strongly basic pyridinium anion exchanger (VP-1AP) gives D_{Pd} values of 64, 77 and 35 for the same acidities respectively [78]. A stronger affinity to Pd(II) is exhibited by a weakly basic anion exchanger (AN-104), which yields $D_{\text{Pd}} = 475, 350$ and 120, respectively, and especially, by a strongly basic phosphonium anion exchanger (KhFO) which yields $D_{\text{Pd}} = 900, 500$ and 200, respectively [79]. Extraction of palladium using imidazolium nitrate anchored groups onto polystyrene-divinylbenzene matrix, have shown fairly good extraction efficiency with $D_{\text{Pd}} \sim 140$ at 3.0 M nitric acid [80].

Since HLLW solutions essentially maintain acidity between 1.0 to 4.0 M HNO_3 , therefore, the anion exchange resin can only be used effectively for solutions with acidity ≥ 3.0 M HNO_3 . For low acidic solutions, effective recovery of Pd can be achieved by adding nitrate ion, preferably salts whose presence does not interfere in further processing of waste.

(ii) Cation Exchangers: Speciation data of Pd in nitric acid medium show that it exists as Pd^{2+} and $\text{Pd}(\text{NO}_3)^+$ at lower acidities (0.5 M to 3.0 M) [77]. Hence, cation exchange resins can also be used for its recovery from such mild acidic solutions. Some of the cation exchangers proposed for palladium sorption include sulfonic acid resin KU-2X8 and phosphoric acid resin KRF-20t-60 the latter gives $D_{\text{Pd}} \sim 9$ at 3.0 M nitric acid [79]. Amino

carboxylic resins, namely VPK, ANKB-2, ANKB-35 and MS-50 have been shown to sorb palladium effectively from 3.0 M nitric acid with distribution ratio 850, 350, 150 and 160 respectively. Another chelating amide oxime exchanger CS-346 was found to sorb Pd (II) well from 0.5 to 3.0 M HNO₃. Also, macroporous silica based anion exchanger containing either pyridine or methyl pyridine functional group have been reported to efficiently sorb palladium ($D_{Pd} \sim 10^2$) at 3.0 M nitric acid concentration [81].

(iii) Active Carbon: Palladium was found to be strongly sorbed on active carbon; both from the highly acidic as well as alkaline media [82]. However, the co-extraction of other fission products makes this method unsuitable for Pd separation from HLLW.

(iv) Chemically modified cedar wood powder: Tertiary amine grafted cedar wood powder showed almost complete sorption of palladium from 0.1 M nitric acid medium, with the sorption decreasing gradually with increase in nitric acid concentration. Thus, at 3.0 M HNO₃, about 60% of palladium is sorbed with almost no uptake of other fission platinum group metals [83]. However, dissolution of parts of the absorbent in highly active HLLW may create problems during further processing.

(v) Extractant immobilized resins: Various extractants have been immobilized on to different solid supports and studied for their extraction behavior for palladium. Thus, bis-(2,4,4-trimethylpentyl)-monothiophosphinic acid (Cyanex-302) encapsulated in microcapsules of Ca alginate gel shows high D_{Pd} of the order of 10^4 from 0.2 to 0.5 M HNO₃ [84]. However, the kinetics of extraction is so slow that the equilibrium is attained only after 3 days. Similarly, tri-isobutyl phosphine sulphide (Cyanex-471X) impregnated on chromosorb-102 gives D_{Pd} of the order of 10^3 within 45 minutes with the complete back extraction in thiourea [85]. Palladium has also been separated using dithiooxamide functionalized resin. However, uptake was found to decrease with increasing acidity, with

the uptake being maximum ($D_{Pd} \sim 80$) at pH~6.0 [86]. Therefore, its use in acidic medium is highly improbable.

Although very efficient extraction and selectivity has been achieved for palladium using these extractant immobilized resins, their stability in terms of leaching out of the extractant from the resin restricts their use.

1.8.4. Solvent Extraction

Solvent extraction, in conventional liquid – liquid form, is the most practicable method used today for partitioning. Important experience has been gained from its use in large scale nuclear separations and from decades of industrial operation of the PUREX process. Extractant proposed for separation of palladium from HLLW should meet the following important criteria:

- (i) The Extractant should be highly selective for palladium; otherwise additional steps will be required to further separate it from co-extracted metal ions which would increase additional waste volumes.
- (ii) The Extractant should show appreciable uptake of palladium so that minimum possible extraction steps will suffice to recover palladium quantitatively.
- (iii) Back extraction of palladium from loaded organic solvent should be easily achievable so that the extractant can be recycled.
- (iv) The Extractant should have sufficient solubility in normal paraffinic diluents like n-dodecane.
- (v) It should be sufficiently stable in nitric acid as well as in radiation environment.
- (vi) It should have high flash and boiling point.
- (vii) It should be easily available on large scale and at low cost.

For liquid - liquid extraction system, the uptake of metal ion is conventionally expressed in terms of distribution ratio (D_M) and Percentage extraction (% E) while the selectivity for a metal ion is presented in terms of separation factor. These terms are defined as

$$\text{Distribution Ratio } (D_M) = [M]_{\text{org.}} / [M]_{\text{raff.}} \quad (2)$$

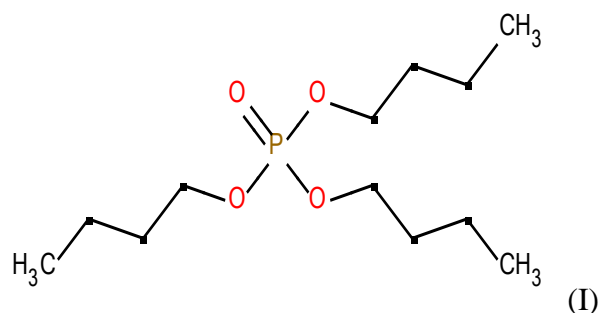
$$\% \text{ Extraction } (\% E) = D_M / (D_M + 1) \text{ \{for equal vol. of org. and aq. phase\}} \quad (3)$$

$$\text{Separation factor } (SF) = D_{Pd} / D_M \quad (4)$$

Various extractants have been proposed for palladium separation from HLW, which can be further categorized as follows:

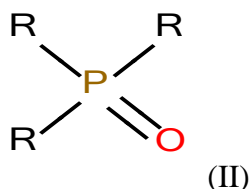
1.8.4.1. Hard donor extractants

(i) **Tributyl phosphate (TBP) (I):** Pd can be extracted with 100% TBP from 0.1–1.0 M HNO_3 with the distribution ratio (D_{Pd}) of 0.6-1.0, whereas, from 4.0 M virtually no Pd is extracted. D_{Pd} was found to decrease with increase in nitric acid concentration. The maximum D_{Pd} was achieved in the acidity range of 0.4 M to 0.8 M, with the extractable species proposed as $\text{Pd}(\text{NO}_3)_2 \cdot 2\text{TBP}$ [87, 88]. However, with such high concentrations of TBP, co-extraction of other actinides and fission products becomes inevitable, thereby restricting its use. Also, the associated hydrodynamic problems with such concentrated extractant make this process highly impractical.



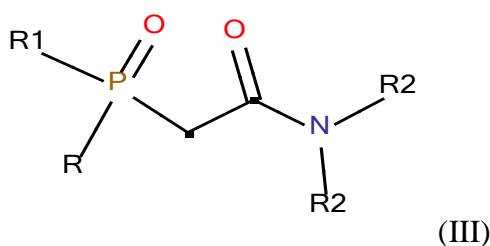
(ii) **Trialkyl phosphine oxide (TRPO) (II):** It is generally known that for organophosphorus class of extractants, the extractability of metal ion increases in the following order: Organophosphate < Organophosphonate < Organophosphine oxide. Based on this trend trialkylphosphine oxides have been studied for effective removal of

Palladium. TRPO(R = butyl, isoamyl or octyl) in benzene diluent extracts Pd(II) nitrate from 0.2 to 4.0 M nitric acid more effectively than TBP. With 0.04 M TOPO in aromatic diluent, D_{Pd} obtained was 2.5 at 0.1 M nitric acid [89]. However, the extraction is highly suppressed by increase in nitric acid concentration and could be of importance only at ≤ 1.0 M HNO_3 .



Where R = butyl, isoamyl or octyl

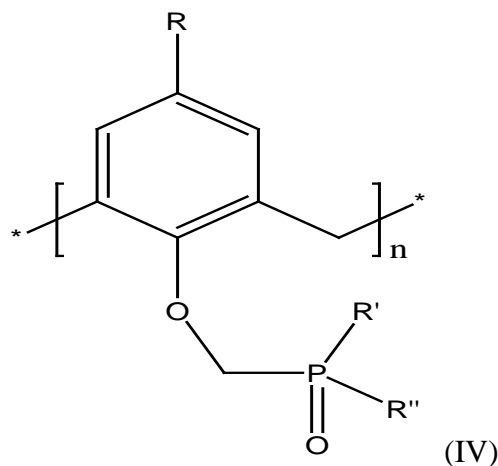
(iii) Carbamoyl methylphosphine oxide (CMPO) (III): Bidentate neutral extractant namely Alkyl(Phenyl)-*N,N*-diisobutylcarbamoyl methylphosphine oxide (CMPO-1) and diphenyl-*N,N*-diisobutylcarbamoyl methylphosphine oxide (CMPO-2) in polar diluent *m*-nitrobenzotrifluoride (NBTF), have shown effective Pd extraction at lower nitric acid concentrations [90]. At 0.1 M HNO_3 , D_{Pd} for 0.2 M CMPO-1/NBTF and 0.2 M CMPO-2/NBTF are 2.1 and 3.6 respectively which decrease to 0.46 and 1.9 respectively at 2.0 M HNO_3 . However, on further increasing the acid concentration, D_{Pd} decreased drastically which makes these extractants unsuitable for the purpose.



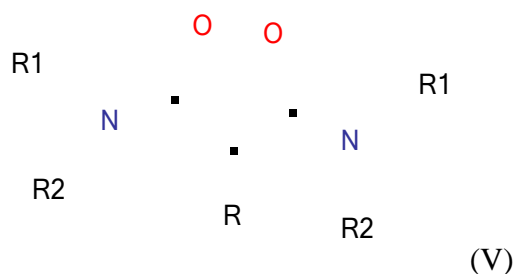
Where R=phenyl, R1=alkyl or phenyl and R2-isobutyl

(iv) Phosphorylated Calixarenes (IV): Calixarenes with donor phosphoryl group, attached to their rigid platform, can be used as effective extractants for palladium at lower acidities. Thus, 0.01 M CIP-67 in NBTF (*m*-nitrobenzotrifluoride) showed $D_{Pd} = 3.0$ and

0.17 at 0.1 and 3.0 M HNO₃ respectively [91]. However, very low distribution ratio at 3.0 M HNO₃ makes this option unattractive. Further, the detailed extraction studies of various other metal ions present in HLLW have still not been reported.

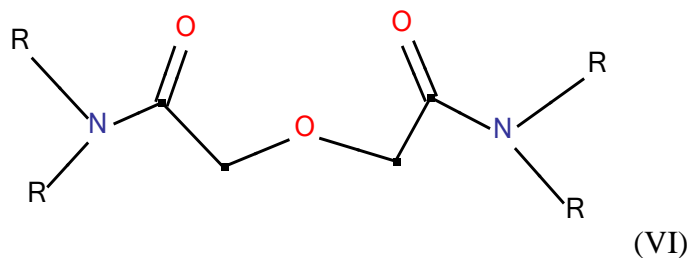


(v) **Malonamides (V):** *N,N'*-dimethyl-*N,N'*-dibutyl-2-tetradecylmalonamide (DMDBTD-MA) in branched alkane diluent gave appreciable D_{Pd} in 2.0 M HNO₃ [92]. However, co-extraction of other fission products makes this option improbable.



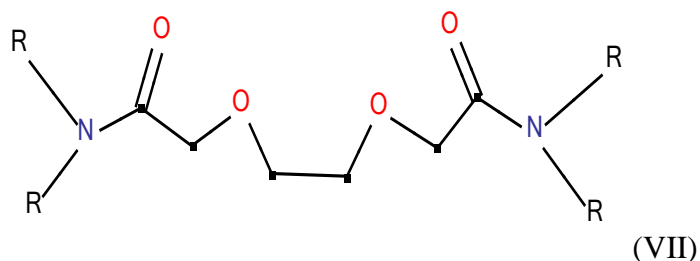
Where R1=methyl, R2=butyl and R=tetradecyl

(vi) **Diglycolamides (VI) and Dioxodiamides (VII):** Tridentate neutral ligands can be used for Pd extraction from nitric acid medium. At 3.0 M HNO₃, D_{Pd} of ~3 was obtained for 0.1 M *N,N,N',N'*-tetraoctyldiglycolamide (TODGA) (VI) in n-dodecane [93]. This can be increased to 10 with 1.0 M TODGA/n-dodecane. However, the co-extraction of other fission products along with palladium restricts its use.



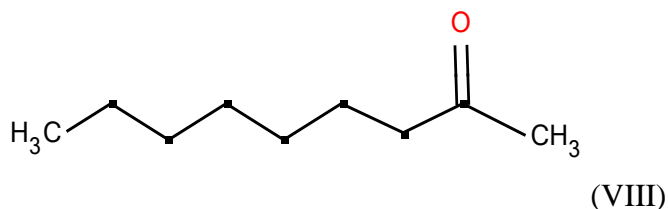
Where R=octyl

On the other hand, tetradentate ligand namely *N,N,N',N'*-tetraoctyl-3,6-dioxo-1,8-diamide (DOODA) (VII) has shown lower D_{Pd} for 0.1M DOODA/n-dodecane from nitric acid medium [94].



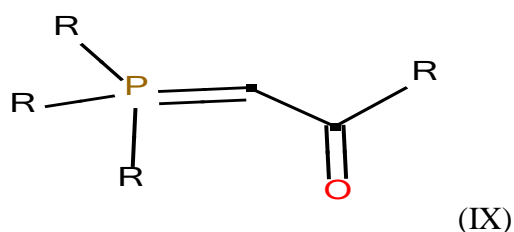
Where R =octyl

(vii) Ketones: Various higher ketones, when dissolved in nitrobenzene, extract palladium from nitric acid medium. With 1.0 M solution of 2-nonanone (VIII) in nitrobenzene D_{Pd} of 5.0 at 2.0 M nitric acid concentration was observed [95]. The extraction was found to increase with increase in nitric acid concentration and finally become constant. However, the use of hazardous nitrobenzene on commercial scale remains problematic.



(viii) Benzoylmethylene triphenylphosphorane (BMTTP) (IX): These phosphorous ylides form stable complexes with palladium. Depending on the conditions prevailing during extraction, different resonant forms of ylides exist which decides the mechanism of

extraction. At higher nitric acid concentration, they exist as quarternary salts which act as anionic exchangers and therefore palladium is extracted as $\text{Pd}(\text{NO}_3)_3^-$ or $\text{Pd}(\text{NO}_3)_4^{2-}$. Thus, 0.05 M BMTTPP (IX) in CHCl_3 showed D_{Pd} of 4.0 at 3.0 M nitric acid concentration, which decreases gradually on further increasing the nitric acid concentration [96]. However, the slow kinetics of extraction as well as limited solubility only in halogenated diluents restricts its use.



Where R = phenyl

From the above discussion, it is evident that extractants with hard donor atoms possess very low extraction capacity for Pd at nitric acid concentrations (~3.0 M) that generally prevail during reprocessing of HLLW. Also, when these extractants are used in higher concentrations in order to get appreciable extraction for palladium, co-extraction of other fission products is generally observed. It is to be noted that since most of the above extractants have been initially designed for other purposes in nuclear fuel reprocessing, therefore, they do not meet the essential criteria for Pd extraction.

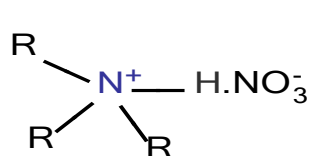
1.8.4.2. Soft donor extractants

Palladium being a soft acid will form stronger complexes with ligands having soft donor atoms like 'N' and 'S'. Among the several 'N' and 'S' donor ligands developed for Pd extraction, the most studied ones are described below:

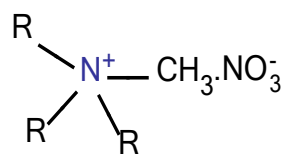
(a) Extractants with 'N' donor atom

(i) **Amines (X) and Quaternary ammonium compounds (XI):** Palladium extraction with amines and quaternary ammonium compounds has been studied in detail at various

laboratories. Both the type of extractants usually work effectively at lower nitric acid concentrations (up to 1.0 M). However, in both cases, D_{Pd} was found to decrease with increase of acidity. For instance, 0.5 M Trioctyl amine (TOA) dissolved in benzene showed D_{Pd} of 2.3 and 0.11 at 3.0 M and 8.0 M nitric acid respectively [97]. Similar concentrations of Tricaprylmethyl ammonium nitrate (Aliquat 336 nitrate) showed D_{Pd} of 18 & 0.3 at 3.0 M and 8.0 M nitric acid respectively. It was proposed that effective extraction at 3.0 M nitric acid and stripping at 6-8 M nitric acid would suffice to recover palladium from HLLW [97]. However, co-extraction of some fission products has also been reported [98]. Furthermore, the stability of these extractants in radiation environment has been found to be reasonable [99], thus showing promise for their use in actual HLLW. However, very low extraction capacity for palladium was observed when normal paraffinic diluents like n-dodecane were used in place of aromatic diluents like benzene, toluene, etc. Since commercial scale use of aromatic diluents in processing of HLLW is still being debated, the use of these extractants for the said purpose becomes doubtful.



(X),

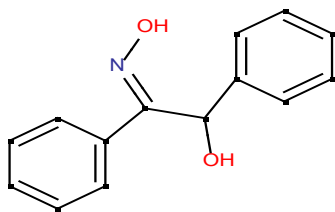


(XI)

Where R=octyl

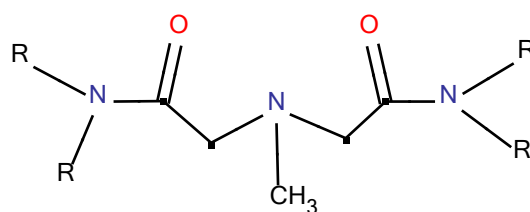
(ii) Benzoin oxime (XII): Oximes have been known for their preferential ligation with soft metals. However, very few studies have been reported involving these extractants for extraction of palladium from nitric acid medium. Recently, Benzoin oxime (XII) has been extensively studied for palladium extraction from HLLW [100]. With 0.0001M α -benzoin oxime dissolved in solvesso-100 (aromatic diluent), D_{Pd} of 1.7 was obtained from 2.0 M nitric acid medium, indicating that appreciable extraction of palladium can be achieved

with higher concentration of α -benzoin oxime for application in actual HLLW. However, the co-extraction of other fission products and use of aromatic diluents can restrict its use.



(XII)

(iii) (Methylimino) bis (N,N-dioctylacetamide) MIDO A: Tridentate extractant having appropriately placed tertiary amine and amide moieties have recently been reported to give high extraction capacity for palladium even at higher nitric acid concentrations. With 0.1 M MIDO A (XIII) dissolved in n-dodecane, $D_{Pd}=10$ was observed from 3.0 M nitric acid medium [101]. However, the extractant also shows significant uptake of various other metal ions like Tc, Zr and Re etc. Thus, appreciable decontamination factor cannot be achieved for palladium vis a vis other metal ions present in HLLW necessitating further studies to separate palladium from co-extracted fission products.

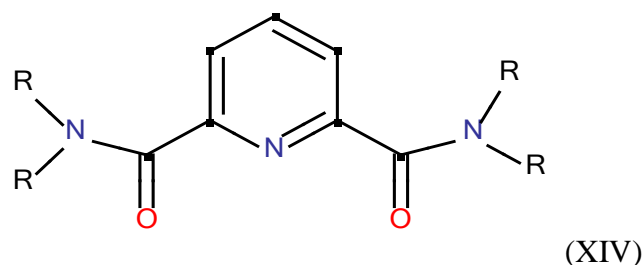


(XIII)

Where R = octyl.

(iv) Dicarboxypyridine diamide (DCPDA): These ligands were initially studied for extraction of trivalent lanthanides and actinides from HLLW. However along with these metal ions, palladium was found to be efficiently extracted. Thus, 0.1 M solution of DCPDA (XIV) in FS-13 (phenyltrifluoromethylsulfone) diluent gave D_{Pd} greater than 100 in 3.0 M nitric acid solutions [102]. However, the co-extraction of other metal

ions still remains a problem with these extractants which may require further separation schemes.

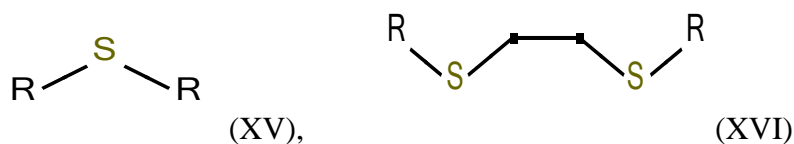


Where R = methyl, phenyl

(b) Extractants with 'S' donor atom

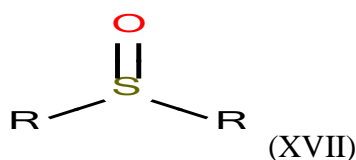
(i) **Dialkyl sulphide:** These extractants have been widely studied for palladium extraction from different acidic media particularly HCl. They exhibit very high extraction efficiency for palladium over other metal ions. For instance, 0.005 M dioctyl sulphide (XV) in solvesso-100 gave D_{Pd} of 13.7 from 3.0 M nitric acid medium [103]. Another homologue namely, dihexyl sulphide (10%(v/v)) in n-dodecane, gave a distribution ratio of palladium of order of 10^3 from 0.1 to 6.0 M nitric acid medium [104]. Further, Dialkyl disulphides (XVI) in aromatic diluents have been reported to show even higher uptake of palladium. For example, dilute solution of Dihexyldithioether (0.001 M) in chloroform gave D_{Pd} of 39 from 1.0 M nitric acid solutions [105].

Though these extractants appear to be very attractive in view of high D_{Pd} values for palladium, their use is severely limited owing to very slow kinetics of extraction and instability in nitric acid medium. Further, these extractants were found to decompose readily in radiation environment.



Where R=hexyl, heptyl, octyl etc.

(ii) Dialkyl sulphoxides: With 0.05 M Dioctyl sulphoxides (DOSO) in solvesso-100, D_{Pd} of 16.5 was achieved from 3.1 M nitric acid solution [103]. However, with branched homologue of the extractant the distribution ratios were found to decrease. D_{Pd} of 3.55 was observed for 0.05 M bis-(2-ethylhexyl) sulphoxide (BESO) (XVII) in toluene. Both the extractants provide appreciable D_{Pd} in simulated HLW conditions. However, the notable co-extraction of other fission products along with actinides poses difficulties in selective separation of palladium from HLLW [106].

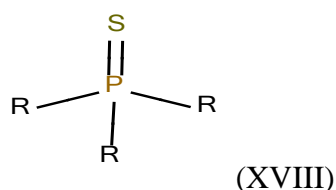


Where R=octyl, 2-ethylhexyl, etc.

(iii) Diesel fuel: It is known to be the cheapest source of sulphide extractant and thus can be used for palladium extraction. Diesel fuel after appropriate treatment with $HNO_3/K_2Cr_2O_7$ and $NaOH/NaNO_3$ solution can be taken as ready to use solvent. When dissolved in mixed paraffin and aromatic diluent, it can extract Pd(II) from 2-3 M HNO_3 with a D_{Pd} of 10-100 [107]. However, their use in palladium recovery from HLLW is questionable in view of the low flash point of diesel fuel. Further, the behavior of sulphur species present in the diesel when exposed to radiation environment has not been studied.

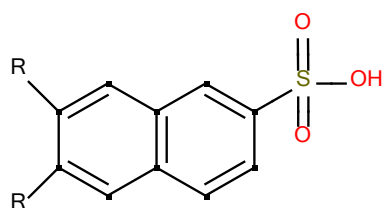
(iv) Triisobutyl phosphine sulphide (TIPS): The extractant has been found to be even more effective than Dialkyl sulphides. For instance, a dilute solution of 0.0001 M TIPS (XVIII) in solvesso-100 extracts palladium with D_{Pd} of 1.4 from 3.0 M nitric acid and equilibrium was attained within 45 minutes [103]. An aromatic homologue, namely, triphenyl phosphine sulphide (0.005M) in benzene shows D_{Pd} of 5.0 at 2.5 M nitric acid

[108]. However, these extractants were found to be insoluble in normal paraffinic diluents. Also, their stability towards oxidation in nitric acid medium remains problematic.

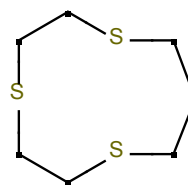


Where R= isobutyl, phenyl

(v) Thiamacrocycles: Thiamacrocycles, particularly 2-octyl-1,4,7-trithiacyclononane (2-octyl-9S3) and 1,4,7-trithiacyclodecane (10S3) (XX) form extractable palladium complexes when used along with dinonyl naphthalene sulfonic acid (HDNNS) (XIX). Thus, with 0.005 M 10S3 and 0.01 M HDNNS, more than 90% extraction of palladium is achieved from 1.0 M nitric acid [109]. However, the extraction decreases drastically at higher nitric acid concentration. Hence, the use of these extractants in separation of palladium from acidic solutions (~3.0 M HNO₃) representing the conditions of HLLW becomes unattractive. Further, their stability in radiation stability has also not been studied.



(XIX),



(XX)

Where R = nonyl

1.9. Motivation for the present work

From above discussion it is evident that separation and recovery of palladium from spent nuclear fuel and especially from HLLW is of prime significance. However, the various

separation methods which are being studied for this purpose, have a number of limitations like low efficiency, slow extraction kinetics, co-extraction of other elements along with palladium, instability in nitric acid medium, solubility in paraffinic diluents etc. In view of this it is important to explore other novel class of ligands for liquid- liquid extraction as well as polymeric sorbents for solid phase extraction of Pd from HLLW.

In the present thesis efforts have been made towards the development of novel class of ligands for liquid-liquid extraction and ligand grafted polymeric resins for solid phase extraction of palladium from HLLW.

Novel class of ligands, namely, *N,N,N',N'*-tetra(2-ethylhexyl) thiodiglycolamide (T(2EH)TDGA) and *N,N,N',N'*-tetra(2-ethylhexyl)dithiodiglycolamide (DTDGA) have been synthesized, characterized and evaluated for extraction of Pd from HLLW. In order to understand the mechanism of uptake of Pd, several techniques like FT-IR, ESI-MS and EXAFS spectroscopy were employed in conjunction with theoretical studies. Further the hydrolytic and radiolytic stability studies were carried out to establish their efficacy at plant scale. Subsequently a flow sheet has been developed for efficient recovery of Pd from HLLW.

Novel class of ligand grafted polymeric resin, namely, 2-acetylpyridine XAD 16 (AP-XAD16) and 2-acetylamine XAD 16 (ACAM-XAD16) have been synthesized, characterized and evaluated for extraction of Pd from HLLW. FT-IR studies have been used to understand the mode of ligation of metal with the ligand grafted resin. Sorption studies were carried out to determine the maximum loading capacity and kinetics parameters.

CHAPTER 2

Synthesis & Characterization of Novel Reagents and Experimental Methodologies

In this chapter, the synthesis and characterization of the two novel ligands, namely, *N,N,N',N'*-tetra-(2-ethylhexyl) thiodiglycolamide (T(2EH)TDGA) & *N,N,N',N'*-tetra-(2-ethylhexyl) dithiodiglycolamide (DTDGA) and the two novel ligand grafted polymeric resin, namely, AP-XAD16 & ACAM-XAD16 resin for separation and recovery of Pd from high level waste (HLLW) solutions has been described. The various experimental methodologies used to evaluate the novel ligands and grafted resins are also described. Subsequently the theoretical and experimental approaches to analyze the species at molecular level are discussed.

2.1. Synthesis and Characterization of ligands and grafted polymeric resins

2.1.1. *N, N, N', N'*-tetra-(2-ethylhexyl)-thiodiglycolamide (T(2EH)TDGA)

2.1.1.1. Synthesis

Synthesis of T(2EH)TDGA has been carried out by the condensation reaction of sodium sulphide nonahydrate with *N,N*-bis-(2-ethylhexyl)-2-chloroacetamide (Fig. 2.1). All chemicals used for this synthesis were of industrially pure grade and used without any further purification. *N,N*-bis-(2-ethylhexyl)-2-chloroacetamide was synthesized according to the procedure described earlier [110]. Approximately 0.05 moles of Na₂S.9H₂O in 200 ml. of ethanol was taken in a 500 ml three necked round bottom flask fitted with reflux condenser. To this 0.1 mole of *N,N*-bis-(2-ethylhexyl)-2-chloroacetamide in 100 ml. of ethanol was added in one lot. The reaction mixture was stirred for 8 hrs without heating and then the temperature was raised to 50-60°C and stirring was continued for another 12 hrs. After cooling, the reaction mixture was filtered off to remove the solid and evacuated

to one third of the original volume. To the residue pure hexane was added and the organic phase was washed with dil. HCl (5%v/v) and subsequently by 5% w/v Na₂CO₃. The organic phase was finally washed with water to neutral pH. After drying over anhydrous sodium sulphate the solvent was concentrated at 60 °C and 0.01 mmHg pressure. The product purity was found to be ≥ 98% with ≥ 85% yield.

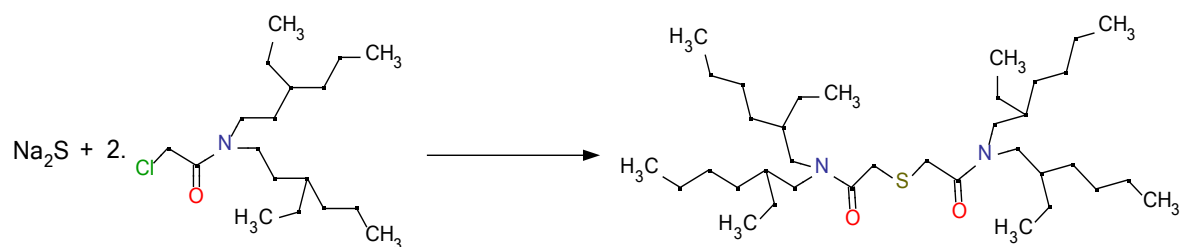


Fig. 2.1. Reaction Scheme for T(2EH)TDGA

2.1.1.2. Characterization

The product has been characterized using Elemental Analysis, GC-MS and ¹H-NMR techniques.

Elemental analysis was performed on CHNS-O Analyzer (FLASHEA 1112 SERIES, THERMO). The method is based on the combustion of the sample in a furnace followed by the assay of the evolved gases by thermal conductivity detector. The furnace temperature was kept at 900 °C while the oven temperature was 60 °C. The conditions of the gas flow of a typical run were: Carrier: 140 ml/min; oxygen: 300 ml/min and reference: 100 ml/min. The quantitative analysis of the gaseous components formed after combustion was done using Thermal Conductivity Detector (TCD) using BBOT as standard. Table 2.1 shows the elemental analysis results of the product. The table shows the closeness of the calculated and the experimental data showing the overall good purity of the product.

Table 2.1. Elemental analysis of T(2EH)TDGA

Element	Calculated (%)	Experimental (%)
Carbon	72.48	71.95
Hydrogen	12.08	12.01
Nitrogen	4.69	4.78
Sulphur	5.36	5.64
Oxygen	5.36	5.59

GC-MS analysis was performed on Shimadzu GCMS QP 2010 Plus instrument with a single quadrupole mass spectrometer at 70 eV using 15 m×0.25 mm DB5 fused silica capillary column. Helium was used as the carrier gas and temperature program was: 40 °C for 2 min, increased to 300 °C at 10 °C/min and held at 300 °C for 50 to 80 min. The injector temperature was 300 °C. The interface temperature and the ion source temperature were kept at 300 and 200 °C, respectively. Table 2.2 shows the GC-MS data of the product. The data shows the purity of the product ~ 98.4% along with some impurities albeit in very less amount.

Table 2.2. GC-MS data of T(2EH)TDGA

Retention time (min.)	Percentage composition	Component	EI-MS (m/z)
21.45	0.30	$(C_8H_{17})_2NCH_2C(O)N(C_8H_{17})_2$	71, 86, 142, 184(bp), 244, 268, 314, 356, 439, 484, 522(M ⁺)
22.47	0.72	$(C_8H_{17})_2NC(O)CH_2CH_2C(O)N(C_8H_{17})_2$	71, 98, 142, 240, 268, 322(bp), 365, 421, 463, 563(M-1) ⁺
24.94	98.38	$S[CH_2C(O)N(C_8H_{17})_2]_2$	71,86, 142, 184(bp), 240, 268, 328, 356, 485, 553, 597 (M+1) ⁺
28.50	1.11	$S_2[CH_2C(O)N(C_8H_{17})_2]_2$	71(bp), 100, 142, 184, 240, 268, 328, 356, 463, 485, 597, 628 (M ⁺)

M⁺: molecular peak, bp: base peak

The $^1\text{H-NMR}$ spectra (Table 2.3) were recorded in CDCl_3 medium using Bruker 200 MHz instrument using TMS (tetramethyl silane) as an internal standard.

Table 2.3. $^1\text{H-NMR}$ of T(2EH)TDGA

δ Value (ppm)	Proton type
0.92-0.95	multiplet, 24H
1.2-1.3	multiplet, 32H
1.34-1.44	multiplet, 4H
2.95	singlet, 4H
3.18	doublet, 4H
3.35	multiplet, 4H
3.37	singlet, 4H

2.1.2. *N, N, N', N'*-tetra-(2-ethylhexyl)-dithiodiglycolamide (DTDGA)

2.1.2.1. Synthesis

KOH (2.8 g, 0.05 moles) was added to 50 ml of MeOH in three necked round bottom flask fitted with air condenser. 1,2-ethane-dithiol (2.35 g, 0.025 moles) dissolved in 50 ml MeOH was added to this mixture in one lot and stirred for 30 minutes. To the stirred solution was added in a dropwise fashion, 15.85 g (0.05 moles) of *N,N*-2-ethylhexyl-2-chloroacetamide dissolved in 100 ml MeOH. The reaction mixture was stirred for 12 hrs at room temperature followed by stirring for 8 hrs at 40 $^{\circ}\text{C}$. The resulting solution was filtered and evacuated to remove the solvent. Hexane was added to the residue and resulting organic solution was successively washed with 0.5 M HCl, 2.5 wt% Na_2CO_3 solution and water, and then dried over anhydrous Na_2SO_4 . This was then concentrated in vacuum (0.01 mmHg) at 60 $^{\circ}\text{C}$ to give DTDGA with 99.2% purity and 95% yield.

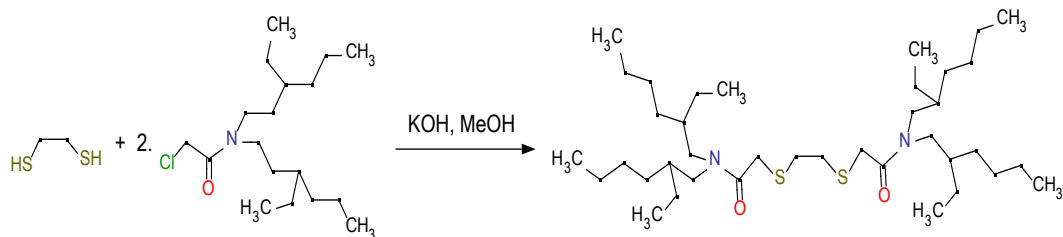


Fig. 2.2. Reaction Scheme for DTDGA

2.1.2.2. Characterization

The product has been characterized using Elemental Analysis (Table 2.4), GC-MS (Table 2.5) and $^1\text{H-NMR}$ (Table 2.6) techniques.

Table 2.4. Elemental analysis of DTDGA

Element	Calculated (%)	Experimental (%)
Carbon	69.45	69.48
Hydrogen	11.65	11.69
Nitrogen	4.26	3.89
Sulphur	9.76	9.77
Oxygen	4.87	5.17

Table 2.5. GC-MS of DTDGA

Retention Time (min.)	Percentage composition	Component	EI-MS (m/z)
23.11	0.89	HS-CH ₂ -CH ₂ -S-CH ₂ -C(O)-N(C ₈ H ₁₇) ₂	69, 71, 142, 184(bp), 268, 342, 375 (M ⁺)
49.58	99.11	(C ₈ H ₁₇) ₂ N-C(O)-CH ₂ -S-CH ₂ -CH ₂ -S-CH ₂ -C(O)-N(C ₈ H ₁₇) ₂ .	71, 142, 184, 268, 342 (bp), 374, 657 (M+1) ⁺

⁺ : molecular peak, bp: base peak

Table 2.6. ¹H-NMR of DTDGA.

δ Value (ppm)	Proton type
0.92-0.95	multiplet, 24H
1.2-1.3	multiplet, 32H
1.34-1.44	multiplet, 4H
2.95	singlet, 4H
3.18	doublet, 4H
3.35	multiplet, 4H
3.37	singlet, 4H

2.1.3. 2-Acetyl pyridine group functionalized Amberlite XAD-16 resin

(i) Synthesis

(a) Acetylation of Amberlite XAD-16

Acetylation of Amberlite XAD-16 was carried out as per the procedure reported earlier [111]. The resin was washed successively with HCl, Na₂CO₃ solution and deionized water, and then dried at 110⁰C for 2 h. About 8 g of it was taken in 250 ml flat bottom flask, anhydrous AlCl₃ dissolved in 40 ml of 1,2-dichloroethane and 16.0 ml of acetyl chloride, were added slowly along the sides of the flask. Anhydrous CaCl₂ drying tube was attached and kept for 10 h with stirring. Thereafter, the reaction mixture was poured into an ice-HCl mixture. The acetylated resin was filtered, washed repeatedly with methanol, water, HCl and dried (Fig. 2.3).

(b) Preparation of acetyl pyridine functionalized resin

Sodium hydride (8.0 g) and 60.0 ml of dry dimethyl formamide (DMF) were added to dried acetylated Amberlite XAD-16 and stirred for 2.0 hrs. 2-chloro pyridine (8.0 g) dissolved in DMF was added to the above solution and stirred for 8 hrs at ambient conditions. The resulting 2-acetyl pyridine functionalized Amberlite XAD-16 (AP-XAD 16 resin) beads were filtered, washed with excess of water and air dried (Fig. 2.3).

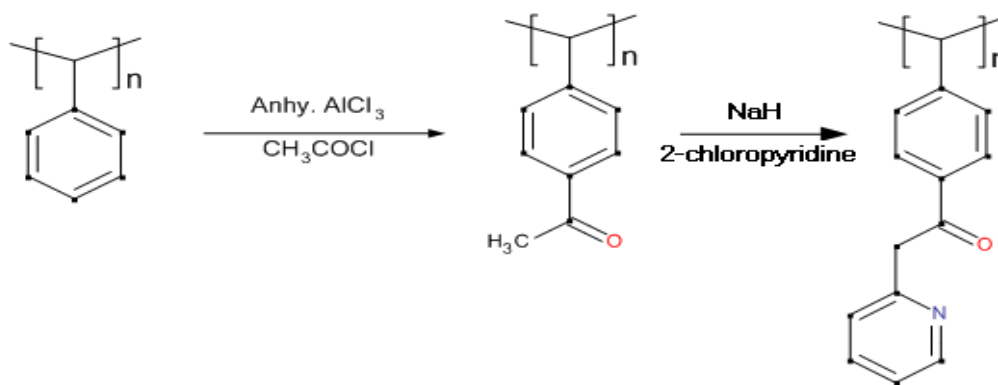


Fig. 2.3. Reaction Scheme for 2-Acetyl pyridine group functionalized Amberlite XAD-16 resin.

2.1.3.1. Characterization

The product has been characterized using FT-IR, Elemental Analysis and thermogravimetric analysis (TGA). IR spectra ($4000\text{--}400\text{ cm}^{-1}$) were taken using diamond ATR probe, using IR Affinity-1 FT-IR spectrophotometer. Table 2.7 shows FT-IR frequency of corresponding functional group of the resin indicating the functionalization of the resin.

Table 2.7. FT-IR data of AP- XAD16 resin.

Frequency (cm^{-1})	Functional group
1683	Carbonyl group
1604.7, 891.1, 707	Pyridine moiety

Table 2.8 shows the elemental composition of the resin.

Table 2.8. Elemental analysis of AP-XAD16 resin.

Element	Calculated (%)	Experimental (%)
Carbon	81.0	80.65
Hydrogen	6.33	6.77
Nitrogen	5.9	5.93
Oxygen	6.75	6.65

Thermogravimetric (TGA) analysis was carried out using STAR^e System METLER TOLEDO instrument. A few mg of the sample was taken in an alumina sample holder, and TG curves were recorded at the heating rate of 15 °C.min⁻¹, from 30 to 900 °C, under dynamic condition, and in N₂ atmosphere (50 ml.min⁻¹). Fig. 2.4 shows the TGA spectra of the AP-XAD 16 resin. The initial weight loss up to 120 °C is due to the water molecules occluded into the polymer matrix. The major weight loss after 350 °C is due to the dissociation of chemically immobilized 2-acetyl pyridine moiety and the polymeric matrix. Resin hydrophilic character is an important parameter which governs the rate of metal ion phase transfer. Water regaining capacity of the resin matrix was thus confirmed by thermal analysis which showed a weight loss of 25% up to 120 °C, which was attributed to the presence of water molecules encapsulated in the polymeric matrix. This reflects the hydrophilic character of the chelating resin, due to the high porosity and pore volume of XAD 16 resin matrix.

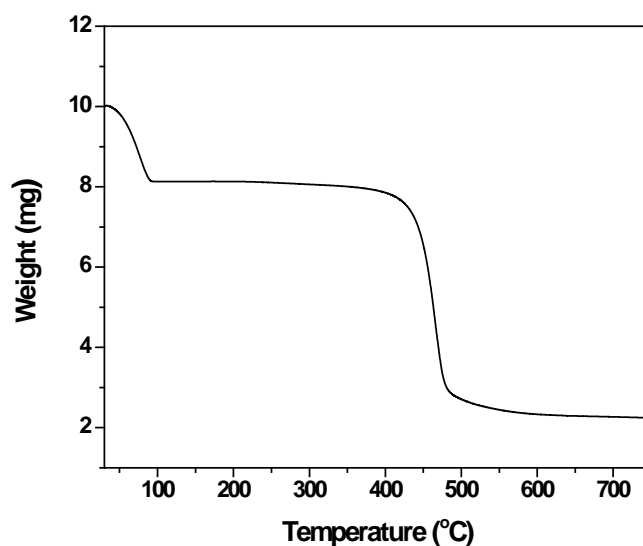


Fig. 2.4. TGA of AP XAD-16

2.2.4. 2-Acetyl amide group functionalized Amberlite XAD-16 resin

2.2.4.1. Synthesis of ACAM XAD-16

Sodium hydride (8.0 g) and dry dimethyl formamide (DMF) (60.0 ml) were added to dried acetylated Amberlite XAD-16 and stirred for 2.0 hrs. *N,N*-di-isobutyl-2-chloro acetamide (8.0 g) dissolved in DMF was added to the above solution and stirred for 8 hrs at ambient conditions. The resulting 2-acetyl amide functionalized Amberlite XAD-16 (ACAM-XAD 16 resin) beads were filtered, washed with excess of water and air dried (Fig. 2.5).

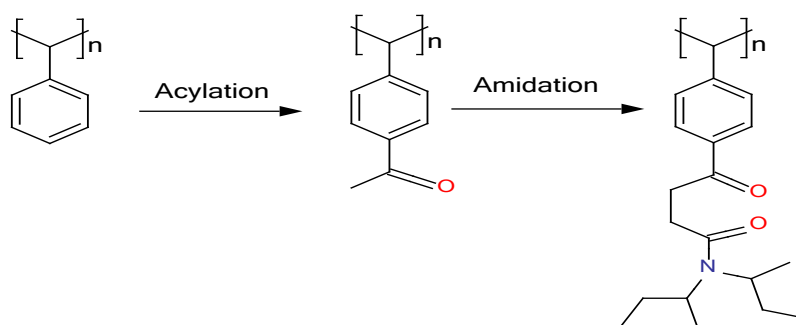


Fig. 2.5. Reaction Scheme for ACAM-XAD16

2.2.4.2. Characterization of ACAM XAD-16

The product has been characterized using FT-IR (Table 2.9) and Elemental Analysis (Table 2.10) and TGA (Fig. 2.6).

Table 2.9. FT-IR of ACAM XAD-16

Frequency (cm^{-1})	Functional group
1683	Carbonyl group (aromatic moiety)
1700	Carbonyl group (amidic moiety)

The FT-IR data shows the functionalization of the resin with the carbonyl group of the aromatic moiety and that of the amidic moiety.

Table 2.10. Elemental analysis of ACAM XAD-16

Element	Calculated (%)	Experimental (%)
Carbon	76.36	76.29
Hydrogen	9.96	8.94
Nitrogen	4.24	4.47
Oxygen	9.69	10.3

TGA of ACAM-XAD 16 resin is as shown in Fig. 2.6. The initial weight loss up to 120 °C is due to the water molecules occluded into the polymer matrix. The major weight loss after 400 °C is due to the dissociation of chemically immobilized 2-acetyl amide moiety and the polymeric matrix. Water regaining capacity of the resin matrix was thus confirmed by thermal analysis which showed a weight loss of 20-22% up to 120 °C, which may be due to the presence of water molecules encapsulated in the polymeric matrix. This reflects the hydrophilic character of the chelating resin as discussed above.

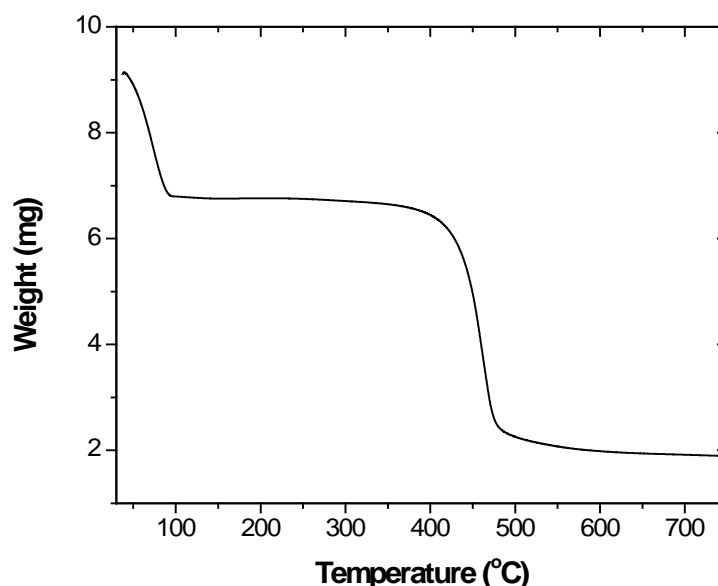


Fig. 2.6. TGA of ACAM XAD-16

2.3. Feed solutions

2.3.1. Palladium feed solution

Palladium nitrate solution was prepared by dissolving appropriate amount of $\text{Pd}(\text{NO}_3)_2 \cdot x\text{H}_2\text{O}$ in nitric acid. The concentration of palladium and nitric acid in the inactive stock solution was 1.06 mg/ml (1×10^{-2} M) and 4 M respectively. This stock solution was diluted appropriately to get desired concentrations of palladium and nitric acid. Aliquots from these solutions were used for different experiments. Quantitative determination of palladium was carried out using Atomic Absorption Spectrophotometry (AAS Avante 1.31, GBC). Detection limit for palladium was 0.06 $\mu\text{g}/\text{ml}$. Error in palladium analysis was within $\pm 2.0\%$.

2.3.2. SHLW Feed Solution

The SHLW solution was obtained from the Waste Management Division, BARC. The concentrations of various metal ions in SHLW solution are given in Table 2.11. Salts in nitrate form were preferred and in the cases where nitrate salts could not be arranged, metal powders were employed. Care was taken to dissolve each of them separately in hot concentrated nitric acid before their addition to the mixture. As the uranium concentration in the HLLW was usually high (~ 20 g/L), it was presumed that HLLW will undergo two to three contacts with 30% TBP to remove uranium before extraction studies. Accordingly, SHLW containing uranium was contacted twice with 30% TBP/ CCl_4 prior to palladium extraction studies. The acidity of the SHLW (3.0 M) was ascertained by acid-base titration. Quantitative determination of various metal ions present in SHLW was carried out using the Inductively Coupled Plasma Atomic Emission Spectrophotometry technique (ICPAES). A JY-50P poly-scan instrument with axial ICP (Jobin Yvon, Longjumeau Cedex, France), operated at 40.68 MHz, was used in this study. The

instrument known as “Panorama” model has the unique facility for simultaneous and sequential operation in the same spectrometer assembly. Thus, the spectrometer has a polychromator covering 35 elements and is also able to function as a sequential unit over a spectral range of ± 2.2 nm around each channel. The error on the measured concentrations was within $\pm 5.0\%$.

Table 2.11. Composition of SHLW for PHWR, 6700 MWD/te; Acidity: 3.0 M HNO₃.

Constituent Element	Concentration (mg/L)	Constituent Element	Concentration (mg/L)
*Cr	142.5	Sm	27.5
*Ni	127.5	Y	1.8
Ba	152.5	Ce	185
*Mn	347.5	La	127.5
*Fe	735.0	Nd	112.5
Mo	137.5	#K	355.0
Sr	40.0	#Na	4450
Zr	3.0	Pr	32.2
Pd	187.5	Cs	60.0
U	20000		

* Structural materials, #Additives.

2.3.3. HLLW feed solution

HLLW originated from reprocessing of Research Reactor spent fuel has the composition of U - 10.56 g/L, Pu -2.19 mg/L, ¹³⁷Cs - 9.29 Ci/L, ¹⁰⁶Ru - 7.99 Ci/L, ¹⁴⁴Ce -27.75 Ci/L, ⁹⁰Sr - 4.0Ci/L [112]. In view of high activity of HLLW, it was diluted by a factor of 10³ to bring down the activity to a measurable level. Consequently, the activity of the radionuclides namely ²⁴¹Am and ¹⁵²⁺¹⁵⁴Eu became too low to determine and hence, had to be spiked.

HLLW originated from reprocessing of spent fuel of PHWR (PREFRE Tarapur) was diluted to bring down its activity to appropriate level. ¹⁰⁹Pd was added as a tracer for

palladium in the HLLW along with some other radioisotopes, viz., ^{99}Mo , $^{85,89}\text{Sr}$ and ^{181}Hf (as a chemical analogue for ^{95}Zr) which were not originally present in the HLLW. ^{109}Pd was prepared by neutron activation of ^{108}Pd at Dhruva reactor.

' γ ' energies along with the half life of various radionuclides used in the present study are given in Table 2.12. Suitable quantity of inactive palladium nitrate salt was added to the diluted solution to obtain the concentration of palladium of about 10^{-3} M. The acidity was finally adjusted to 3.0 M HNO_3 .

Known and equal volumes of the aqueous and organic fractions were counted for the activity of the radionuclides on a high purity germanium detector coupled to a 4096 channel analyzer. The peak areas of the gamma-rays were obtained by linear subtraction of Compton background, as most of the peaks were well resolved. The D_M value was calculated as the ratio of the count rate of the gamma-ray in organic phase to that in the aqueous phase. Uranium analysis was carried out spectrophotometrically using Br-PADAP as chromogenic reagent [113].

Table 2.12 Nuclear data of actinides and long lived fission products present in the HLLW.

Element	Half life ($t_{1/2}$)	' γ ' energy (keV)
^{241}Am	432.6 years	59.5
^{152}Eu	13.54 years	121.8
^{144}Ce	284.89 days	133
$^{85+89}\text{Sr}$	$^{85}\text{Sr} \sim 64.84$ days $^{89}\text{Sr} \sim 50.52$ days	514
^{106}Ru	367 days	512
^{137}Cs	30.17 years	661.6
^{99}Mo	65.94 hours	740
^{181}Hf	42.4 days	133, 482
^{109}Pd	13.47 hours	88

2.4. Experimental methodologies

2.4.1. Solvent extraction studies

All liquid-liquid extraction experiments were carried out under ambient conditions by shaking equal volume (1-10 mL each) of organic and aqueous phase in a separatory funnel using wrist action shaker. After phase separation, the aqueous phase was analyzed for palladium concentration. The concentration of palladium in the organic phase was calculated by mass balance. The contact time for the entire batch extraction studies were 10 min. which was fixed based on the kinetics experiment, whereas in the case of extraction equilibrium studies the contact time was varied.

The distribution ratio (D_M) of the metal was determined as the ratio of metal ion concentration in organic phase to that in aqueous phase. Separation factor ($SF=D_{Pd}/D_M$) of palladium with respect to other metal ion was also determined. Percentage extraction of metal ion was determined by equation:

$$\% E = \frac{D_M}{D_M + 1} \times 100 \quad (1)$$

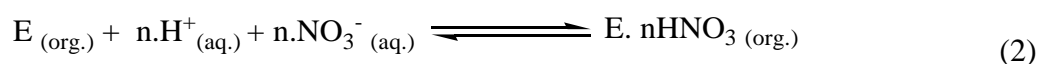
Errors in D_M and % E values were within $\pm 5.0\%$ and $\pm 2.0\%$ respectively. However, for elements with very small distribution ratios in the range of 10^{-2} to 10^{-3} , the error was within $\pm 10.0\%$.

2.4.2. Acid Uptake Studies

Nitric acid uptake is a common property exhibited by amidic extractants. Dithiodiglycolamides, having both the thioetheric and amidic functional group, are also expected to show similar properties. For the acid distribution studies, equal volumes of the

organic phase containing 0.1 M ligand dissolved in n-dodecane and an aqueous phase of varying acidity (0.5 to 5.0 M HNO₃) were equilibrated in a separatory funnel for 10 minutes using a wrist-action shaker. After phase disengagement, the acidity of both the organic and aqueous phase was determined according to the method described earlier [114].

Metal extractant (ligand) interacts with the nitric acid according to the following mechanism.



where E is the extractant and n is the number of nitric acid molecules involved in the formation of the adduct. The acid uptake constant K_H is given by

$$K_H = \frac{[E.nHNO_3]_{org.}}{[E]_{org.} [H^+]_{aq.}^n [NO_3^-]_{aq.}^n} \quad (3)$$

where [E]_{org.} is the concentration of free organic extractant and is determined as

$$[E]_{org.} = [E]_{initial} - [E.nHNO_3]_{org.}$$

As the data for the activities of nitric acid and free DTDGA in the organic phase are not available, therefore, the equilibrium constant is referred to as conditional acid uptake constant.

Considering [H⁺] = [NO₃⁻] in aqueous medium, the above equation can be written as,

$$K_H = \frac{[E.nHNO_3]_{org.}}{[E]_{org.} [H^+]_{aq.}^{2n}} \quad (4)$$

Taking logarithm on both side of the above equation and rearranging,

$$\log K_H = \log [E \cdot nHNO_3]_{org.} - \log [E]_{org.} - 2n \log [H^+]_{aq.} \quad (5)$$

Since $[E \cdot nHNO_3]$ is equal to the concentration of H^+ in the organic phase, therefore, the equation (5) can be written as,

$$\log [H^+]_{org.} - \log [E]_{org.} = \log K_H + 2n \log [H^+]_{aq.} \quad (6)$$

$[H^+]_{aq.}$ can be calculated from the titre value (T) and acid dissociation constant of HNO_3 ($\log K_a = 23.5$).

$$K_a = \frac{[H^+]_{aq.} [NO_3^-]_{aq.}}{[HNO_3]_{aq.}} \quad (7)$$

where the titre value (T) is the total acidity in the aqueous phase comprising of dissociated and undissociated nitric acid, hence, $T = [HNO_3]_{aq.} + [H^+]_{aq.}$

Thus, from equation (6), the plot of $\log [H^+]_{org.} - \log [E]_{org.}$ vs. $\log [H^+]_{aq.}$ gives a straight line with intercept of $\log K_H$ and slope of $2n$.

2.4.3. Gamma Radiolysis Experiments

It is well known that in an extraction process involving HLLW, the extractant will inevitably be exposed to continuous high radiation dose in contact with nitric acid. Since the nuclear radiation energies are higher by several orders of magnitude than the chemical bond energies, the extractant will eventually experience radiolytic degradation. The radiolysis results in breakdown of the active extracting molecule and formation of radiolysis products, which usually have deleterious effect on the extractant performance. The severity of the degradation is determined by stability of the extractant towards radiolysis. Thus it becomes necessary to evaluate the radiolytic stability of the extractant if it is to be used for the extraction process involving HLLW. Recently, Mincher et al have

reported the detailed investigations into production of the reactive species in an irradiated system as well as their reaction with solvent extraction ligand [115] and the radiation chemistry of the ligands proposed for the use in the extraction of cesium and strontium fission products [116]. Likewise several extractants, namely, tributyl phosphate (TBP), trioctyl phosphine oxide (TOPO), *N,N'*-dimethyl- *N,N'*-dibutyl tetradecyl malonamide (DMDBTDMA), *n*-octyl(phenyl) *N,N*-diisobutylcarbonyl methyl phosphine oxide (CMPO), *N,N,N',N'*-tetraoctyldiglycolamide (TODGA) and *N,N,N',N'*-tetra(2-ethylhexyl) diglycolamide (TEHDGA) have been studied in detail for hydrolytic and radiolytic stabilities [117-121]. These studies revealed that organophosphorous extractants generally decompose to lower phosphoric acids which have deleterious effect on extraction process whereas the amidic extractants degrade to amines and carboxylic acids which are relatively innocuous. Further, the diluents play a major role in radiolysis of extractants. For example, aromatic diluents suppress the degradation, whereas the saturated aliphatic diluents like *n*-dodecane enhance radiolysis sensitivity [122, 123]. Radiolytic stability of T(2EH)TDGA and DTDGA, the two promising extractants for separation and recovery of palladium from HLLW has been studied.

Three types of samples were prepared in glass vials for irradiation, namely, (1) neat ligand, (2) 0.025–0.1 M ligand dissolved in *n*-dodecane and (3) 0.025–0.05M ligand/*n*-dodecane in contact with equal volume of 3.0 M nitric acid, which was occasionally shaken during irradiation. These samples were placed in a ⁶⁰Co gamma irradiation chamber at a dose rate of 25 Gy/min in air at room temperature. The dose rate was determined by Fricke dosimetry. After a particular absorbed dose the samples were removed from the chamber and analyzed for distribution ratios and degradation products as per procedure described earlier.

2.4.4. Hydrolysis Experiments

100 ml of 0.025 M ligand/*n*-dodecane solvent, in a single necked round bottom flask, was continuously stirred with equal volume of 3.0 M nitric acid at room temperature for 2 weeks. The degradation products were analysed by GC-MS and FT-IR.

2.4.5. Sorption Studies

2.4.5.1. Static batch method

This method uses a batch extraction process wherein an aqueous solution containing known metal ion concentration is equilibrated with a definite amount of functionalized resin beads (mg scale) for limited time duration on a mechanical shaker at 200 rpm. The distribution coefficient (D) and equilibrium adsorption capacity (Q_e , mg/g) were calculated with the following formulae:

$$D = \frac{c_0 - c_e}{c_e} \cdot \frac{V}{m} \quad (8)$$

$$Q_e = (c_0 - c_e) \cdot \frac{V}{m} \quad (9)$$

where C_0 and C_e are the initial concentration and concentration at equilibrium (mg/L) in the solution, V is the total volume of solution (mL); and W is the mass of adsorbent (g).

2.4.5.2. Sorption kinetics

In order to investigate the kinetics of the sorption process of palladium onto the resin, two kinetic models namely, pseudo-first- and second-order models, were proposed.

(i) Pseudo-first-order Model

The pseudo-first-order equation can be written as

$$\frac{dq_t}{dt} = k_f(q_e - q_t) \quad (10)$$

where q_t (mg/g) is the amount of metal ion sorbed at time t (min), q_e (mg/g) is the sorption capacity at equilibrium, and k_f (min^{-1}) is the rate constant for pseudo-first-order model.

After integration and by applying the initial conditions $q_t = 0$ at $t = 0$ and $q_t = q_t$ at $t = t$, the equation becomes

$$\log(q_e - q_t) = \log q_e - \left(\frac{k_f t}{2.303} \right) \quad (11)$$

(ii) Pseudo-second-order Model

The pseudo-second-order model can be presented in the following form:

$$\frac{dq_t}{dt} = k_s(q_e - q_t)^2 \quad (12)$$

Where k_s is the rate constant of pseudo-second-order model (in g/mg min). By definite integration of Eq. (12) for boundary conditions $q_t = 0$ when $t = 0$ and $q_t = q_t$ at $t = t$, the following equation is obtained:

$$\frac{t}{q_t} = \frac{1}{(k_s q_e^2)} + \left(\frac{1}{q_e} \right) t \quad (13)$$

The initial sorption rate constant, h (mg/g min), at $t = 0$ can be defined as

$$h = k_s q_e^2 \quad (14)$$

2.4.5.3. Adsorption isotherm models

The equilibrium adsorption of palladium onto AP XAD-resins was analyzed using Langmuir and Freundlich isotherms.

(i) Langmuir isotherm

Langmuir model is the simplest theoretical model for monolayer adsorption onto a surface with finite number of identical sites. The general Langmuir equation is as follows:

$$q_e = \frac{K_L C_e}{1 + a_L C_e} \quad (15)$$

When linearized, Eq. (15) becomes

$$\frac{C_e}{q_e} = \frac{\alpha_L C_e}{K_L} + \frac{1}{K_L} \quad (16)$$

K_L and α_L are the equilibrium constants of Langmuir equation. Plotting C_e/q_e against C_e yields a straight line with slope, α_L/K_L , and intercept $1/K_L$. The ratio α_L/K_L indicates the theoretical monolayer saturation capacity, Q_0 . The shape of the isotherm can determine whether the adsorption is favorable or not.

(ii) Freundlich isotherm

Freundlich expression is an empirical equation applicable to non-ideal sorption on heterogeneous surface as well as multilayer sorption. The isotherm follows the equation,

$$q_e = K_F C_e^{1/n} \quad (17)$$

K_F is relative indicator of sorption capacity, while the dimensionless, $1/n$ suggests the favorability and capacity of the adsorbent/adsorbate system. According to the theory, $n > 1$ represents favorable adsorption conditions. Eq. (17) is linearized into logarithmic form for data fitting and parameter evaluation as follows:

$$\log q_e = \log K_F + \frac{1}{n} \log C_e \quad (18)$$

By plotting $\log q_e$ versus $\log C_e$, constant K_F and exponent $1/n$ can be calculated.

2.4.6. Structural investigation studies

With a view to understand the structure of Pd complexes with T(2EH)TDGA and DTDGA, X-ray absorption spectroscopy and density functional theory (DFT) based studies were carried out. Extended X-ray Absorption Fine Structure (EXAFS) is a frontier tool to determine the number, type and the distance of near neighbor atoms around the probe atom [124, 125]. This technique thus provides valuable information about the

coordinating atoms to the metal ion. The information obtained by EXAFS is sometimes required to be corroborated by theoretical calculations to obtain the geometry of the complex. The general description of EXAFS and DFT based calculation is given below.

2.4.6.1. EXAFS Studies

EXAFS is an X-ray absorption technique which gives detailed local structure information around the probe atom. When an X-ray photon interacts with the probe atom, it may undergo photoelectric absorption, which is followed by emission of photoelectrons from the atomic shells. The photoelectrons travel outwards as a spherical wave and may get backscattered from the neighboring atoms. The constructive and destructive interference between the outgoing and backscattered electron waves, gives rise to oscillations in the X-ray absorption spectrum (μx vs E), which is obtained by varying the incident X-ray energy and measuring the intensity of incident (I_0) and transmitted (I) X-rays, viz.,

$$\mu(E)x = \ln (I_0/I) \quad (19)$$

Where $\mu(E)$ is the absorption coefficient of X-ray photon of energy, E , and x is the thickness of the sample. The absorption spectrum shows the sharp rise in the cross section at the binding energy of the shell (K.L. etc.), with the oscillations riding on the sharply decreasing intensity after the edge. The spectral region from pre-edge up to ~ 30 eV is called X-ray absorption near edge spectrum (XANES) and contained information about the valency and coordination number of the probe atom, while the spectral region above 30 eV of the edge and extending to a few hundreds of eV is called extended X-ray absorption fine structure (EXAFS), which provides the information about the Z , number and distance of the near neighboring atoms.

The EXAFS fine-structure function, $\chi(E)$, is defined as,

$$\chi(E) = \frac{\mu(E) - \mu_0(E)}{\Delta\mu_0(E_0)} \quad (20)$$

where $\mu(E)$ is the measured absorption coefficient, $\mu_0(E)$ is a smooth background function representing the absorption of an isolated atom, and $\Delta\mu_0(E_0)$ is the measured jump in the absorption $\mu(E)$ at the threshold energy. It is convenient to analyse the XAFS spectra when represented in terms of photo-electron wave number (k), defined as,

$$k = \sqrt{\frac{2m(E - E_0)}{\hbar^2}} \quad (21)$$

The EXAFS spectrum ($\chi(K)$), represents a sum of damped, phase shifted sine waves, from all the scattering atoms.

$$\chi(k) = \sum_j \frac{S_0^2 N_j f_j(k) e^{-2R_j/\lambda(k)} e^{-2k^2\sigma_j^2}}{kR_j^2} \text{Sin}[2kR_j + \delta_j(k)] \quad (22)$$

where, R_j is the distance of j^{th} scattering atom from the probe atom, σ_j^2 is the variance of R_j , N_j is the number of j^{th} scatterer, S_0^2 is the amplitude reduction factor, f_j , δ_j are the scattering parameters based on identity of scattering atom(s) and λ is the mean-free path of the photoelectron. The $\chi(k)$ spectra are Fourier transformed to obtain the $\chi(R)$ spectra, which contain the information about the near neighbor atoms and are fitted into the theoretical function for final metric parameters.

In the present work, X-ray absorption spectra at the Pd-K edge were collected at XAFS beamline of Elettra synchrotron facility under dedicated ring conditions (2.4 GeV, 150 mA) using a Si(311) double crystal monochromator. Measurements were carried out in transmission mode using three ionization chambers, one each for initial X-ray intensity (I_0), transmitted intensity (I) through the sample and intensity (I_m) after the monitor foil

(Fe) placed downstream of the second ionization chamber for simultaneous energy calibration. The higher order harmonic content of the beam was rejected with detuning the crystals in the monochromator by about 45% of its maximum at the scan ending energy. Spectra were collected over the energy range of 24200-25200 eV focusing on Pd-K edge energy (24350 eV), with the pre-edge energy step of 5 eV, 0.20 eV in the edge region and 0.03 \AA^{-1} in extended XAFS region. Typically ten scans were taken for each sample at 295 K and averaged to improve the statistics. To aid in the spectrum analysis, XAFS spectra for one reference sample, that is, palladium nitrate in 1.0 M HNO_3 was also acquired. The Pd K-edge X-ray absorption spectra of the reference compound and the samples were analyzed by the software package IFEFFIT. Data reduction step was carried out using standard procedure of background removal and normalization in Athena. Absorption data, $\mu(x)$ vs. E , was converted into representation involving momentum space vector (k) and subsequently Fourier transformed into R-space. Final fitting of the spectra was done on the normalized, background subtracted data in R-Space using all shells simultaneously in Artemis after fitting the spectra shell wise either in R space or after back transformation to k space. The fitting involved optimization of parameters of EXAFS equation for hypothetical structure to match the experimental data. EXAFS data for the hypothetical structure was generated using FEFF 6.01 program. For each fitting, the bond lengths (R), the coordination numbers (CN), and the Debye-Waller factors (σ^2) were kept as free parameters. All fits included contributions from the first shell of directly coordinated 'O' atoms from water and 'S' and 'O' atoms from the extractants. It is to be noted that in all the fits, the Fourier transforms (FT) represent a pseudo radial distribution function of the palladium near-neighbor environment, and the peaks appear at lower R values relative to the true near neighbor distances as a result of the EXAFS phase shifts which are different for each neighboring atom ($\alpha = 0.2\text{-}0.5 \text{ \AA}$).

2.4.6.2 DFT Calculations

Density functional theory (DFT) was used to determine the optimized geometries and related thermochemical properties of all species. All DFT calculations were performed with Firefly Gamess Package [126]. For each molecular species (free ligands and Pd-ligand complexes), a geometry optimization was first performed in the gas phase. A vibrational frequency analysis was then carried out in order to confirm the minimum energy and determine the thermal corrections. In a few cases, but such small imaginary frequencies are known to be often merely computational (numerical) artifacts and therefore can be neglected. From the thermal corrections and electronic energies, the Gibbs free energy of each species was calculated in the gas phase. Finally, Gibbs free energies for the solvated species were obtained from single-point energy calculations for the gas-phase-optimized structure in the presence of a polarizable continuum model to describe solvent effects. For all calculations, B3LYP functional was used along with 6-31G** basis set for C, H, N, O and S and Stuttgart RSC ECP (effective core potential) basis set for palladium [127].

CHAPTER 3

Evaluation of T(2EH)TDGA for separation of Pd(II) from high level liquid waste

Separation and recovery of palladium from HLLW originating from PUREX process of spent nuclear fuel is necessary from the viewpoint of various problems encountered during vitrification [52] as well as the conceptualization of the process where HLLW can be treated as a secondary source of this valuable metal [26]. Since the palladium is a soft acid, its selective extraction is possible with soft donor based extractants containing thioetheric 'S' atoms. Based on this presumption various extractants, namely, dioctyl sulfide (DOS) [103], dihexyl disulfide (DHDS) [105], dioctyl sulfoxide (DOSO) [103] and triisobutylphosphinesulfide (TIPS) [103], have been studied in detail. Though proved to be selective for 'Pd', these extractants suffer from several limitations like slow kinetics of extraction, low solubility in paraffinic diluents and instability in acidic medium. In view of these limitations, it becomes imperative to look for other class of ligands, which can selectively extract palladium with better efficiency. It is already known that amidic extractants like malonamide (MA) and diglycolamide (DGA) when used in higher concentrations can extract palladium from nitric acid medium with simultaneous co-extraction of other FPs [92, 93]. Sulphur analogue of diglycolamides has been used to selectively separate palladium from platinum in hydrochloric acid medium [128]. Such ligands have not been investigated for the extraction of palladium from nitric acid medium. Among the thiodiglycolamide class of ligands, *N,N,N',N'*-tetra-(2-ethylhexyl)thiodiglycolamide has been chosen owing to the following reasons

- (i) Thioetheric sulphur atom (soft base) acting as the primary donor atom would impart selectivity towards Palladium ion (soft acid).

- (ii) Carbonyl oxygen of amidic moiety would impart more chelation thereby forming the more stable metal ligand complex.
- (iii) Bulkier alkyl groups on the amidic moieties tend to increase the solubility of ligand as well as Pd-ligand complex in paraffinic diluents.
- (iv) The possibility of complete incineration of the spent solvent leading to reduced volume of the secondary waste.

3. Evaluation of the extractant

The synthesis and characterization of T(2EH)TDGA has been discussed in detail in chapter 2. In this chapter its evaluation for Pd extraction has been described.

3.1. Extraction of nitric acid

Nitric acid uptake is a common property exhibited by amidic extractants. Thiodiglycolamides, having both the thioetheric and amidic functional group, should also show similar properties. Therefore, nitric acid extraction of 0.1 M T(2EH)TDGA/ n-dodecane solvent system was studied and the ratio of concentration of HNO₃ to T(2EH)TDGA in organic phase was determined at different initial nitric acid concentrations. Figure 3.1 shows the variation of $[\text{HNO}_3]_{\text{org.}}/[\text{T(2EH)TDGA}]_{\text{ini}}$ ratio as a function of initial aqueous nitric acid concentration. The amount of acid extracted in the organic phase increases with an increase in the concentration of nitric acid present in the aqueous phase. At nitric acid concentration above 3.5 M, the ratio of HNO₃ to T(2EH)TDGA was found to be unity.

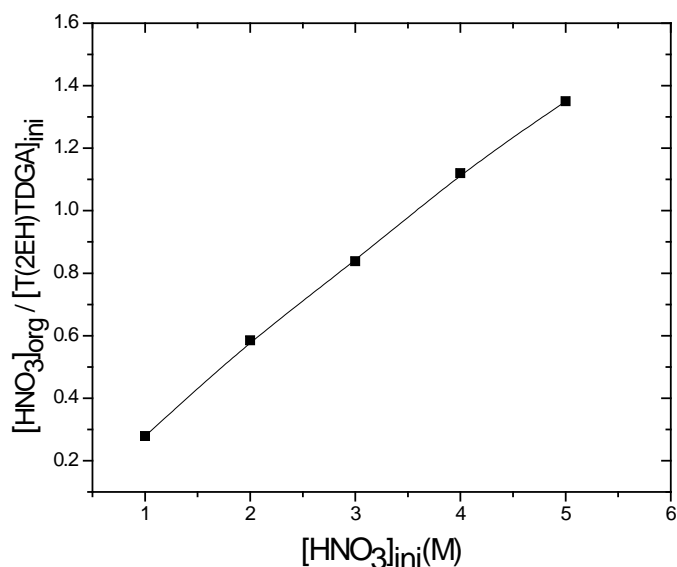


Fig. 3.1. Extraction of HNO₃ from aqueous solution by 0.1 M T(2EH)TDGA/n-dodecane at different initial nitric acid concentrations.

In order to compare its basicity with other extractants, it becomes imperative to have the quantitative knowledge of its basicity in terms of conditional acid uptake constant.

As discussed in the earlier chapter the plot of $\log [H^+]_{org} - \log [E]_{org}$ vs. $\log [H^+]_{aq}$ gives a straight line with intercept of $\log K_H$ and slope of $2n$. The slope value obtained from graph is 2.07 ± 0.228 (Fig. 3.2), suggesting the stoichiometry of adduct being 1:1 for T(2EH)TDGA to HNO₃. The conditional acid uptake constant K_H of T(2EH)TDGA obtained from the intercept is 0.62 ± 0.07 . The basicity of T(2EH)TDGA could be attributed to the presence of carbonyl group of two amidic moieties attached to the sulphur atom through methylene bridge.

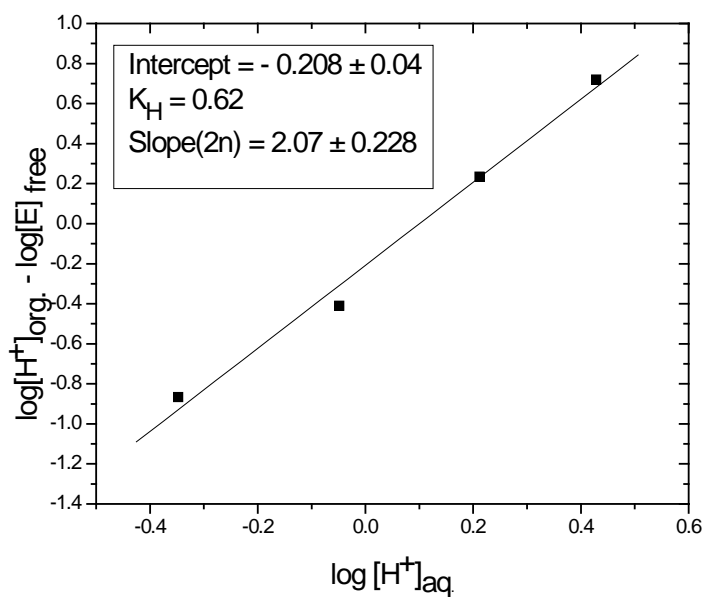


Fig. 3.2. Extraction of nitric acid from aqueous solution by 0.1 M T(2EH)TDGA/n-dodecane.

3.2. Extraction equilibrium studies

Figure 3.3 shows the variation of percentage extraction (%E) of Pd(II) as a function of contact time. Under chosen experimental conditions the extraction equilibrium was achieved in less than five minutes. However, for further studies the equilibration time was kept as 10 minutes to ensure complete equilibration.

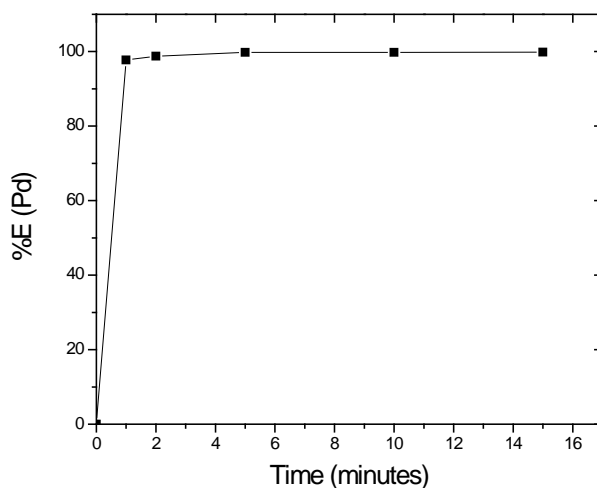


Fig. 3.3. Variation of % E of palladium as a function of contact time. Organic phase: 0.01 M T(2EH)TDGA/n-dodecane, Aqueous phase: 10^{-3} M palladium in 4.0 M nitric acid.

3.3. Effect of nitric acid concentration on Pd(II) extraction by T(2EH)TDGA

Influence of nitric acid concentration on the extraction of palladium was studied by determining D_{Pd} at various concentrations of nitric acid. Fig. 3.4 shows the variation of D_{Pd} with 0.005 M T(2EH)TDGA/n-dodecane as a function of initial nitric acid concentration. It can be seen that D_{Pd} increases with increase in nitric acid concentration and quantitative extraction of palladium was observed above 4.0 M nitric acid. No change was observed in D_{Pd} on further increase in the nitric acid concentration.

The above observations suggest that the nitric acid plays a vital role in extraction of palladium. It was therefore of interest to investigate the participation of nitric acid in the extraction reaction. D_{Pd} was determined from nitric acid solutions of fixed ionic strength of 4.0 M (H, Na)NO₃. Fig. 3.5 shows that D_{Pd} remains unchanged with nitric acid variation at fixed ionic strength. This indicates that HNO₃ molecule itself does not participate in the complex formation. Hence, with increase in nitric acid concentration the

increase in D_{Pd} (cf. fig. 3.4) could be attributed to the increase in nitrate ion concentration which participates in complex formation.

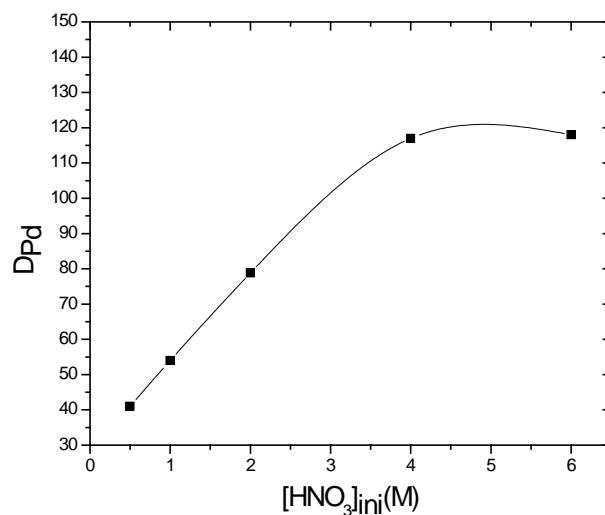


Fig. 3.4. Dependency of D_{Pd} on HNO_3 concentration. Aqueous phase: 10^{-3} M Pd in 0.5 M to 6.0 M HNO_3 . Organic phase: 0.005 M T(2EH)TDGA/n-dodecane.

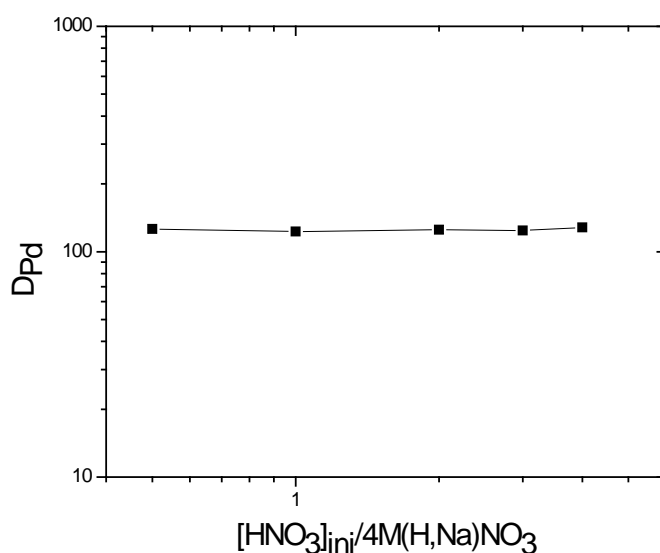


Fig. 3.5. Extraction dependency of D_{Pd} in 4.0 M(H, Na) NO_3 . Org. phase: 0.005 M T(2EH)TDGA /n-dodecane, Aqueous phase: 4M(H, Na) NO_3 .

3.4. Effect of nitrate ion concentration

Figure 3.6 shows the variation of D_{Pd} against nitrate ion concentration. The extraction of palladium increases with the increase in nitrate ion concentration. A plot of $\log D_{Pd}$ vs. $\log [NO_3^-]$ gave a straight line with a slope of 1.78 ± 0.01 which is close to 2. This indicates that Pd is extracted in the form of $Pd(NO_3)_2$.

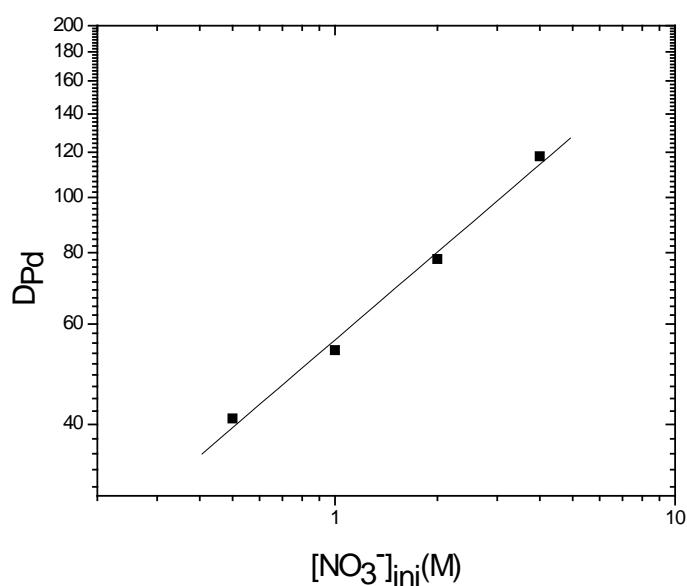
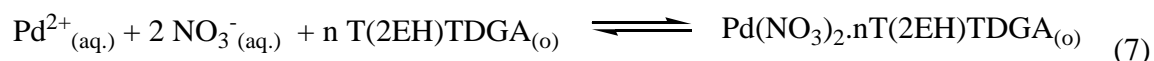


Fig. 3.6. Extraction dependency of palladium on initial nitrate ion concentration. Organic phase: 0.005M T(2EH)TDGA/n-dodecane, Aqueous Phase: $10^{-3}M$ palladium in $(0.5H+Na)NO_3$.

3.5. Effect of concentration of T(2EH)TDGA

To provide insight into the composition of palladium extractant species formed into the organic phase, the variation of D_{Pd} as a function of extractant concentration was investigated. The results are shown in figure 3.7. It was observed that D_{Pd} values increase with an increase in the concentration of T(2EH)TDGA. As the extractant is neutral, it

follows that it extracts the metal ion solely through solvation. Therefore, the extracted species formed should also be neutral. Extraction of palladium by T(2EH)TDGA from nitrate solution can be represented as



In the chosen experimental conditions, the conditional extraction constant K'_{ex} is given by

$$K'_{\text{ex}} = \frac{[\text{Pd(NO}_3)_2 \cdot n\text{T(2EH)TDGA}]_{(\text{o})}}{[\text{Pd}^{2+}]_{(\text{aq.})} [\text{NO}_3^{-}]_{(\text{aq.})}^2 [\text{T(2EH)TDGA}]_{(\text{o})}^n} \quad (8)$$

where the distribution ratio of palladium, $D_{\text{Pd}} = [\text{Pd(NO}_3)_2 \cdot n \text{T(2EH)TDGA}]_{(\text{o})} / [\text{Pd}^{2+}]_{(\text{aq.})}$.

Taking logarithm on both the sides of above equation and rearranging gives

$$\log D_{\text{Pd}} = \log K'_{\text{ex}} + n \log [\text{T(2EH)TDGA}] + 2 \log [\text{NO}_3^{-}] \quad (9)$$

Here, it was assumed that $[\text{NO}_3^{-}]$ remains constant in the chosen experimental conditions.

A plot of $\log D_{\text{Pd}}$ vs $\log [\text{T(2EH)TDGA}]$ is shown in figure 3.7. The plot is a straight line with a slope of 2.17 ± 0.12 , which indicates that the extracted species in the organic phase is $\text{Pd(NO}_3)_2 \cdot 2\text{T(2EH)TDGA}$. This was further confirmed by loading experiments.

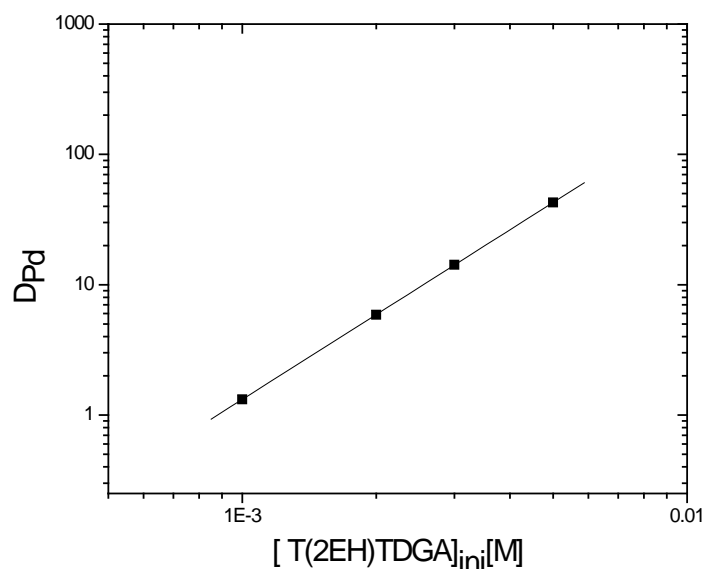


Fig. 3.7. Dependency of the distribution ratio of Pd on T(2EH)TDGA concentration.

Aqueous phase: 10^{-3} M Pd in 0.5 M HNO_3 . Organic phase: 0.001 to 0.005 M T(2EH)TDGA in n-dodecane.

3.6. Effect of diluents

The extraction of 10^{-3} M palladium in 4.0 M nitric acid medium using 0.01M T(2EH)TDGA in various diluents such as n-dodecane, benzene, toluene, 1-octanol and dichloromethane was investigated. No significant change with respect to diluents on D_{Pd} was observed. It was found that more than 99% of palladium is extracted in single step in all of the diluents. In the given experimental conditions the extraction of palladium with this extractant is so high that, slight variation in the distribution ratio due to the interaction between extracted species and diluents will have insignificant effect on percentage extraction of Pd.

3.7. Loading studies

Loading capacity of T(2EH)TDGA was determined by contacting 10 ml of 10^{-3} M T(2EH)TDGA/n-dodecane repeatedly with equal volume of aqueous solution containing 10^{-3} M palladium in 0.5 M nitric acid. The phases were separated after equilibration and palladium content in the aqueous phase was determined. The amount of palladium transferred into the organic phase in each contact was calculated by mass balance and the cumulative concentration in the organic phase after each contact was determined. It was found that 5.44×10^{-4} M palladium was loaded in two contacts after which no further loading was observed. Also, the loaded organic was stripped using 0.01 M thiourea in 0.1 M nitric acid and palladium content analyzed in the strip solution was found to be same as obtained by mass balance. The loading capacity of palladium in the organic phase corresponds to 1:2 stoichiometry between the palladium and the extractant, thus confirming the previously determined values of stoichiometry by slope analysis method.

3.8. Back extraction studies

Back extraction of Pd from loaded organic was carried out by dilute nitric acid and thiourea. The organic phase obtained on equilibrating 0.01 M T(2EH)TDGA/n-dodecane with aqueous phase containing 1.0×10^{-3} M palladium dissolved in 4.0 M nitric acid, was contacted with stripping solutions namely 0.1 M nitric acid and 0.01 M thiourea in 0.1 M nitric acid. It was observed that dilute nitric acid alone is not suitable for recovering palladium from loaded organic phase. However, it is quantitatively recovered with a single contact using a solution of 0.01 M thiourea in 0.1 M nitric acid.

3.9. Recovery of palladium from stripping solution

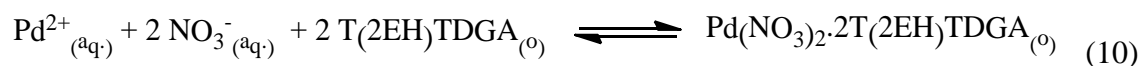
Recovery of metals from stripping solution is of prime concern which may provide the option of either recycling or discarding the barren strip solutions. Moreover this will provide an option to reduce the waste volume as well as an alternative approach to recover palladium in stable chemical form for long term storage. In view of this, effort has been made to recover palladium from strip solutions. It is known that thiourea decomposes in alkaline solutions to give sulphide ions [129]. It is also known that noble metals especially palladium readily precipitate in presence of sulphide ions, the solubility product being of the order of 10^{-58} [130]. It was envisaged that under alkaline conditions, sulphide ions formed on decomposition of thiourea would precipitate palladium as palladium sulphide. Accordingly, the strip solution was treated with aqueous ammonia (25% v/v) and stirred for 30 minutes at ambient conditions to facilitate precipitation. The precipitate was filtered and the filtrate was analyzed for palladium, which was found to be below detection limit. Furthermore, the precipitate was dried in vacuum and analyzed by EDX as well as elemental analyzer. The XRD showed the powder as amorphous. Neutron activation analysis of precipitate showed 29% 'Pd' while S content was determined to be 14% by elemental analysis whereas the composition of PdS is 77.15% Pd and 22.85% S. This shows that the precipitate may be consisting of different phases of palladium sulfide along with some water molecules. However, the exact structure of the compounds will require more detailed investigations.

3.10. Thermodynamic studies

Owing to the presence of α/β emitting radionuclides in HLLW, its temperature may rise well above the ambient conditions. Variation in temperature may affect the extraction and

therefore, it become imperative to study the effect of temperature on the extraction behavior of palladium using T(2EH)TDGA.

The extraction of palladium from nitric acid medium with T(2EH)TDGA can be represented as



In the chosen experimental conditions, the conditional extraction constant K'_{ex} is given by

$$K'_{\text{ex}} = \frac{[\text{Pd(NO}_3)_2 \cdot 2\text{T(2EH)TDGA}]_{(\text{o})}}{[\text{Pd}^{2+}]_{(\text{aq})} [\text{NO}_3^{-}]^2_{(\text{aq})} [\text{T(2EH)TDGA}]^2_{(\text{o})}} \quad (11)$$

where the distribution ratio of palladium, $D_{\text{Pd}} = [\text{Pd(NO}_3)_2 \cdot 2\text{T(2EH)TDGA}]_{(\text{o})} / [\text{Pd}^{2+}]_{(\text{aq})}$.

Taking logarithm on both the sides of above equation and rearranging

$$\log D_{\text{Pd}} = \log K'_{\text{ex}} + 2 \log [\text{T(2EH)TDGA}] + 2 \log [\text{NO}_3^{-}] \quad (12)$$

From previously determined value of acid uptake constant ($K_{\text{H}} = 0.62$), at 0.2M nitric acid concentration in aqueous phase, the amount of acid extracted in the organic phase was found to be very small and can be safely ignored. Hence, it was assumed that $[\text{NO}_3^{-}]$ remains constant in the chosen experimental conditions. A plot of $\log D_{\text{Pd}}$ with $\log [\text{T(2EH)TDGA}]$ gives a straight line with an intercept equal to $\log K'_{\text{ex}} + 2 \log [\text{NO}_3^{-}]$. Thus at a given temperature, conditional extraction constant (K'_{ex}) was determined by plotting $\log D_{\text{Pd}}$ vs. $\log \text{T(2EH)TDGA}$. Similar experiments were carried out at different temperatures and corresponding $\log K'_{\text{ex}}$ were also determined.

At a given temperature 'T', the Gibbs free energy change (ΔG_{ex}) associated with the extraction process of palladium can be calculated from the value of conditional extraction constant (K'_{ex}) by employing the following equation

$$\Delta G_{\text{ex}} = - 2.303 RT \log K'_{\text{ex}} \quad (13)$$

Combining the equation 13 with the Gibbs's Helmholtz equation

$$\Delta G = \Delta H - T\Delta S \quad (14)$$

and rearranging, we get

$$\log K'_{\text{ex}} = - \Delta H_{\text{ex}}/RT + \Delta S_{\text{ex}}/R \quad (15)$$

Thus from above equation a plot of $\log K'_{\text{ex}}$ vs. $1/T$ gives a straight line with slope value of $\Delta H_{\text{ex}}/R$ and intercept equal to $\Delta S_{\text{ex}}/R$. From these ΔH_{ex} and ΔS_{ex} can be determined.

Fig. 3.8 shows the variation of D_{Pd} as a function of $[T(2\text{EH})\text{TDGA}]$ at various temperatures. From the intercept, conditional extraction constant ($\log K'_{\text{ex}}$) were determined.

Fig. 3.9 shows the variation of D_{Pd} as a function of temperature. From the plot it is evident that palladium extraction decreases with the increase in temperature. Thus the extraction process is found to be exothermic in nature.

Fig. 3.10 shows the variation of $\log K'_{\text{ex}}$ as a function of $1/T$. The slope value obtained from the plot is 2879.16 ± 84.17 which gives the enthalpy of extraction (ΔH_{ex}) equal to $-55.12 \text{ kJmol}^{-1}$ whereas, the intercept value obtained from the plot is -2.31 ± 0.26 giving the entropy of extraction (ΔS_{ex}) equal to $-44.04 \text{ JK}^{-1}\text{mol}^{-1}$. The negative value of enthalpy suggests the extraction of palladium to be exothermic which corroborates the above observations (cf. fig 3.9). The extraction process is disfavored by the negative entropy, a result observed for most extraction processes in which a number of extractant molecules

combine with metal ions and associated anions to form highly ordered extracted complex in the organic phase.

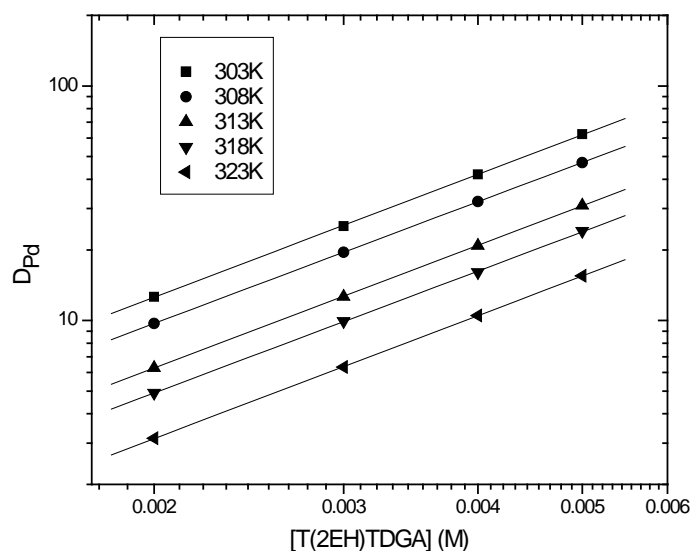


Fig. 3.8. Dependence of D_{Pd} on T(2EH)TDGA concentration. Aqueous phase: 2.5×10^{-4} M Pd in 0.2 M HNO_3 . Organic phase: 0.002 M to 0.005 M T(2EH)TDGA in n-dodecane.

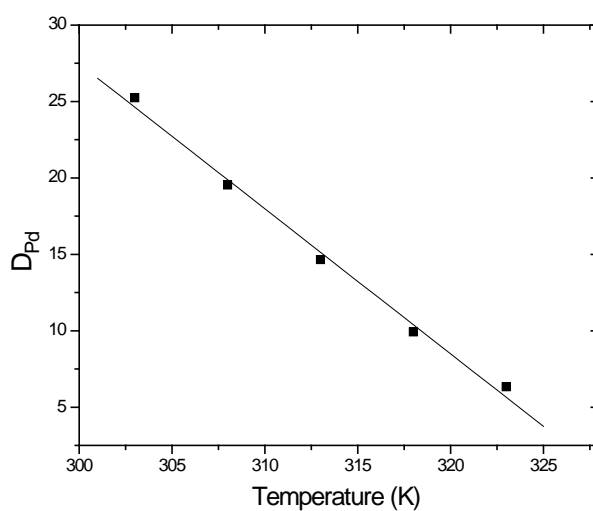


Fig. 3.9. Dependence of D_{Pd} on temperature. Aqueous phase: 2.5×10^{-4} M Pd in 0.2 M HNO_3 . Organic phase: 0.003 M T(2EH)TDGA /n-dodecane.

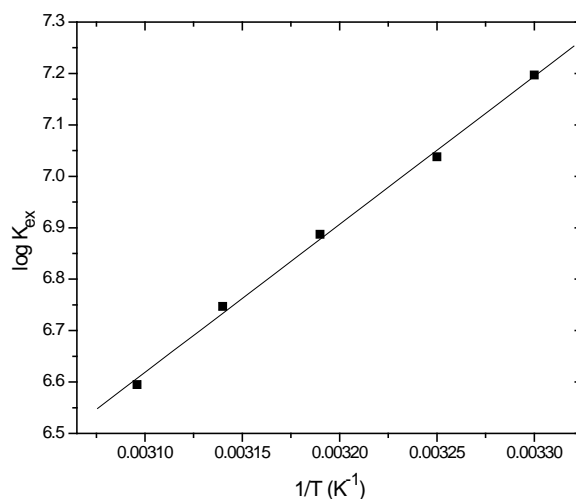


Fig. 3.10 Dependence of conditional extraction constant (K'_{ex}) on temperature.

3.11. FTIR and FT-Raman Studies

It was observed that T(2EH)TDGA possesses very high extractability and selectivity for palladium as compared to other extractants containing 'S' as donor atom. To account for this an effort was made to understand the mode of ligation by T(2EH)TDGA vis a vis dialkylsulphoxides (BESO) as a representative of 'S' donor extractants. Earlier reports have suggested that extractants of the class of dialkylsulphoxides being monodentate, bind with the palladium through 'S' atom of S=O functional group [106, 131-132]. Since T(2EH)TDGA is a multidentate ligand containing both the thioetheric sulphur and amidic groups. It became imperative to examine whether 'S' alone or both the thioetheric sulphur and amidic groups coordinate with palladium. FT-IR and FT-Raman spectra of neat T(2EH)TDGA/n-dodecane and T(2EH)TDGA/n-dodecane after contacting with 10^{-2} M Pd (II) in 4.0 M nitric acid were recorded. Infrared spectra were recorded on a FT-IR spectrometer (JASCO FT-IR-4100) in NaCl cell. Peaks are recorded in cm^{-1} .

FT-Raman spectra were recorded at ambient temperature using a CCD based Raman spectrograph. The 488nm laser line of Ar⁺ laser was used as the excitation wavelength and the laser power was 30 mW. Scattered light was analyzed by a 0.9 m single monochromator coupled with a super-notch filter and detected using a cooled CCD (Andor Technology). The resolution limited line width at 510 nm is measured to be about 3 cm⁻¹ for an entrance slit opening of 50 μm.

The sharp band at 1658 cm⁻¹ (Fig. 3.11) which was assigned to ν(C=O) in the ligand shifted to lower energy suggesting the coordination of the carbonyl group with the palladium.

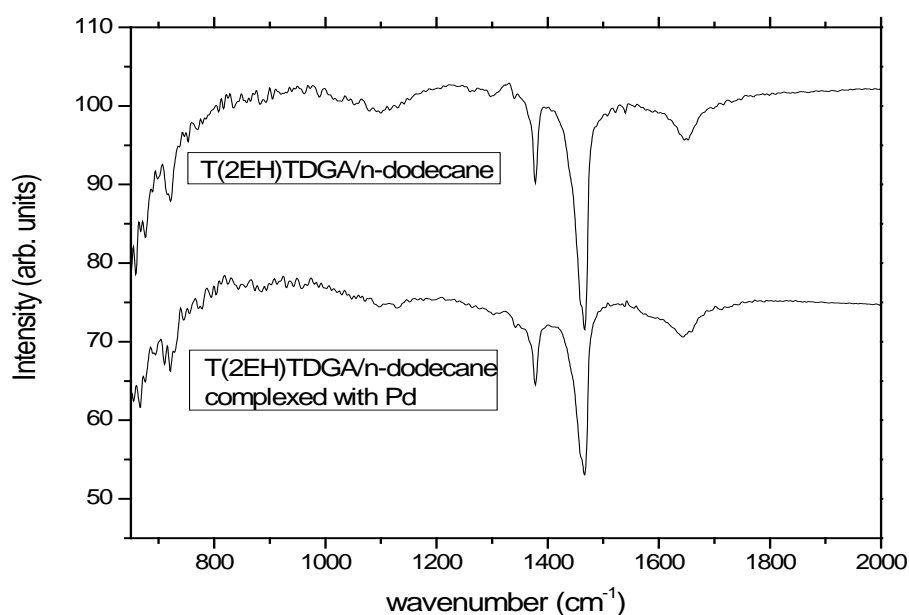


Fig. 3.11. FT-IR spectra of T(2EH)TDGA and Pd(II)- T(2EH)TDGA.

Bands at 677 and 771 cm⁻¹ in FT-Raman spectra (Fig. 3.12) which have contribution from ν(C-S) in the ligand [133] have also been shifted to lower energy indicating the ligation of thioetheric 'S' with the palladium as well. Thus as compared to other monodentate

ligands, T(2EH)TDGA coordinates with palladium through multidonor sites leading to very high stability of extracted complex. This enhanced ligation could be the reason for very high extractability of palladium for T(2EH)TDGA over BESO.

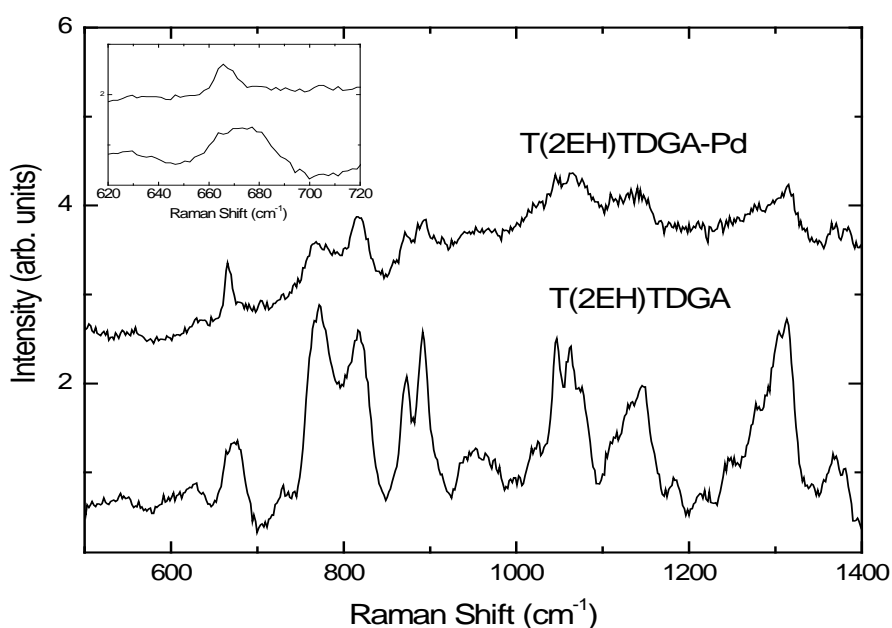


Fig. 3.12. FT-Raman spectra of T(2EH)TDGA and Pd(II)-T(2EH)TDGA.

3.12. Extraction studies with SHLW Solution

To evaluate the distribution behavior of various elements present in SHLW, the batch extraction of SHLW elements was carried out by contacting SHLW with varying concentration of T(2EH)TDGA in n-dodecane. Table 3.2 shows the distribution ratio of various metal ions present in SHLW. From the results it is evident that except palladium, all other metal ions are hardly extracted in the organic phase thus giving very high separation factor ($\geq 10^5$) of palladium with respect to other metal ions. Further, the distribution ratio of palladium is sufficiently high to enable complete extraction possible in single contact.

Table 3.1 Distribution ratio of various metal ions present in SHLW

Aqueous phase: SHLW feed solution, Organic Phase: T(2EH)TDGA/n-dodecane

Constituent Element	Distribution Ratio	
	0.01M T(2EH)TDGA	0.025M T(2EH)TDGA
Pd	282	650*
Cr	$< 10^{-3}$	$< 10^{-3}$
Ni	$< 10^{-3}$	$< 10^{-3}$
Ba	$< 10^{-3}$	$< 10^{-3}$
Mn	$< 10^{-3}$	$< 10^{-3}$
Fe	$< 10^{-3}$	$< 10^{-3}$
Mo	$< 10^{-3}$	$< 10^{-3}$
Sr	$< 10^{-3}$	$< 10^{-3}$
Zr	$< 10^{-3}$	$< 10^{-3}$
Sm	$< 10^{-3}$	$< 10^{-3}$
Y	$< 10^{-3}$	$< 10^{-3}$
Ce	$< 10^{-3}$	$< 10^{-3}$
La	$< 10^{-3}$	$< 10^{-3}$
Nd	$< 10^{-3}$	$< 10^{-3}$
Ca	$< 10^{-3}$	$< 10^{-3}$
Na	$< 10^{-3}$	$< 10^{-3}$
Cs	$< 10^{-3}$	$< 10^{-3}$

*Pd concentration in raffinate was below 0.3ppm.

3.13. Extraction behavior of HLLW elements

To evaluate the feasibility of T(2EH)TDGA/n-dodecane solvent system for palladium separation from HLLW, the extraction behavior of some of the HLLW elements such as U(VI), Am(III), Eu(III), Cs(I), Ru(III) and Sr(II) were studied. Table 3.1 shows the distribution ratio of these elements obtained by equilibrating different concentrations of T(2EH)TDGA/n-dodecane with HLLW feed solution at 3.0 M nitric acid concentration. The results showed negligible extraction of these elements. However, with the increase in concentration of T(2EH)TDGA from 0.001 M to 0.05 M, a slight increase in distribution

ratio of U(VI) and Ru(III) was observed. With the use of 0.01M T(2EH)TDGA/*n*-dodecane, very high distribution ratio of palladium was obtained as compared to other HLLW elements. Therefore, 0.01M T(2EH)TDGA/*n*-dodecane can be used to selectively separate palladium from HLLW elements in nitric acid medium.

Table 3.2. Distribution ratios of HLLW elements. Organic phase: T(2EH)TDGA/*n*-dodecane, aqueous phase: HLLW feed solution.

[T(2EH)TDGA]	D_{Am}	D_{Eu}	D_{Sr}	D_{Cs}	D_{Ru}	D_U
0.001M	$< 1.0 \times 10^{-4}$	$< 1.0 \times 10^{-3}$	$< 1.0 \times 10^{-4}$			
0.01M	$< 1.0 \times 10^{-4}$	$< 1.0 \times 10^{-4}$	$< 1.0 \times 10^{-4}$	$< 1.0 \times 10^{-3}$	0.0014	0.016
0.05M	$< 1.0 \times 10^{-4}$	$< 1.0 \times 10^{-4}$	$< 1.0 \times 10^{-4}$	$< 1.0 \times 10^{-3}$	0.011	0.064

3.14. Reusability of the Extractant

The reusability of the extractant was investigated by contacting the organic phase containing 0.025M T(2EH)TDGA/*n*-dodecane with SHLW followed by stripping with 0.01 M thiourea in 0.1 M HNO₃ in five successive cycles. The stability of the resultant lean organic phase was then evaluated by determining D_{Pd} values from SHLW. It was observed that even after five successive cycles of loading and stripping, the D_{Pd} was almost constant at the original value of 650 (Table 3.3) suggesting excellent reusability of the extractant.

Table 3.3. Distribution data of Pd in five successive cycles of extraction and stripping;

Aqueous phase: SHLW feed solution. Organic phase: 0.025 M T(2EH)TDGA/n-dodecane.

Number of cycles	Distribution Ratio
1	652
2	648
3	659
4	645
5	642
Mean	649.2
S.D.	6.61
R.S.D. (%)	1.02

3.15. Hydrolytic and radiolytic stability studies

Hydrolysis of T(2EH)TDGA by aqueous nitric acid solution and radiolysis of T(2EH)TDGA by gamma irradiation were investigated. The effects of radiolysis and hydrolysis on the extraction behavior of SHLW elements were also studied.

3.15.1. Hydrolysis of T(2EH)TDGA solvent system

Solvent extraction experiments of SHLW elements carried out with 0.025 M T(2EH)TDGA/n-dodecane kept in contact with 3.0 M nitric acid for two weeks revealed that palladium is quantitatively extracted ($E\% \sim 100\%$) with negligible extraction of other elements present in SHLW (Table 3.4). Further the GC-MS of the organic phase does not show any hydrolyzed product. This indicates that T(2EH)TDGA/n-dodecane solvent system does not deteriorate upon contact with 3.0 M nitric acid at least for 2 weeks.

Table 3.4. Distribution ratio of various metal ions present in SHLW

Aqueous phase: SHLW feed solution, Organic Phase: T(2EH)TDGA/n-dodecane.

Constituent Element	Distribution Ratio	
	0.025M T(2EH)TDGA/ n-dodecane(neat) acid	0.025M T(2EH)TDGA/n-dodecane kept in contact with 3.0M nitric for two weeks
Pd	632	618
Cr	$< 10^{-3}$	$< 10^{-3}$
Ni	$< 10^{-3}$	$< 10^{-3}$
Ba	$< 10^{-3}$	$< 10^{-3}$
Mn	$< 10^{-3}$	$< 10^{-3}$
Fe	$< 10^{-3}$	$< 10^{-3}$
Mo	$< 10^{-3}$	$< 10^{-3}$
Sr	$< 10^{-3}$	$< 10^{-3}$
Zr	$< 10^{-3}$	$< 10^{-3}$
Sm	$< 10^{-3}$	$< 10^{-3}$
Y	$< 10^{-3}$	$< 10^{-3}$
Ce	$< 10^{-3}$	$< 10^{-3}$
La	$< 10^{-3}$	$< 10^{-3}$
Nd	$< 10^{-3}$	$< 10^{-3}$
Ca	$< 10^{-3}$	$< 10^{-3}$
Na	$< 10^{-3}$	$< 10^{-3}$
Cs	$< 10^{-3}$	$< 10^{-3}$

Earlier it has been reported that ‘S’ donor extractants, namely, DHS, TIPS etc., undergo oxidation in strong nitric acid medium [103]. Since the acidity of SHLW solution was 3.0 M and T(2EH)TDGA being a sulphur donor extractant, it becomes necessary to study the oxidizing effect of nitric acid on the extractant. For this we investigated the oxidation of sulphur to sulphoxide or sulphone by monitoring the S-O stretching ($\nu(\text{S-O})$) band in the

FT-IR spectra that usually appear in the frequency range of $1000\text{-}1200\text{cm}^{-1}$ [134]. Fig. 3.13 shows the FT-IR spectra of aliquots taken at regular time intervals from T(2EH)TDGA/n-dodecane solvent system kept in contact with 3.0 M nitric acid. No band corresponding to S-O stretching frequency was observed indicating that 'S' atom present in T(2EH)TDGA molecule is resistant to oxidation by the strong acid under given experimental conditions. This can be attributed to the presence of two carbonyl groups present in vicinity of 'S' that itself get protonated and thereby prevent the sulphur atom from being attacked by strong acid. In addition, electron density withdrawal from 'S' atom by amide group can resist the oxidation of sulphur atom.

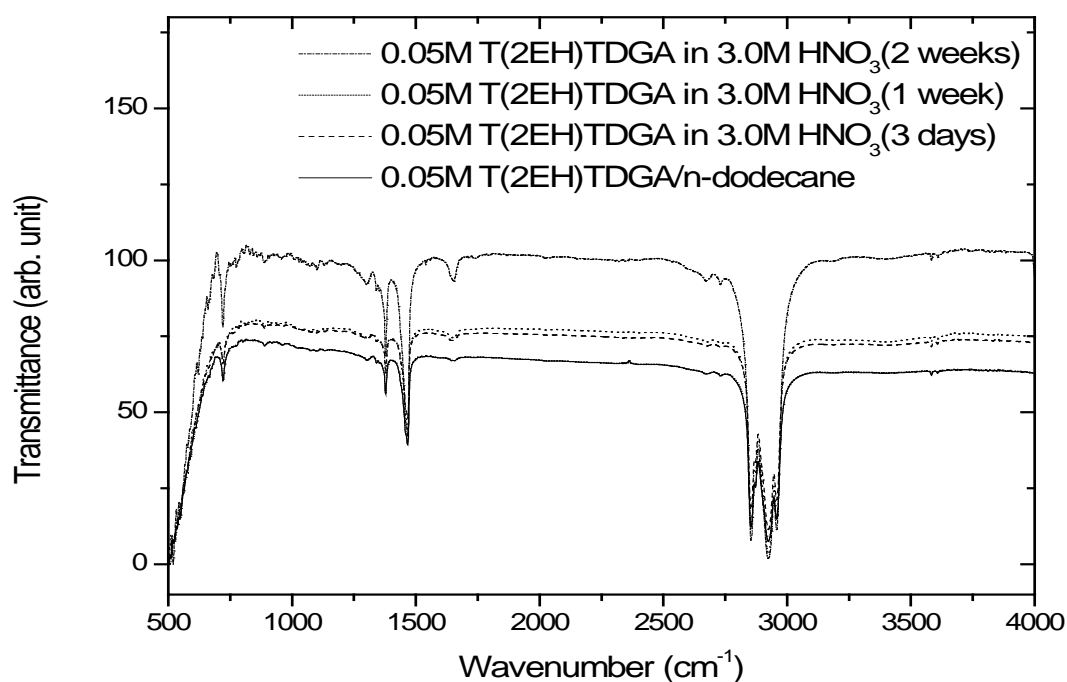


Fig. 3.13. FT-IR spectra of 0.05 M T(2EH)TDGA/n-dodecane kept in 3.0 M Nitric acid.

3.15.2. Qualitative analysis of radiolytic degradation products

The products obtained on radiolysis were identified by GC-MS. The results indicate that the degradation of T(2EH)TDGA by γ irradiation involved the cleavage of amide and thioether linkages. Degradation products of T(2EH)TDGA in case of neat T(2EH)TDGA

and T(2EH)TDGA/n-dodecane were found to be the same and consist mainly of neutral products along with very small quantities of acidic degradation products. Fig. 3.14 shows the GC-MS spectra of neat T(2EH)TDGA whereas Fig. 3.15 shows the GC-MS of neat T(2EH)TDGA after a total dose of 0.5 MGy. The major degradation products were identified as bis(2-ethylhexyl)amine (BEHA), *N,N*-bis-(2-ethylhexyl) formamide (BEHFA), *N,N*-bis-(2-ethylhexyl)-2-[(2-oxoethyl) sulfanyl] acetamide (BEHOMSAA) *N,N*-bis-(2-ethylhexyl) acetamide (BEHAA), *N,N*-bis-(2-ethylhexyl) (methyl sulfanyl) formamide (BEHMSFA), *N,N*-bis(2-ethylhexyl) thioglycolamide (BEHTGA). The chromatogram (Fig. 3.16) shows the degradation products formed by radiolysis of solvent system in contact with 3.0 M nitric acid at 0.5 MGy. The degradation products were found to be the same as in case of neat T(2EH)TDGA and 0.025 M T(2EH)TDGA/n-dodecane.

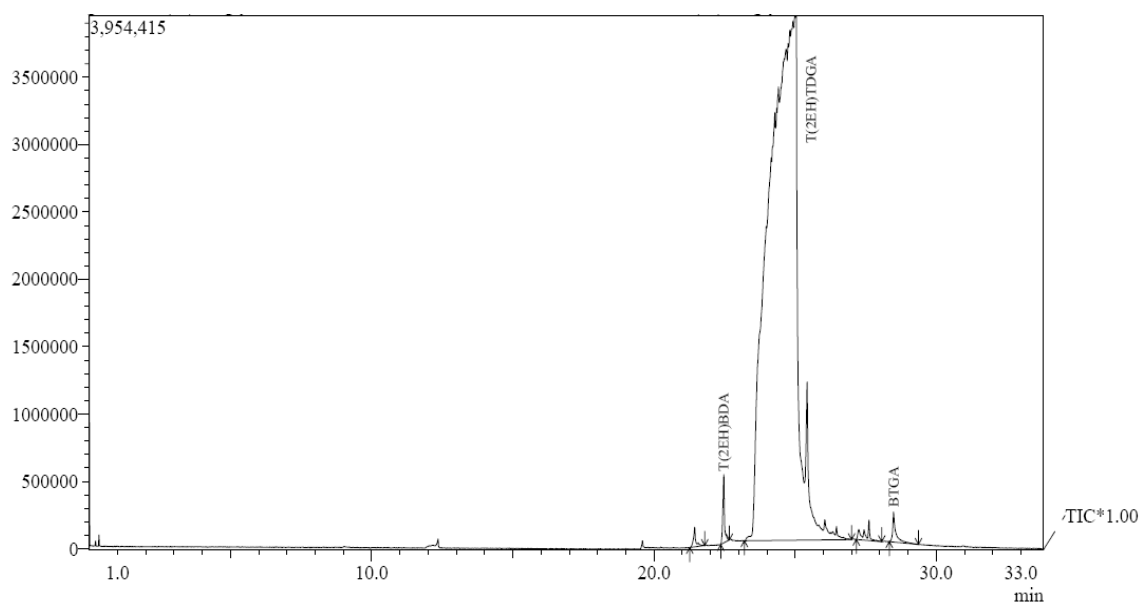


Fig. 3.14. GC-MS of pure T(2EH)TDGA

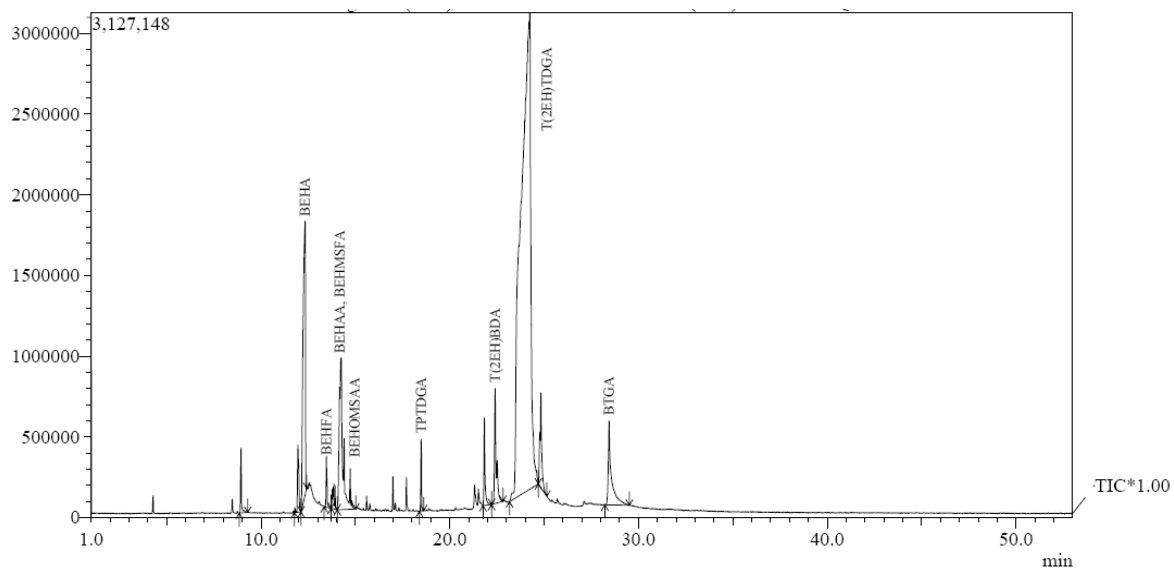


Fig. 3.15. GC-MS of neat T(2EH)TDGA after an absorbed dose of 0.5 MGy.

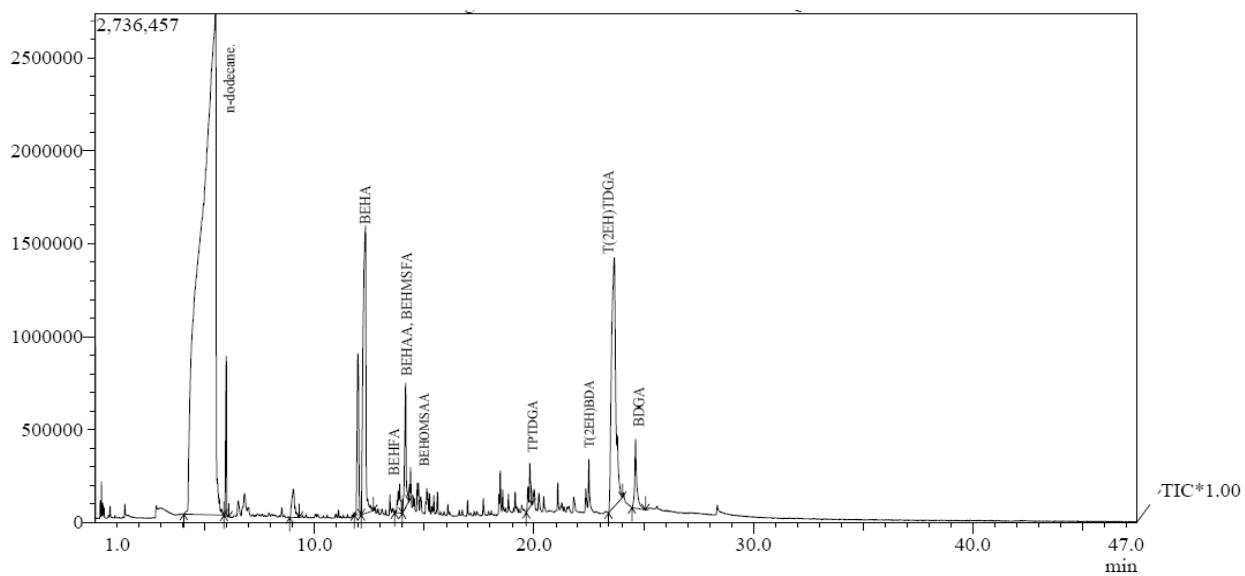


Fig. 3.16. GC-MS of 0.05M T(2EH)TDGA/n-dodecane in contact with 3.0M nitric acid after an absorbed dose of 0.5 MGy.

EI-MS data for T(2EH)TDGA and its degradation products are shown in Table 3.5. From these degradation products, the probable path of degradation can be predicted.

Table 3.5. EI-MS of degradation products found in T(2EH)TDGA after an absorbed dose of 0.5 MGy.

S. No.	Compound	EI-MS
1	BEHA	240 (M ⁺), 185, 142 (bp), 86, 71
2	BEHFA	268 (M ⁺), 200, 142, 102 (bp), 71
3	BEHAA	282 (M ⁺), 268 (bp), 216, 142, 118, 71
4	BETGA	313 (M ⁺), 281, 268, 185, 129, 69 (bp)
5	BEHMSFA	329 (M ⁺), 268, 230, 142 (bp), 118, 71
6	BEHOMSAA	356 (M ⁺), 313, 268, 216 (bp), 117, 71
7	TPTDGA	424 (M ⁺), 313, 240 (bp), 227, 142, 71
8	T(2EH)BDA	562(M ⁺), 463, 322 (bp), 240, 118,71
9	T(2EH)TDGA	596 (M ⁺), 553, 356, 268, 184 (bp), 71
10	BTGA	627 (M ⁺), 596, 521, 268, 184 (bp), 71

*bp is base peak

Fig. 3.17 shows the probable paths, indicated as (a), (b) and (c) for the formation of degradation products of T(2EH)TDGA. The products of path (a) namely BEHA and TDGAMA are formed by cleavage of amide bond. BEHAA and BEHGA of path (b) are formed by cleavage of thioether bond. Products of path (c), namely BEHMSFA and BEHFA are formed by cleavage of carboxyl linkage of amide. Additionally there is another product namely TPTDGA which is assumed to be formed by the cleavage of alkyl groups from the amidic moiety.

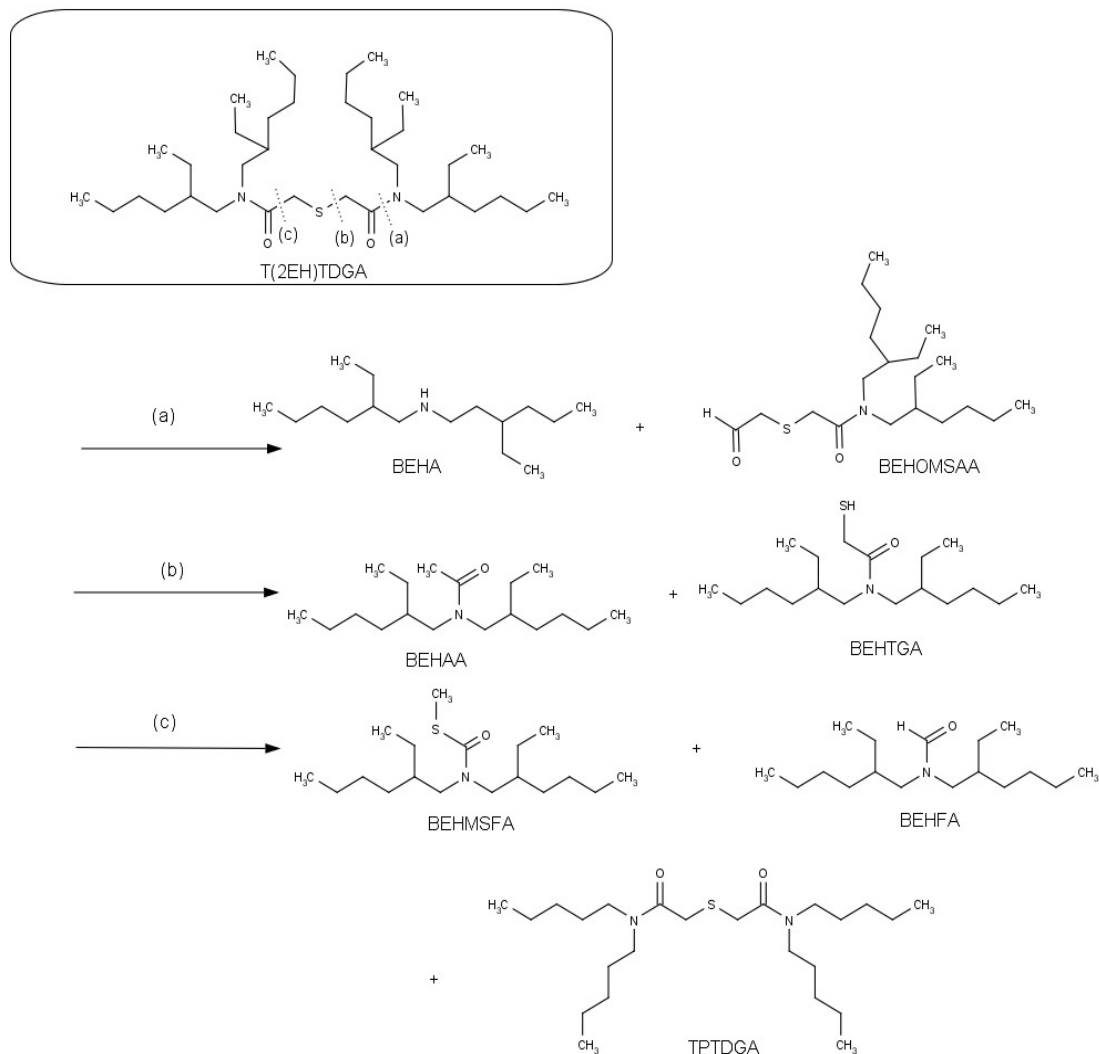


Fig. 3.17. Radiolytic degradation paths of T(2EH)TDGA

3.15.3. Radiolytic stability of T(2EH)TDGA solvent system

Pure T(2EH)TDGA, 0.025 M - 0.1 M T(2EH)TDGA/n-dodecane and 0.025 M - 0.05 M T(2EH)TDGA /n-dodecane in contact with 3.0 M HNO₃ were irradiated with γ radiations. The plot of residual concentration of T(2EH)TDGA represented as [T(2EH)TDGA]_{irr} against the absorbed dose is shown in Fig. 3.18. The figure shows that the decrease in concentration of T(2EH)TDGA is considerably less in case of neat solvent compared to T(2EH)TDGA in n-dodecane. The degree of degradation by radiation is

estimated from the slope of the line. The following equation defined by Mincher and Cury [135] is used to estimate the slope.

$$C = C_0 \cdot \exp(-k \cdot d) \quad (16)$$

Where C is the concentration of T(2EH)TDGA (in mol/L) after irradiation, C_0 is the initial concentration of T(2EH)TDGA before irradiation, d is the dose absorbed by the sample and k is the dose constant. The absolute value of dose constant indicates the degree of degradation by radiation and obtained by slopes of the plots of Fig. 3.18. From the plot it is evident that slope of T(2EH)TDGA/n-dodecane is greater than neat T(2EH)TDGA indicating that the presence of n-dodecane have sensitization effect on degradation of T(2EH)TDGA. This is also seen when, on decreasing the concentration of T(2EH)TDGA from 0.1 M to 0.025 M, that is, on increasing the dodecane content, the degradation rate increases. Mincher et al have reported the radiolysis of aliphatic diluents such as dodecane, where the major product of the radiolysis were found to be carbon centered radical cations [115]. These radical cations undergo charge transfer reaction with the extractant molecule due to difference in their ionization potentials resulting in formation of radical cation of the extractant molecule, thus making the latter more susceptible for degradation. These findings are in line with our observations where dodecane was found to sensitize radiolysis of T(2EH)TDGA. The degradation curve of 0.025 M T(2EH)TDGA/n-dodecane in contact with 3.0 M nitric acid was found to be almost similar to 0.025 M T(2EH)TDGA/n-dodecane indicating that nitric acid has less effect on the extent of radiolysis. However, the presence of small amount of acidic degradation products could be attributed to the oxidation/hydrolysis of intermediate degradation products by various species formed from radiolysis of nitric acid and dodecane. The plot also indicates that the loss of T(2EH)TDGA in all the studies is less than 10% up to an absorbed dose of 0.2 MGy, above which the degradation rate was found to increase.

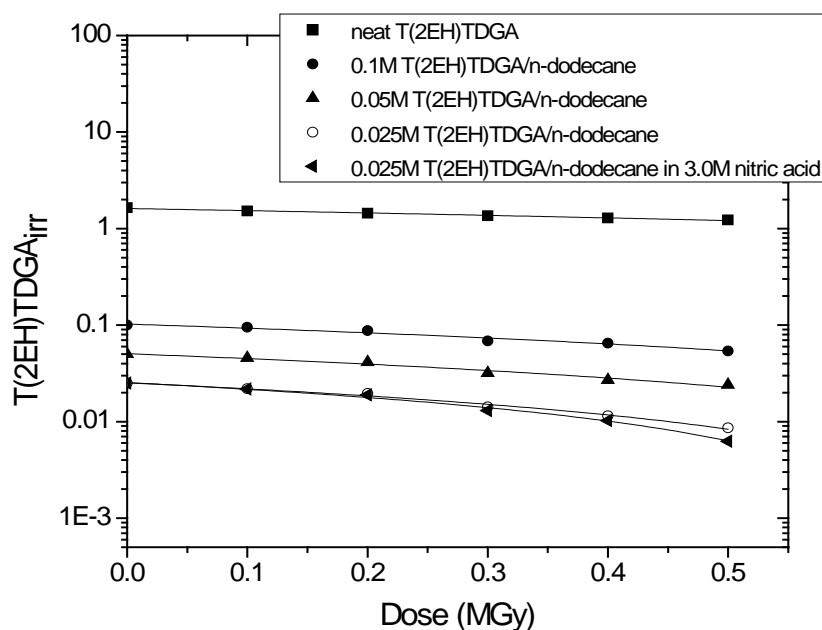


Fig. 3.18. Degradation curve of T(2EH)TDGA as a function of absorbed dose.

As far as the effect of gamma irradiation on speciation of Pd is concerned, there is no literature available on this aspect. However, most of the earlier reports on palladium extraction from HLW have indicated the presence of palladium as Pd(II) ($\text{Pd}(\text{NO}_3)_2$) in PUREX process raffinate. Therefore, we have assumed that palladium will remain predominantly in +2 oxidation state.

The radiation chemical yield 'G' defined as the number of T(2EH)TDGA molecules decreased by absorption of 100 eV energy, is calculated by using the following equation:

$$C = C_0 \cdot \exp(-1.04 \times 10^{-10} \text{ GMD}) \quad (17)$$

where, M is the molecular weight of T(2EH)TDGA and D is the absorbed dose (Gy). By

rearranging the above equation and taking logarithm of both the sides of the equation we get,

$$\ln(C/C_0) = -1.04 \times 10^{-10} \text{ GMD} \quad (18)$$

A plot of $\ln(C/C_0)$ vs. D gives a straight line whose slope will be equal to 1.04×10^{-10} GM. From the slope, 'G' value for neat T(2EH)TDGA was determined to be 9.19 (Fig. 3.19). The 'G' value of T(2EH)TDGA is comparable with other extractants used for processing of HLW for various applications. This indicates good radiolytic stability of T(2EH)TDGA for use in the separation of Pd from HLW.

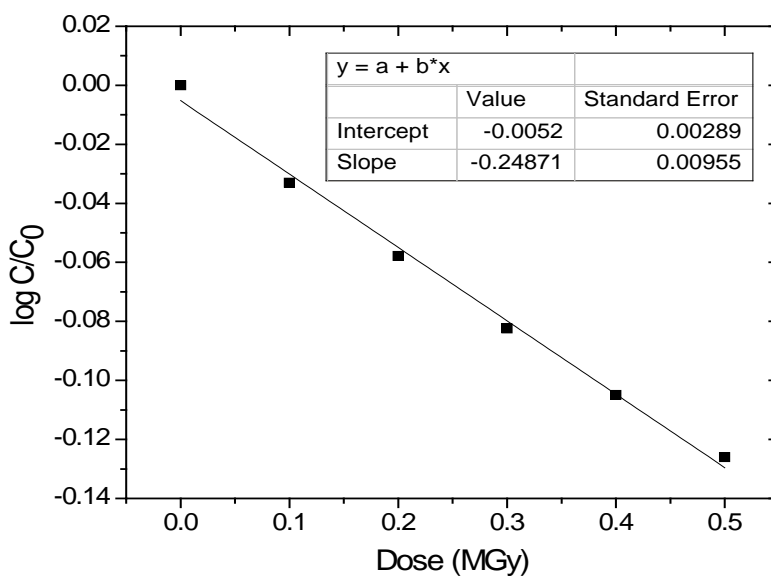


Fig. 3.19. Plot of $\log C/C_0$ vs. Dose (MGy) for neat T(2EH)TDGA.

3.15.4. Effect of radiolysis of solvent on extraction behavior of Pd(II) and other SHLW Elements

Fig. 3.20 shows the distribution ratio of palladium present in 3.0 M nitric acid as a function of absorbed dose. The solvents used were 0.025 M T(2EH)TDGA/n-dodecane, 0.05 M T(2EH)TDGA/n-dodecane, which were irradiated in contact with 3.0 M nitric acid. The decrease in distribution ratio of palladium was observed with increase with absorbed dose. Though, the distribution ratio decreases with increase in absorbed dose, the high extraction (%E) of palladium was maintained even up to 0.5 MGy (Fig. 3.21). For

0.025 M T(2EH)TDGA/n-dodecane, the distribution ratio was less affected up to an absorbed dose of 0.2 MGy after which it decreases significantly. However, for 0.05 M T(2EH)TDGA/n-dodecane the decrease in distribution ratio of palladium is gradual even up to 0.5 MGy. This could be due to sensitization effect of n-dodecane which would be larger in the case of 0.025 M T(2H)TDGA/n-dodecane as compared to that in the case of 0.05 M T(2EH)TDGA/n-dodecane.

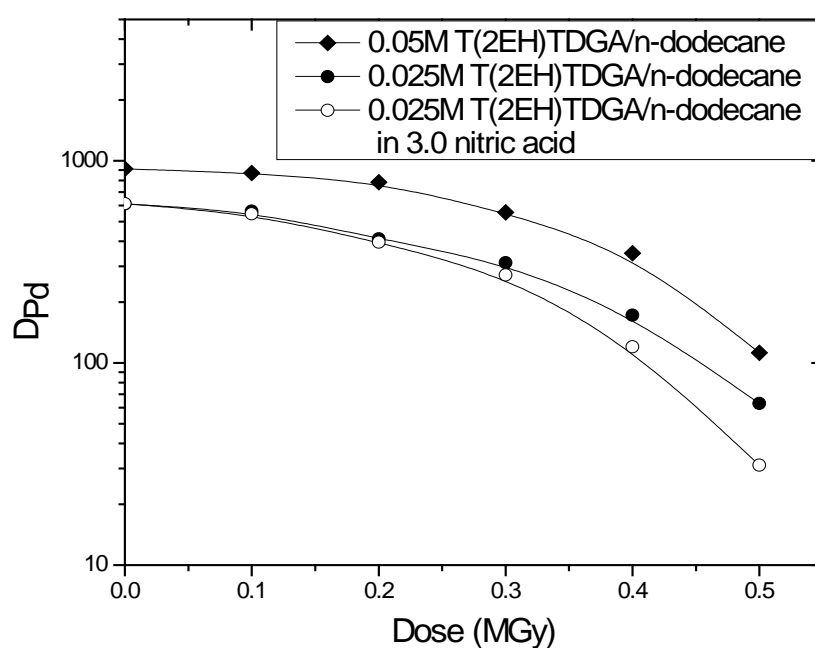


Fig. 3.20. Extraction of Pd as a function of absorbed dose. Aq. phase: 1×10^{-3} M Pd in 3.0 M HNO₃.

For other elements present in SHLW, the distribution ratios were found to be very small ($D_M \leq 10^{-3}$) and remained so even with increase in absorbed dose. This shows that even under high radiation environments the extractant retained its remarkable selectivity for palladium over other metal ions present in SHLW.

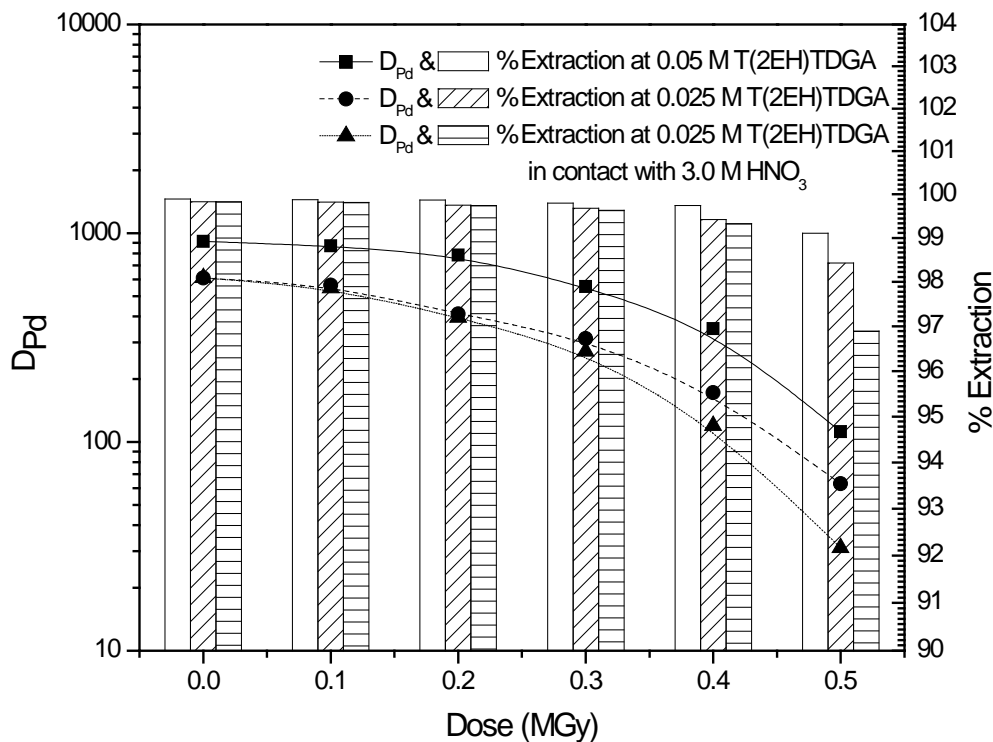


Fig. 3.21. Comparison of D_{Pd} and % Extraction of palladium as a function of absorbed dose. Aq. phase: 1×10^{-3} M Pd in 3.0 M HNO_3 .

Since the back extraction of palladium from the loaded organic phase was done using 0.01 M thiourea in 0.1 M nitric acid solution, it was of interest to study the stripping behavior under radiation environment. For this purpose, the irradiated solvent namely 0.05 M T(2EH)TDGA/n-dodecane was contacted with SHLW solutions and then the loaded palladium was back extracted using 0.01 M thiourea in 0.1 M nitric acid medium. The back extraction efficiency of the unirradiated and irradiated solvent was nearly the same regardless of absorbed dose. This suggests the possible recovery of palladium even in radiation environment using thiourea as a stripping agent.

During the reprocessing of actual high level waste solution the solvent is expected to receive dose in the range of few kGy per year [136] which is much lower than the dose of even 0.2 MGy. The findings, thus suggest that the solvent is fairly stable and retains its extraction and stripping properties after gamma radiation dose of 0.2 MGy and it is therefore suitable for use in palladium separation from high level liquid waste.

3.16. Extractive Spectrophotometric Determination of Palladium

Extractive spectrophotometric methods are simple techniques and have been widely used for determination of palladium. Palladium forms intensely colored complexes with hydrazones, dyes, dithiocarbonates, oximes, and thio compounds. Using this property a number of extractive spectrophotometric methods of palladium determination with various reagents such as di-2-pyridylmethanone-2-(5-nitro)pyridylhydrazone [137], pyridine-2-acetaldehydesalicyloylhydrazone [138], di-2-pyridylketonebenzoylhydrazone [139], Isonitrosobenzoylacetone [140], isonitrosothiocamphor [141], o-butyl dithiocarbonate [142], diphenylthiovioluric acid [143], 2-carboxy-2'-hydroxy-5-methylazobenzene [144], Pyridoxal-4-phenyl-3-thiosemicarbazone [145], Benzylloxybenzaldehyde thiosemicarbazone (BBTSC) [146], N-ethyl-3-carbazolecarbaxaledethiosemicarbazone [147] and α -benzoin oxime (ABO) [148] have been developed. However, the existing methods suffer from various limitations such as longer extraction periods [137-139, 143], temperature control [142], narrow pH range [138, 140-142, 145-147], less stability [140], and interference from other metal ions [137, 142, 144, 148]. Moreover, in some methods [139-141], the extraction is not quantitative. Therefore, there is a need of more effective reagent for extractive and spectrophotometric determination of Pd. It has been observed that *N,N,N',N'*-tetra-(2-ethylhexyl) thiodiglycolamide (T(2EH)TDGA) is itself colorless but forms a colored complex with palladium. Since, the extractant is found to be selective for Pd, therefore, it was envisaged to use this extractant as a reagent for spectrophotometric determination of Pd. The use of this reagent is advantageous as it can be synthesized at low cost with high purity and yield.

Thus the extraction and spectrophotometric determination of palladium using T(2EH)TDGA have been investigated. The extractant have also been evaluated for its use in separation and estimation of palladium present in simulated HLW.

3.16.1. Extraction and Absorbance Measurements

An aliquot of sample containing 1–20 $\mu\text{g ml}^{-1}$ of palladium (II) solution in desired acidity was taken in a separatory funnel and was contacted with equal volume (4 ml each) of dodecane containing appropriate concentration of T(2EH)TDGA for 15 min. The two phases were allowed to separate and the organic phase was dried over anhydrous sodium sulphate. The absorbance of the solution was measured against neat T(2EH)TDGA/n-dodecane solution.

The absorption spectra of Pd bearing solutions were recorded using a UV–vis spectrophotometer (JASCO V-550) in the wavelength range of 200–700 nm in steps of 2 nm. A special cell with path length 1 mm was used for absorbance measurement.

Fig. 3.22 shows the absorbance spectra of both the neat T(2EH)TDGA/n-dodecane and Pd-T(2EH)TDGA/n-dodecane complex. The yellow colored complex absorbed strongly at ~ 300 nm. Since neat T(2EH)TDGA/n-dodecane also shows absorption in this region, it has been used as reagent blank during the absorbance measurement of Pd-T(2EH)TDGA complex.

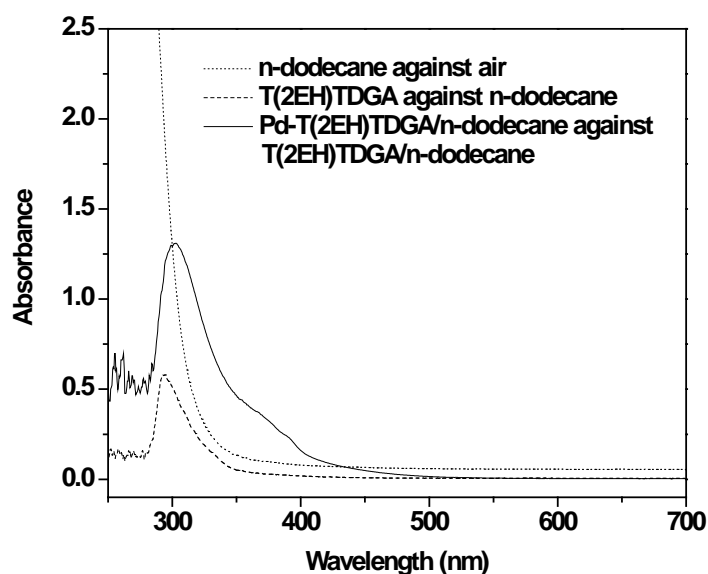


Fig. 3.22. Absorption spectrum of T(2EH)TDGA/n-dodecane and Pd-T(2EH)TDGA/n-dodecane complex. Concentration of Pd = 1.0×10^{-4} M in 1.0 M nitric acid. Concentration of T(2EH)TDGA = 2.0×10^{-3} M.

3.16.2. Effect of diluents

10^{-4} M Pd in 1.0 M nitric acid was contacted with 0.002 M T(2EH)TDGA dissolved in different diluents. Fig. 3.23 shows the absorption spectra of Pd loaded T(2EH)TDGA in different diluents. Almost comparable absorbance observed for the diluents could be due to the fact that uptake of palladium by T(2EH)TDGA is quantitative irrespective of the nature of the diluents as observed earlier. Furthermore, since palladium is extracted as neutral species $[\text{Pd}(\text{NO}_3)_2 \cdot \text{T}(2\text{EH})\text{TDGA}]$ its extraction and, therefore, the absorbance of extracted complex is maximum in neutral diluents like n-dodecane. Therefore, in subsequent experiments, n-dodecane was used as diluent.

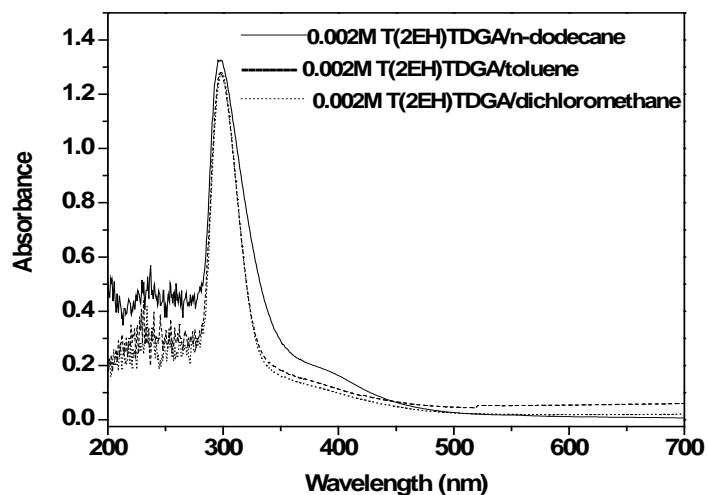


Fig. 3.23. Effect of diluents. Concentration of Pd = 1.0×10^{-4} M in 1.0 M nitric acid. Concentration of T(2EH)TDGA = 2.0×10^{-3} M.

3.16.3. Effect of acids

Fig. 3.24 shows the absorption spectra of 0.002 M T(2EH)TDGA/n-dodecane after contacting with palladium solutions in different acids, namely, nitric, sulfuric and hydrochloric acid. Low absorbance values observed in sulphuric acid medium could be attributed to low uptake of palladium by T(2EH)TDGA in sulphuric acid medium. The maximum absorbance was obtained in nitric acid medium and hence it was used in all subsequent experiments. To investigate the effect of nitric acid concentration on absorbance, 0.002 M T(2EH)TDGA/n-dodecane was contacted with palladium in nitric acid solution of 0.5 M to 3.0 M. The absorbance was found to be almost same for the acid range studied. Thus the analysis of Pd can be done in the nitric acid concentration range of 0.5 M to 3.0 M.

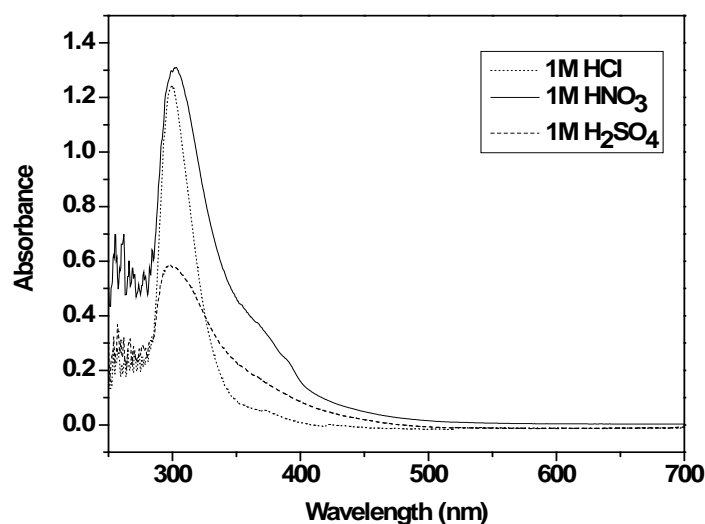


Fig. 3.24. Effect of acid. Concentration of Pd = 1.0×10^{-4} M, concentration of T(2EH)TDGA = 2.0×10^{-3} M.

3.16.4. Validity of Beer law

Aqueous solutions containing varying amount of palladium in 0.5 M nitric acid were contacted with 0.002 M T(2EH)TDGA/n-dodecane. Fig. 3.25 shows that there is a linear

increase in the absorbance within the concentration range of 1.0 to 15 μgml^{-1} of palladium (II) at ~ 300 nm, indicating that Beer's law is applicable within this range. The molar absorptivity of the complex was found to be $1.29 \times 10^5 \text{ M}^{-1}\text{cm}^{-1}$ at ~ 300 nm.

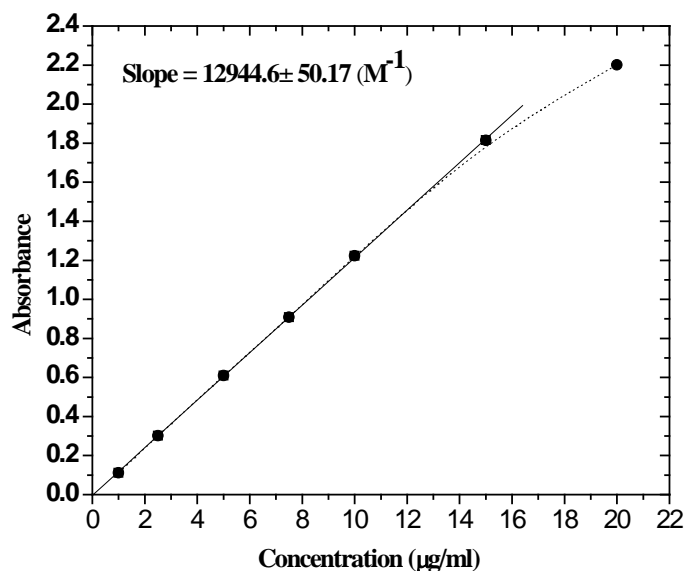


Fig. 3.25. Calibration plot. Concentration of Pd = 1.0 $\mu\text{g/ml}$ to 20 $\mu\text{g/ml}$, concentration of T(2EH)TDGA = 2.0×10^{-3} M.

3.16.5. Nature of the extracted species

The composition of Pd-ligand complex was determined by Job's continuous variation method [14] (Fig. 3.26). Equimolar solution of T(2EH)TDGA and Pd (1.0×10^{-4} M) having different volumes (1-7 ml) were contacted to obtain the different ratio of T(2EH)TDGA and Pd(II). Absorbance of the organic phase was plotted against the mole fraction of palladium. The ratio of metal to ligand was found to be 1:2. This stoichiometry corroborates well with the previously determined values using slope analysis method.

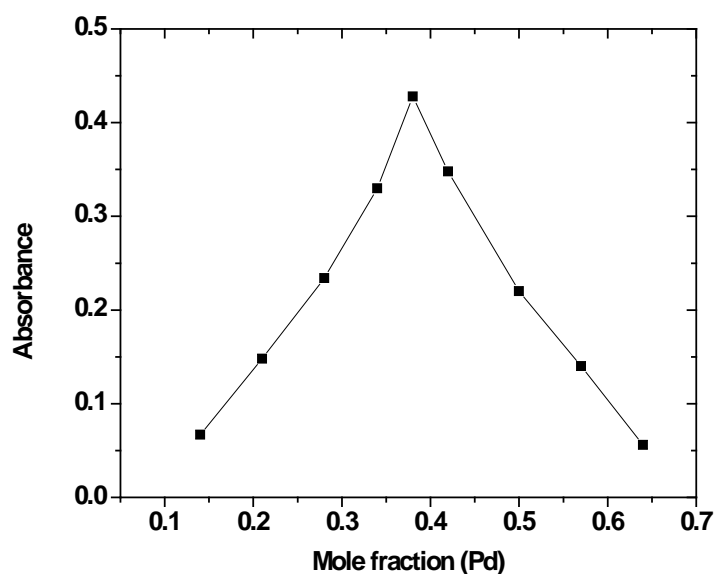


Fig. 3.26. Job's plot. Concentration of Pd = 1.0×10^{-4} M in 0.5 M HNO₃, concentration of T(2EH)TDGA = 1.0×10^{-4} M.

3.16.6. Precision and Accuracy

Table 3.6 shows the average palladium concentration of four samples, each containing $10 \mu\text{gml}^{-1}$ of palladium (II). Very small values of the standard deviation, relative standard deviation and standard error for this method clearly indicate good precision and accuracy of this method.

Table 3.6. Determination of concentration of Pd using Spectrophotometric method.

Organic phase: 2.0×10^{-3} M in n-dodecane. Aqueous phase acidity: 1.0 M HNO₃.

Pd taken ($\mu\text{g/ml}$) in each sample	10
Pd found ($\mu\text{g/ml}$) in samples	9.89 ± 0.04 (1σ)
Relative standard deviation = 0.45%	
Standard error = 0.02	

3.16.7. Extraction and spectrophotometric determination of Pd in SHLW

Determination of palladium in HLW solution is of interest because the concentration of palladium affects its solubility in glass matrix during vitrification process. Accordingly, a SHLW was made representing the actual concentrations of various metal ions present in HLW. This SHLW was analyzed, in triplicate, for palladium by the procedure developed above and the same solution was also analyzed for palladium using ICP-AES. The results are shown in Table 3.7. The palladium concentration in simulated HLW obtained by extractive spectrophotometry is close to that obtained by ICP-AES within 2.0 to 5.0%. Corrosion products and most of the fission products present in simulated high level liquid waste do not interfere in the determination of palladium. The method has shown adequate tolerance for all the major metal ions expected to be present along with palladium in HLW.

Table 3.7. Determination of concentration of palladium using ICP-AES and Spectrophotometric method. Organic phase: 2.0×10^{-3} M in n-dodecane, Aqueous phase: SHLW diluted 20 times (Final acidity 1.0 M HNO₃).

Pd estimated using ICP-AES	9.37 µg/ml
Pd estimated using Spectrophotometric method	9.22 ± 0.04 µg/ml

In table 3.8, the various methods available of estimation of Pd have been summarized and thus can be compared with this work. It can be noted that with this ligand the highest molar absorptivity have been achieved and thus this method can appropriately be used for palladium estimation.

Table 3.8. Comparison of the present method with the other spectrophotometric methods for the determination of palladium(II).

S. No.	Reagent	Conditions	λ_{\max} (nm)	ϵ_{\max} (L.mol ⁻¹ cm ⁻¹)
1.	Di-2-pyridyl-methanone-2-(5-nitro)pyridyl-hydrazone	Dichloroethane, 0.1M to 2.5M HCl	560	37, 800
2.	Pyridine-2-acetaldehyde salicyloyl hydrazone	Chloroform, pH 2.0 to 4.25	425	13, 087
3.	Di-2-pyridylketonebenzoylhydrazone	Benzene, 0.1M H ₂ SO ₄	455	9.3 x 10 ³
4.	Isonitrosobenzoylacetone	Benzene, 0.5M acetic acid solution	405	1.0 x 10 ⁴
5.	Diphenylthiovioluric acid	Acetone, CHCl ₃ , pH 1.0 to 3.5	425	-
6.	2-carboxy-2'-hydroxy-5-methylazobenzene	pH 1.5 to 3.8	560	7,109
7.	Pyridoxal-4-phenyl-3-thiosemicarbazone	Benzene, pH 3.0	460	2.2 x 10 ⁴
8.	Benzoyloxybenzaldehydethiosemicarbazone	Cyclohexanol, pH-5.	365	0.4 x 10 ⁴
9.	N-ethyl-3-carbazolecarbaxaledehyde-thiosemicarbazone	n-butanol, pH- 4.0.	410	1.6 x 10 ⁴
10.	α -benzoin oxime	Hexone, 1M HNO ₃ .	332	4.0 x 10 ³
11.	T(2EH)TDGA (present work)	Dodecane, 0.5 to 4.0 M HNO ₃ .	300	1.3 x 10 ⁵

Conclusions

A novel neutral multidentate ligand, namely, *N,N,N',N'*-tetra-(2-ethylhexyl)thiodiglycolamide (T(2EH)TDGA) was evaluated for Pd extraction from HLLW. The extraction equilibrium was achieved in less than 5 min. Palladium was quantitatively extracted above 3.0 M nitric acid and its complete back extraction was achieved in single contact using 0.01M thiourea in 0.1 M nitric acid. The stoichiometry of species extracted into the organic phase was found to be $\text{Pd}(\text{NO}_3)_2 \cdot 2\text{T}(2\text{EH})\text{TDGA}$. Acid uptake studies have shown 1:1 stoichiometry between T(2EH)TDGA and HNO_3 at nitric acid concentration above 3.5 M. The acid uptake constant (K_H) of T(2EH)TDGA molecule was found to be 0.62. The temperature variation studies have shown that the extraction process of palladium by T(2EH)TDGA is exothermic in nature and is enthalpy driven whereas the entropy factor counteracts it. Extraction studies with HLLW elements have shown negligible uptake of U, Am, Eu, Sr, Cs and Ru. Reusability of the extractant was demonstrated and the quantitative recovery of palladium from the stripping solution was attained. T(2EH)TDGA is found to be stable towards hydrolysis under ambient conditions, “S” atom being protected by neighboring amidic groups towards oxidation under strong nitric acid medium. 0.05M T(2EH)TDGA/*n*-dodecane solvent system retained its extraction and stripping properties up to a high gamma radiation dose of 0.2 MGy, thereby making it one of the most promising candidates for separation and recovery of palladium from HLLW. The radiolysis of T(2EH)TDGA is found to be enhanced by the presence of *n*-dodecane. Degradation of T(2EH)TDGA molecule occurs mainly through cleavage of thioetheric and amidic linkages. The radiation chemical yield “G” of T(2EH)TDGA was determined to be 9.19 which is comparable to that of other extractants proposed for reprocessing of HLLW for different applications. Solvent extraction studies

with SHLW elements revealed the possible application of extractant for selective separation and recovery of palladium from high level liquid waste.

A simple and highly selective method has been developed for the extractive spectrophotometric determination of Pd (II) with T(2EH)TDGA. The complex is stable and obeys Beer's law over the range of 1–15 $\mu\text{g ml}^{-1}$ Pd at ~ 300 nm with molar absorptivity of $1.29 \times 10^5 \text{ M}^{-1} \text{ cm}^{-1}$. The method was found to be precise with relative standard deviation less than 0.5%. The proposed method was satisfactorily applied to the determination of palladium in simulated high level liquid waste samples.

CHAPTER 4

Evaluation of *N,N,N',N'*-tetra-(2-ethylhexyl)-dithiodiglycolamide (DTDGA) for separation of Pd(II) from HLLW

In chapter 3, evaluation of novel 'S' donor ligand namely *N,N,N',N'*-tetra-(2-ethylhexyl) thiodiglycolamides (T(2EH)TDGA) for separation and recovery of palladium from HLLW solution was described. The extractant has shown remarkable extractability and selectivity for Pd over other metal ions present in HLLW which makes it one of the most promising candidates for the said purpose. High selectivity and extractability of the ligand was attributed to the presence of thioetheric sulphur and amidic moiety appropriately placed in the ligand to chelate through more than one donor sites. However, there are various aqueous streams where the concentration of palladium is in sub ppm levels for which even more efficient extractant is required along with high selectivity. To seek an even more efficient ligand for the said purpose, another novel ligand, namely, *N,N,N',N'*-tetra-(2-ethylhexyl)-dithiodiglycolamide (DTDGA) has been explored by us. It was envisaged that judicious incorporation of one more sulphur atom would result in more chelation thereby increasing the overall extractability & hence increasing the ligand economy while retaining the selectivity.

4.0. Evaluation of the Extractant

The synthesis and characterization of the ligand has been discussed in chapter 2. In this chapter the evaluation of the ligand for the extraction of Pd(II) vis-à-vis other metal ions present in HLLW has been discussed.

4.1. Extraction equilibrium studies

Figure 4.1 shows the variation of percentage extraction (% E) of palladium as a function of contact time. It is evident that under chosen experimental conditions the extraction equilibrium was achieved within two to five minutes.

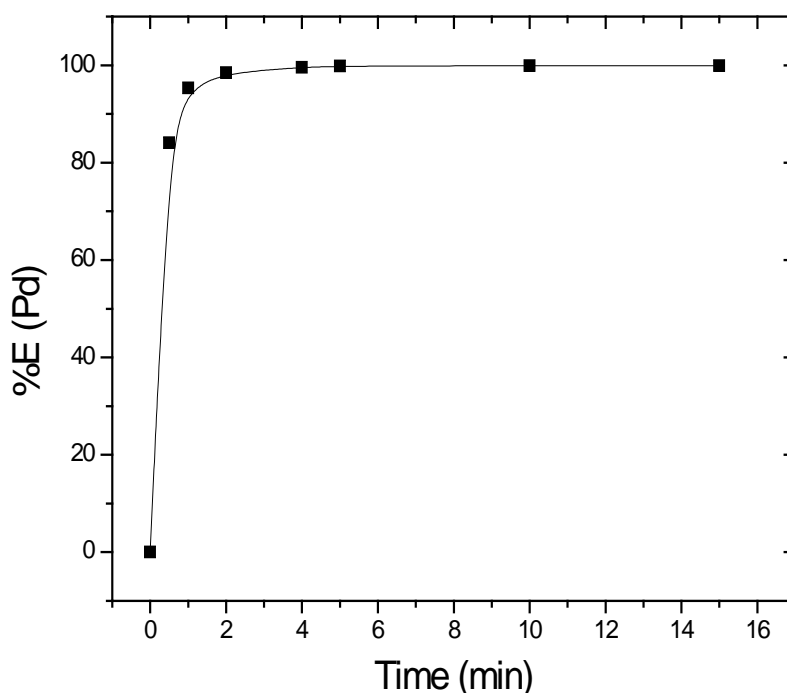


Fig. 4.1. Variation of % E of palladium as a function of contact time. Organic phase: 0.0015 M DTDGA/n-dodecane, Aqueous phase: 10^{-3} M palladium in 3.0 M nitric acid.

4.2. Effect of nitric acid concentration on palladium extraction

Figure 4.2 shows the variation of D_{Pd} with 0.0015 M DTDGA/n-dodecane against initial nitric acid concentration. From figure it is evident that D_{Pd} increases with increase in nitric acid concentration up to 3.0 M, after which D_{Pd} remains almost constant. The initial

increase in D_{Pd} could be attributed to either the salting out effect due to increase in nitrate ion concentration or the participation of nitric acid molecule in the formation of metal complex. Thus, to investigate the participation of nitric acid in the extraction reaction, D_{Pd} was determined from nitric acid solutions of fixed ionic strength of 3.0 M (H, Na)NO₃. Figure 4.3 shows that D_{Pd} remains unchanged with nitric acid concentration at fixed ionic strength. This indicates that HNO₃ molecule itself does not participate in the complex formation. However, with increase in nitric acid concentration the increase in D_{Pd} (cf. fig. 4.2) could be attributed to the salting out effect of nitrate ion which participates in complex formation.

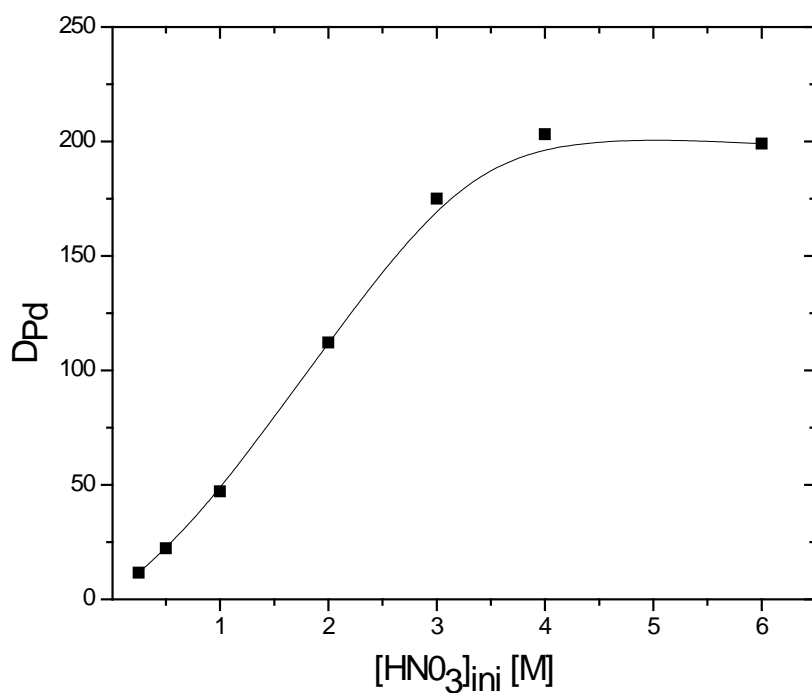


Fig. 4.2. Effect of nitric acid concentration on distribution ratio of palladium (D_{Pd}). Org. phase: 0.0015 M DTDGA/n-dodecane, aqueous phase: 10^{-3} M Pd at different initial nitric acid concentrations.

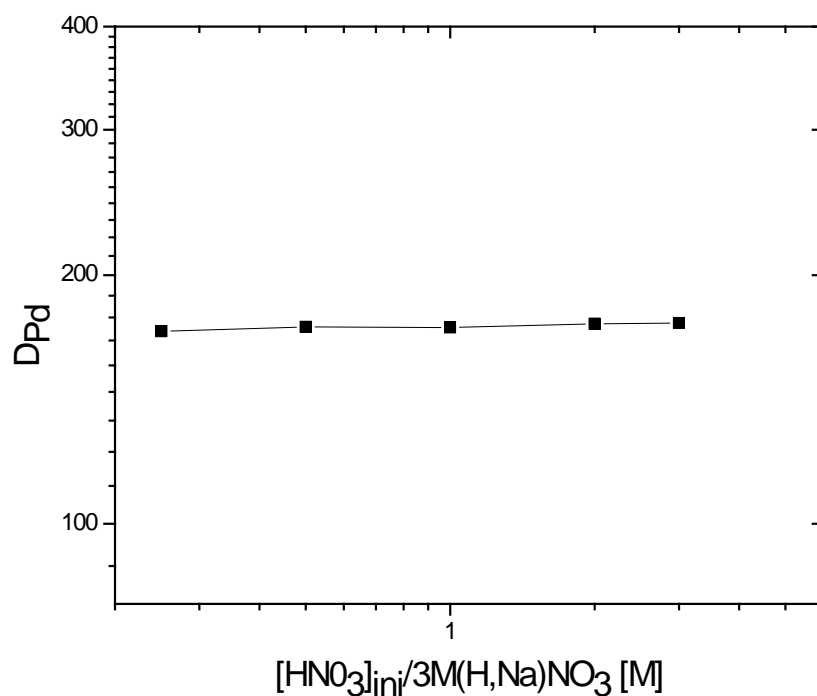


Fig. 4.3. Variation of D_{Pd} with $[\text{HNO}_3]$ at fixed ionic strength. Org. phase: 0.0015 M DTDGA/n-dodecane, aqueous phase: 3 M (H, Na) NO_3 .

4.3. Nitric acid uptake

Nitric acid extraction by 0.1 M DTDGA/ n-dodecane was studied and the ratio of concentration of HNO_3 to that of DTDGA in organic phase was determined at different initial nitric acid concentrations. Figure 4.4 shows the variation of $[\text{HNO}_3]_{\text{org}}/[\text{DTDGA}]_{\text{ini}}$ ratio (R) as a function of initial aqueous nitric acid concentration. The amount of acid extracted in the organic phase increases with an increase in the concentration of nitric acid present in the aqueous phase. At 3.5 M HNO_3 , the R value was found to be unity.

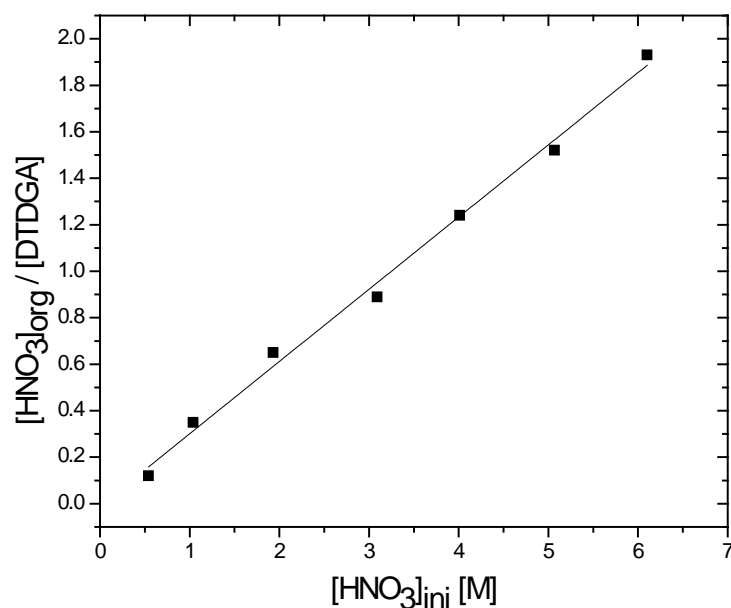


Fig. 4.4. Extraction of HNO₃ from aqueous solutions by 0.1 M DTDGA/n-dodecane at different initial nitric acid concentrations.

In order to compare the basicity of DTDGA with other extractants, it becomes imperative to have the quantitative knowledge of its basicity in terms of conditional acid uptake constant. As discussed in chapter 2, section 2.4, the acid uptake constant (K_H) can be determined from plot of $\log [H^+]_{org.} - \log [E]_{org.}$ vs. $\log [H^+]_{aq.}$, which gives a straight line with intercept of $\log K_H$ and slope of $2n$.

The slope value obtained from graph is 2.28 ± 0.22 (fig. 4.5), suggesting the stoichiometry of adduct being 1:1 for DTDGA to HNO₃. The conditional acid uptake constant K_H of DTDGA obtained from the intercept is 0.60 ± 0.07 which is comparable to that of T(2EH)TDGA. The similar basicity of DTDGA and T(2EH)TDGA could be attributed to the presence of carbonyl group of two amidic moieties attached to the sulphur atom through methylene bridge. Further, the additional 'S' atom did not increase the acid uptake.

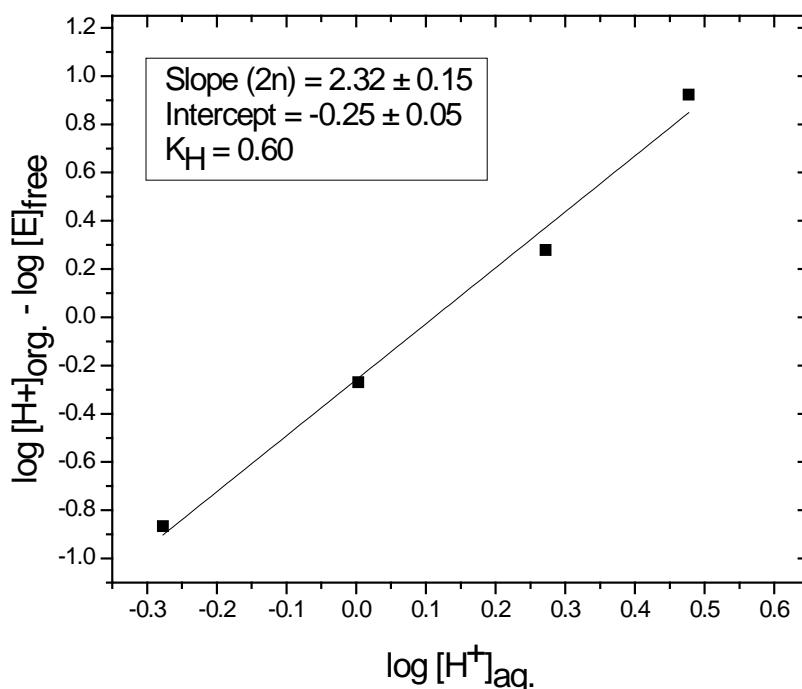


Fig. 4.5. Determination of Acid uptake constant (K_H). Org. phase: 0.1 M DTDGA/n-dodecane, Aq. phase: nitric acid at different concentrations.

4.4. Effect of diluents

It is commonly observed that the extractability of metal ions by a given extractant is highly influenced by the nature of diluents used. To investigate this effect the extraction behavior of Pd(II) was evaluated by contacting 10^{-3} M Pd (II) in 3.0 M HNO_3 with 0.0015 M DTDGA dissolved in various diluents such as n-dodecane, benzene, toluene, 1-octanol, dichloromethane and solvesso-100. It was observed that D_{Pd} remained nearly constant irrespective of the diluents used. Since more than 99% of palladium is extracted in single step in all of the diluents it can be concluded that under the given experimental conditions the extraction of palladium with this extractant is so high that slight variation in the distribution ratio due to the interaction between extracted species and diluents will have insignificant effect on percentage extraction of Pd. Since normal paraffinic diluents have

been proposed to be best suited diluents for HLLW processing, further studies are carried out with DTDGA/n-dodecane solvent system.

4.5. Loading Studies

To determine the loading capacity of DTDGA, 10 ml of 1.5×10^{-3} M DTDGA/n-dodecane was repeatedly contacted with equal volume of aqueous solution containing 10^{-3} M palladium in 3.0 M HNO_3 . The amount of palladium transferred into the organic phase in each contact was calculated by mass balance and the cumulative concentration in the organic phase after each contact was determined. It was found that 1.63×10^{-3} M palladium was loaded in two contacts after which no further loading was observed. Also, Pd(II) loaded in the organic phase was stripped using 0.01 M thiourea in 0.1 M nitric acid and palladium content in the strip solution was found to be same as obtained by mass balance. The loading capacity of palladium in DTDGA corresponds to 1:1 stoichiometry between the palladium and the extractant. No third phase was observed even at very high loading (\sim g/L) of palladium for corresponding concentrated solution of DTDGA in n-dodecane. This is important from the view point of reduction of waste volumes, where palladium from dilute aqueous streams can be extracted into relatively smaller volumes of DTDGA solvent system.

4.6. Back extraction and subsequent recovery of palladium from strip solution

Back extraction studies of Pd from loaded organic phase were carried out by using different stripping solutions. The organic phase obtained on equilibrating 0.0015 M DTDGA/n-dodecane with aqueous phase containing 1.0×10^{-3} M palladium in 3.0 M nitric acid, was contacted with equal volumes of various stripping solutions. Table 1 shows the percentage back extraction achieved in single contact. It is evident that with DI water there is no back extraction, while with 0.05 M ammonium acetate and 0.05 M HEDTA alone,

less than 10% back extraction is achieved and with 0.05 M ammonium carbonate + 0.05 M ammonium nitrate and 0.05 M ammonium acetate + 0.05 M ammonium nitrate, about 20-25% back extraction is obtained. Also, it was observed that dilute nitric acid alone is not suitable for recovering palladium from loaded organic phase. However, it is quantitatively recovered with a single contact using a solution of 0.01 M thiourea in 0.1 M nitric acid. Since, for efficient back extraction of palladium with 0.05 M ammonium carbonate + 0.05 M ammonium nitrate or 0.05 M ammonium acetate + 0.05 M ammonium nitrate, higher aqueous to organic phase ratio will be required, this will lead to increase in waste volume. The use of thiourea as stripping agent was found to be the most appropriate. Finally, it is of interest to recover palladium from the corresponding strip solution. Earlier, we have demonstrated that Pd can be effectively recovered as palladium sulphide (precipitate) from thiourea strip solution by making it alkaline and stirring for 30 minutes. Pd can also be directly recovered from thiourea strip /ammonia strip solution by electrodeposition.

Table 4.1. Back extraction (% E) of palladium from loaded organic phase (0.0015 M DTDGA/n-dodecane)

S. No.	Stripping Agent	(% E)
1.	0.05 M Ammonium Acetate	7.11
2.	0.05 M Ammonium Acetate + 0.05 M Ammonium nitrate	11.13
3.	0.05 M Ammonium carbonate + 0.05 M Ammonium nitrate	19.17
4.	Ammonia solution (v/v, 5%)	22.02*
5.	Ammonia solution (v/v, 5%) + 0.05 M Ammonium nitrate	23.10*
6.	0.05 M HEDTA	5.12
7.	0.05 M Ammonium carbonate + 0.05 M Ammonium nitrate + 0.05 M HEDTA	32.11
8.	DI water (pH=7)	≤ 1.0
9.	0.01 M HNO ₃	≤ 1.0
10.	0.01 M Thiourea in 0.1 M nitric acid	≥ 99.8

* Slight turbidity is observed at the interphase

4.7. Determination of Pd-DTDGA complex stoichiometry

To establish the nature of extracted species, both the chemical (mole ratio method) as well as physical (ESI-MS) approaches were followed. Fig. 4.6 shows the variation of $[\text{Pd}]_{\text{org.}}$ vs $[\text{DTDGA}]_{\text{org.}} / [\text{Pd}]_{\text{aq.}}$. It can be inferred from the figure that the stoichiometry of the species (Pd to DTDGA) is 1:1. Fig. 4.7 shows the ESI-MS of the extracted species, peak at m/z 888 corresponds to $\text{Pd}(\text{NO}_3)_2$. DTDGA thus confirming the stoichiometry determined earlier.

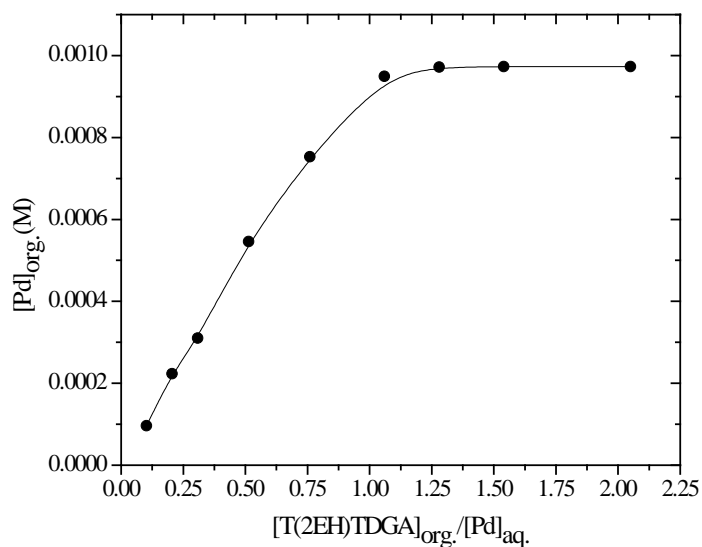


Fig. 4.6. Mole Ratio Plot, Org.: DTDGA/n-dodecane, Aq.: 0.98×10^{-3} M Pd in 3.0 M HNO_3 .

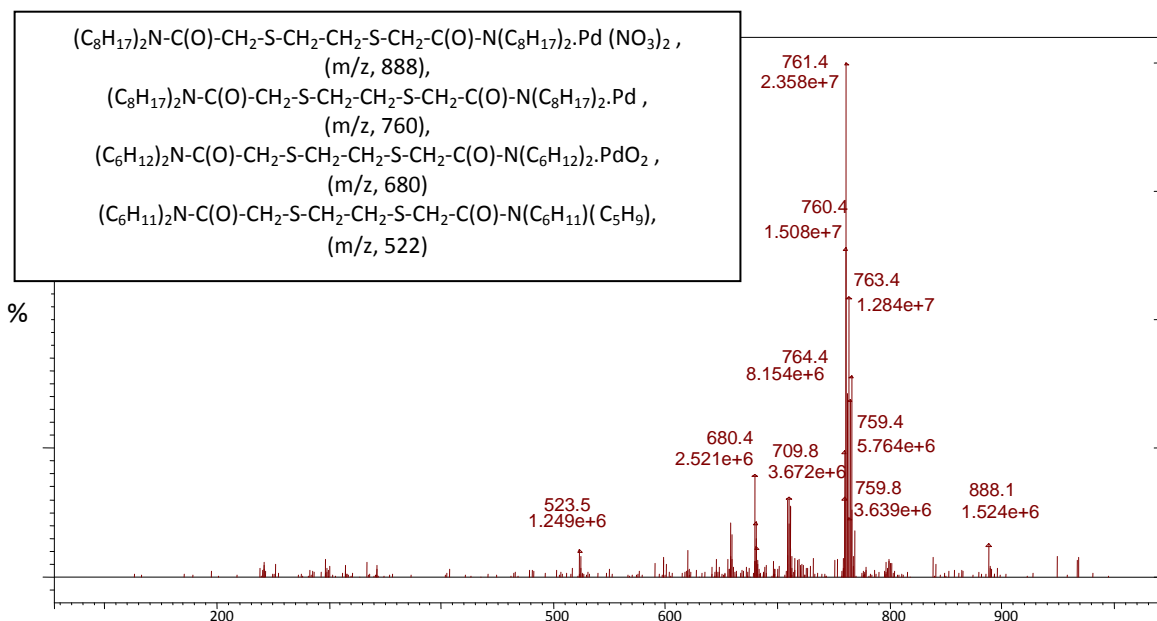


Fig. 4.7. ESI-MS (% abundance vs m/z) of 10^{-4} M DTDGA/n-hexane after contacting with 10^{-4} M Pd in 3.0 M nitric acid medium.

4.8. Comparison of ligands

Fig. 4.8 shows the comparison of extraction efficiency of DTDGA with ligands namely, tertiary and quaternary amines (tri-n-octylamine, tri-n-octylmethylammonium chloride (TOMAC) and tri-n-octylmethylammonium nitrate (TOMAN)) [97-98, 149], α -benzoin oxime (ABO) [100], dihexyl/dioctyl sulfide (DHS/ DOS) and dihexyl disulfide (DHDS) [103-105], dioctyl and bis-(2-ethylhexyl) sulfoxide (DOSO and BESO) [105, 106], tributyl phosphine sulphide (TIPS) [103], benzoylmethylene triphenylphosphorane (BMTTP) [96] and T(2EH)TDGA. Since most of the ligands work under different conditions, their comparison with DTDGA has been made under the best conditions, reported in the literature. It can be seen that very high distribution ratio of palladium was obtained with DTDGA as compared to other previously known extractants thus making it one of the highly efficient extractants for the same purpose.

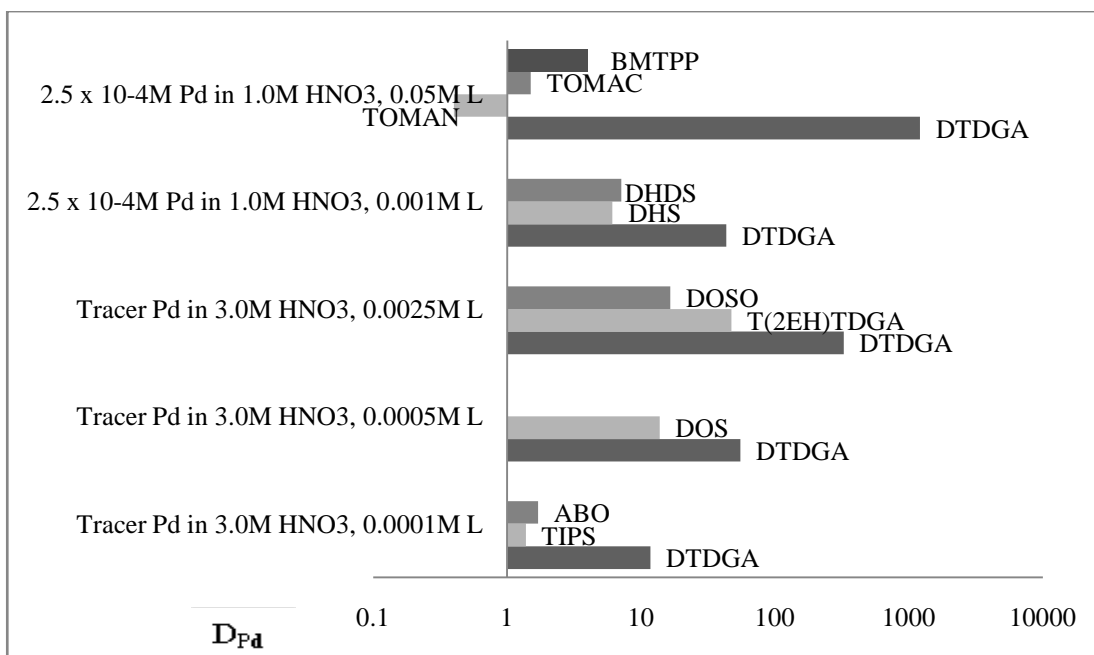


Fig. 4.8. Comparison of extraction efficiency of various extractants (L).

4.9. Extraction Studies with SHLW Solution

Earlier we have demonstrated that DTDGA could be used for the extraction of palladium from nitric acid medium. To evaluate the distribution behavior of various elements present in SHLW, the batch extraction of SHLW elements was carried out by contacting SHLW with varying concentration of DTDGA in n-dodecane. Figure 4.9 shows the distribution ratio of various metal ions present in SHLW. From the results it is evident that except palladium, all other metal ions are hardly extracted in the organic phase, thus giving a very high separation factor ($\geq 10^5$) of palladium with respect to other metal ions. Further, the distribution ratio of palladium is sufficiently high to enable the quantitative extraction possible in a single contact. Thus, very high selectivity and extractability for palladium makes this extractant very promising for extraction of palladium from HLLW.

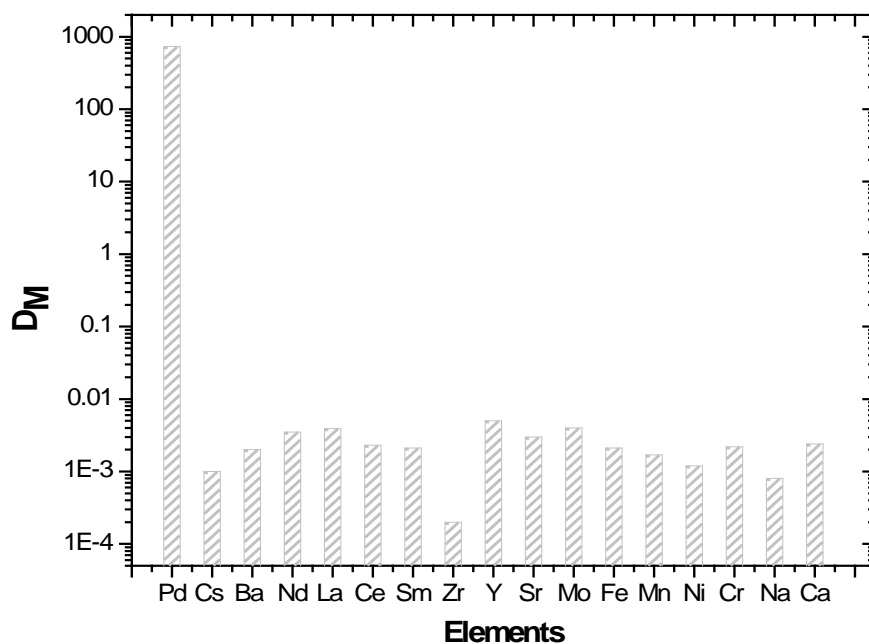


Fig. 4.9. Distribution ratio of various metal ions present in SHLW. Aqueous phase: SHLW feed solution, Organic Phase: 0.025 M DTDGA/n-dodecane.

4.10. Extraction Studies with tracer spiked HLLW

The HLLW from the reprocessing plant of spent fuel (PHWR) was spiked with some of the ‘ γ ’ emitting radioisotopes and was subjected to liquid-liquid extraction with DTDGA/n-dodecane. Figure 4.10 shows the ‘ γ ’ spectra of the feed (bottom) and the organic phase after extraction (top). The high selectivity of the ligand for Pd is evident from the figure.

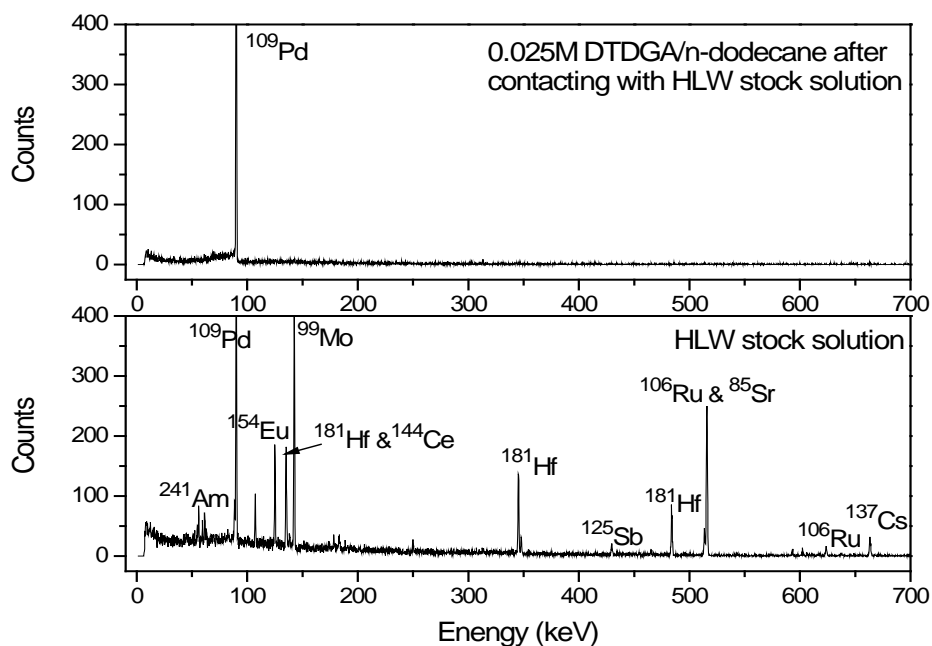


Fig. 4.10. ‘ γ ’-spectra of HLW stock solution and organic phase after extraction.

Table 4.2 shows the distribution ratio of various elements present in HLLW, the separation factor (D_{Pd}/D_M) of the order of $\geq 10^5$ for palladium over other HLLW elements makes this extractant very promising for further studies.

Table 4.2. Extraction of HLLW elements, Org.: 0.0025 M DTDGA/n-dodecane, Aq.: 3.0 M HNO_3 solutions spiked with HLLW and other ‘ γ ’ tracers.

Element	²⁴¹ Am	¹⁵²⁺¹⁵⁴ Eu	¹⁴⁴ Ce	⁹⁹ Mo	¹²⁵ Sb	¹⁸¹ Hf	¹⁰⁶ Ru	¹³⁷ Cs	¹⁰⁹ Pd
Distribution ratio (D_M)	0.0011	0.0006	0.0008	0.0003	0.0007	0.0001	0.0002	0.00014	325.3

4.11. Reusability of the Extractant

To evaluate the reusability of the extractant, the organic phase containing 0.0015 M DTDGA/n-dodecane was contacted with SHLW followed by stripping with 0.01 M thiourea in 0.1 M HNO_3 in five successive cycles. The stability of the resultant lean

organic phase was then evaluated by determining D_{Pd} values with SHLW. It was observed that even after five successive cycles of loading and stripping, the D_{Pd} remained almost constant at the original value of 252 (Table 4.3) suggesting excellent reusability of the extractant.

Table 4.3. Distribution data of Pd in five successive cycles of extraction and stripping; Aqueous phase: SHLW feed solution. Organic phase: 0.0015 M DTDGA/n-dodecane.

Number of cycles	Distribution Ratio
1	252
2	247.9
3	259.3
4	245.2
5	241.9
Mean	249.2
S.D.	6.7
R.S.D. (%)	2.7

4.12. McCabe-Thiele Diagram

From above discussion it can be suggested that palladium can be quantitatively extracted from HLW with 0.0025 M DTDGA/n-dodecane solvent system. Generally, the number of theoretical stages required for the quantitative extraction of metal ions in dynamic conditions is determined by a graphical method using the McCabe-Thiele diagram. In the construction of the McCabe-Thiele diagram, the extraction isotherm, which represents the relation between the equilibrium concentration of the metal ions in the aqueous phase to that in the organic phase, was first drawn as shown in Fig. 4.11. A vertical line is then drawn from a point representing the concentration of metal ions in the feed solution on the x -axis. The operating line was then inserted, passing through the origin whose slope is equal to the proposed phase ratio ($A/O = 2.65$). The figure suggested that for $A/O = 2.65$,

two extraction stages were sufficient for complete extraction of palladium from a feed solution containing 100 mg/L Pd.

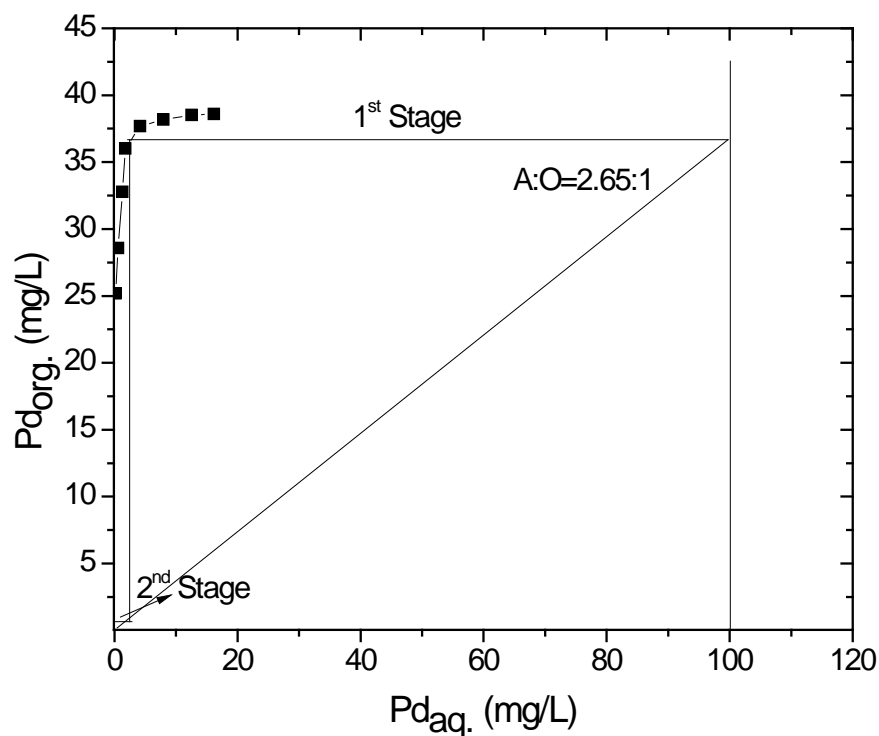


Fig. 4.11. McCabe-Thiele plot for extraction of palladium from 3.0 M nitric acid solution.

Organic: 0.0025 M DTDGA/n-dodecane, aqueous phase: 200 mg/L Pd in 3.0 M nitric acid (O/A varied from 8:2 to 2:8).

4.13. Flow sheet for separation and recovery of palladium from SHLW

Based on the data obtained for the extraction of palladium, initial tests with HNO₃ solutions and stripping with thiourea/ammonia solution, and from tests with simulated HLW solution, a flow sheet (Fig. 4.12) using DTDGA as the extractant is proposed for the recovery of palladium from the HLLW of PUREX process origin.

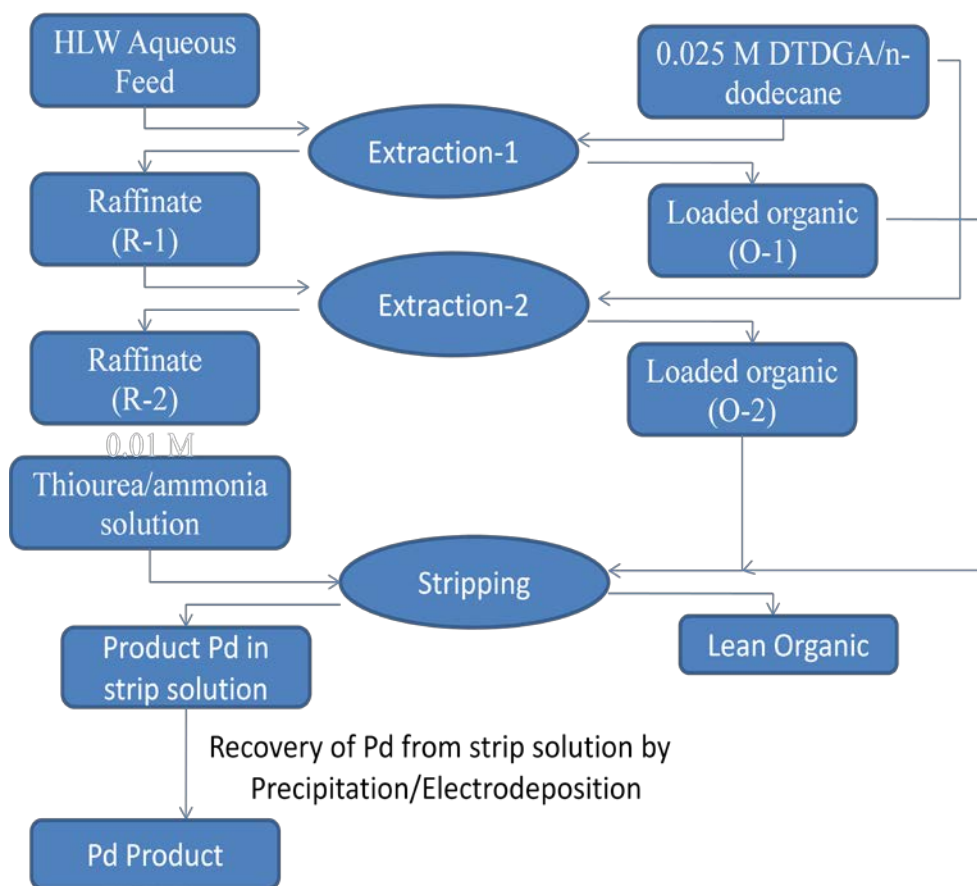


Fig. 4.12. Flow sheet for extraction and recovery of palladium from HLLW.

4.13. Stability Studies of *N,N,N',N'*-tetra-(2-ethylhexyl) dithiodiglycolamide (DTDGA)

In chapter 3 we have evaluated the stability of novel extractant, namely, T(2EH)TDGA in nitric acid and radiation environment. The extractant was found to be fairly stable and therefore can possibly be used in separation and recovery of palladium from HLLW. Since, DTDGA was found to be even more effective than T(2EH)TDGA, its stability in nitric acid and radiation environment was also studied following similar method as employed for T(2EH)TDGA.

4.13.1. Hydrolysis of DTDGA solvent system

0.025 M DTDGA/n-dodecane kept in contact with 3.0 M nitric acid for two weeks when contacted with SHLW solution, shows almost quantitative extraction of Pd with negligible extraction of other elements present in SHLW. Thus, DTDGA/n-dodecane solvent system does not deteriorate upon contact with nitric acid solution at least up to 2 weeks. The resistance of thioetheric 'S' atoms to oxidation by the strong acid under given experimental conditions has been discussed in the earlier chapter.

4.13.2. Qualitative analysis of radiolytic degradation products

Identification of various radiolytic degradation products of DTDGA was done by GC-MS. Majority of the products were found to be formed by the cleavage of amide and thioether linkages, with few products formed by scissoring of alkyl chains. Degradation products of neat DTDGA and DTDGA/n-dodecane were found to be the same and consist mainly of neutral products. Fig. 4.13 shows the GC-MS spectra of neat DTDGA whereas Fig. 4.14 shows the GC-MS of neat DTDGA after a total dose of 0.5 MGy. The major degradation products were identified as *N,N*-bis-(2-ethylhexyl) formamide (BEHFA), *N,N*-bis-(2-ethylhexyl) acetamide (BEHAA), *N,N*-bis-(2-ethylhexyl)-2-sulfanylacetamide (BEHSAA), *N,N*-bis-(2-ethylhexyl)-2-(ethylsulfanyl)acetamide (BEHESAA), *N,N*-bis-(2-ethylhexyl)-2-[(2-sulfanylethyl)-sulfanyl]acetamide (BEHSESAA), *N,N*-bis-(2-ethylhexyl)-2-[[2-(methylsulfanyl) ethyl]sulfanyl] acetamide (BEHMSESAA) & *N,N,N'*-trihexyl-*N'*-methylhexyl dithiodiglycolamide (THMHDTDGA). The chromatogram (Fig. 4.15) shows the degradation products formed by radiolysis of DTDGA/n-dodecane in contact with 3.0 M nitric acid at 0.5 MGy. The degradation products were found to be the same as in case of neat DTDGA and 0.025 M DTDGA/n-dodecane along with some acidic degradation products.

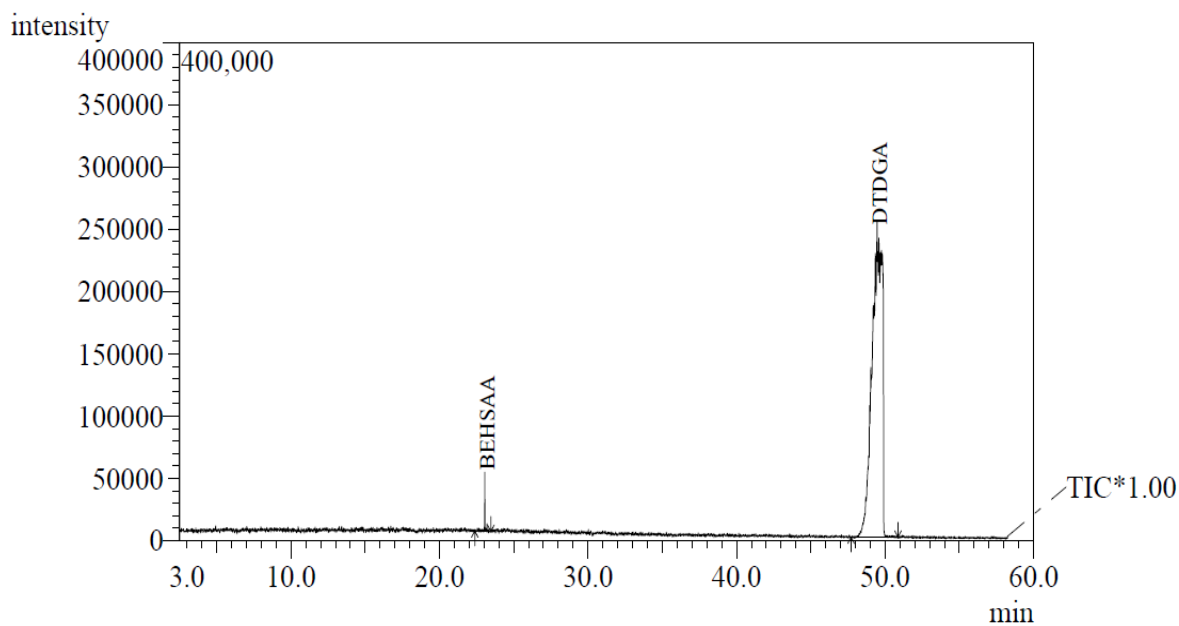


Fig. 4.13. GC-MS of pure DTDGA

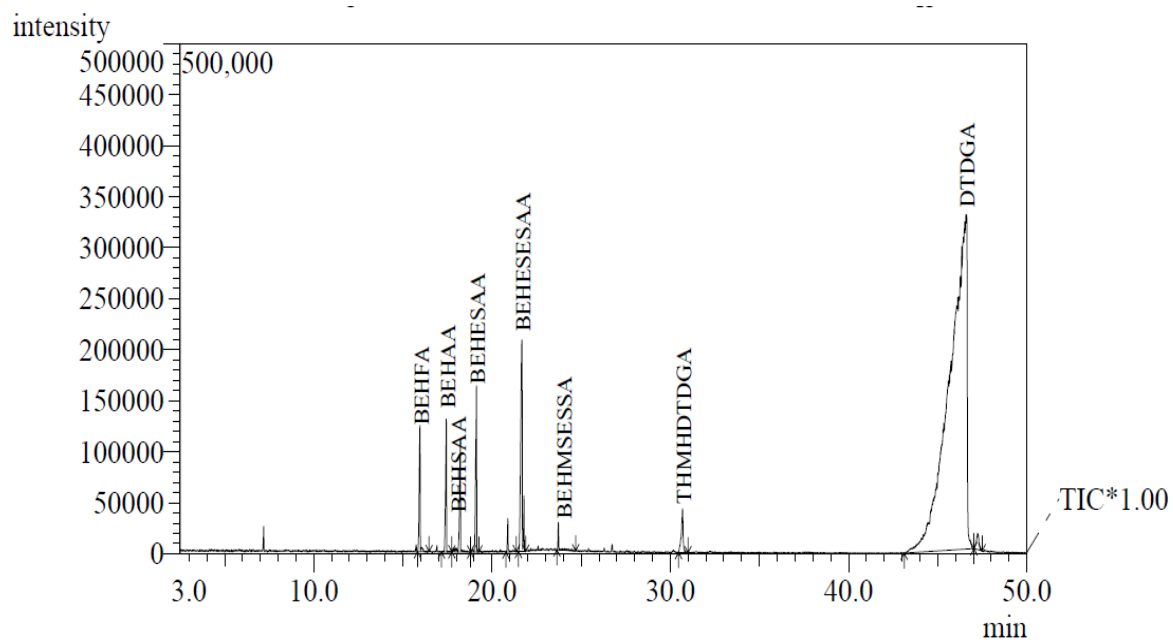


Fig. 4.14. GC-MS of neat DTDGA after an absorbed dose of 0.5MGy.

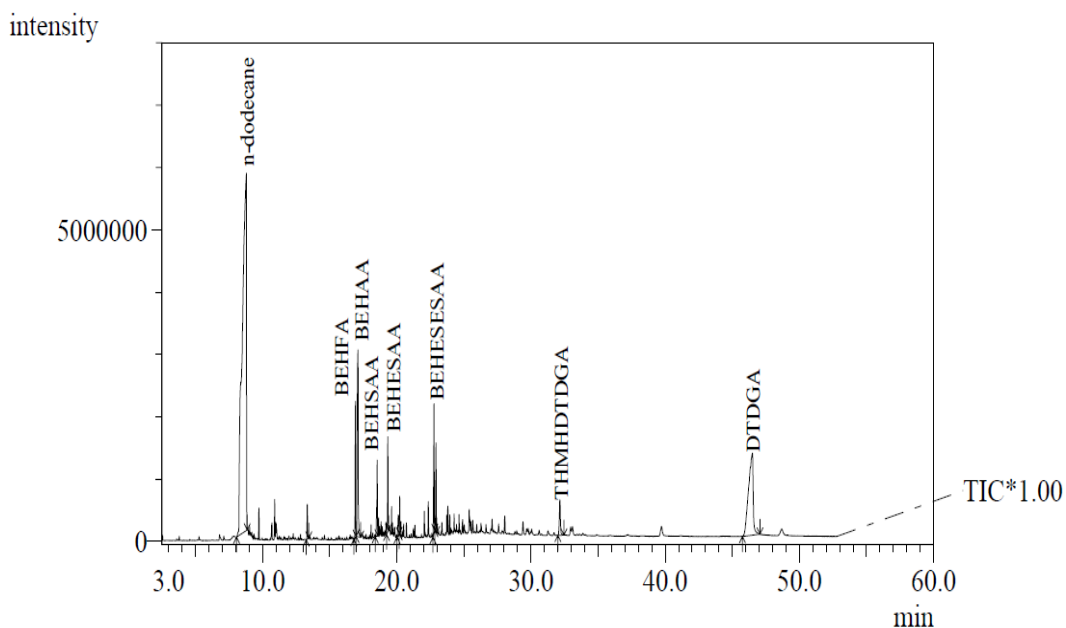


Fig. 4.15. GC-MS of 0.05 M DTDGA/n-dodecane in contact with 3.0 M nitric acid after an absorbed dose of 0.5 MGy.

EI-MS data for DTDGA and its degradation products are shown in Table 4.4. From these degradation products, the probable path of degradation can be predicted.

Table 4.4. EI-MS of degradation products found in DTDGA after an absorbed dose of 0.5 MGy.

S. No.	Product	EI-MS (“*” base peak)
1.	<i>N,N</i> -bis-(2-ethylhexyl)formamide (BEHFA)	71*, 86, 142, 184, 268
2.	<i>N,N</i> -bis-(2-ethylhexyl)acetamide (BEHAA)	69, 120*, 170, 218, 268, 282
3.	<i>N,N</i> -bis-(2-ethylhexyl)-2-sulfanylacetamide (BEHSAA)	71, 118, 142, 170, 268*, 282, 315
4.	<i>N,N</i> -bis-(2-ethylhexyl)-2-(ethylsulfanyl)acetamide (BEHESAA)	71, 142*, 184, 242, 282, 341
5.	<i>N,N</i> -bis-(2-ethylhexyl)-2-[(2-sulfanylethyl)sulfanyl]acetamide (BEHSESAA)	69, 71, 142, 184*, 268, 342, 375
6.	<i>N,N</i> -bis-(2-ethylhexyl)-2-[[2-(methylsulfanyl)ethyl]sulfanyl]acetamide (BEHMSESAA)	71, 109, 142*, 268, 342, 389
7.	<i>N,N,N'</i> -triethylhexyl- <i>N'</i> -methylhexyl dithiodiglycolamide (THMHDTDGA)	71, 142, 184*, 268, 328, 411, 554
8.	<i>N,N,N',N'</i> -tetra-(2-ethylhexyl)dithiodiglycolamide (DTDGA)	71, 142, 184, 268, 342*, 374, 657

Fig. 4.16 shows the probable paths, indicated as (A), (B) and (C) for the formation of degradation products of DTDGA. The products of path (a) namely BEHFA and BEHMSSESAA are formed by cleavage of amide bond. BEHAA and BEHSESAA of path (b) are formed by cleavage of thioether bond. Products of path (c), namely BEHSAA and BEHESAA are formed by cleavage of another thioether linkage of DTDGA. Additionally there is another product namely THMHDTDGA which is found to be formed by the cleavage of alkyl groups from the amidic moiety.

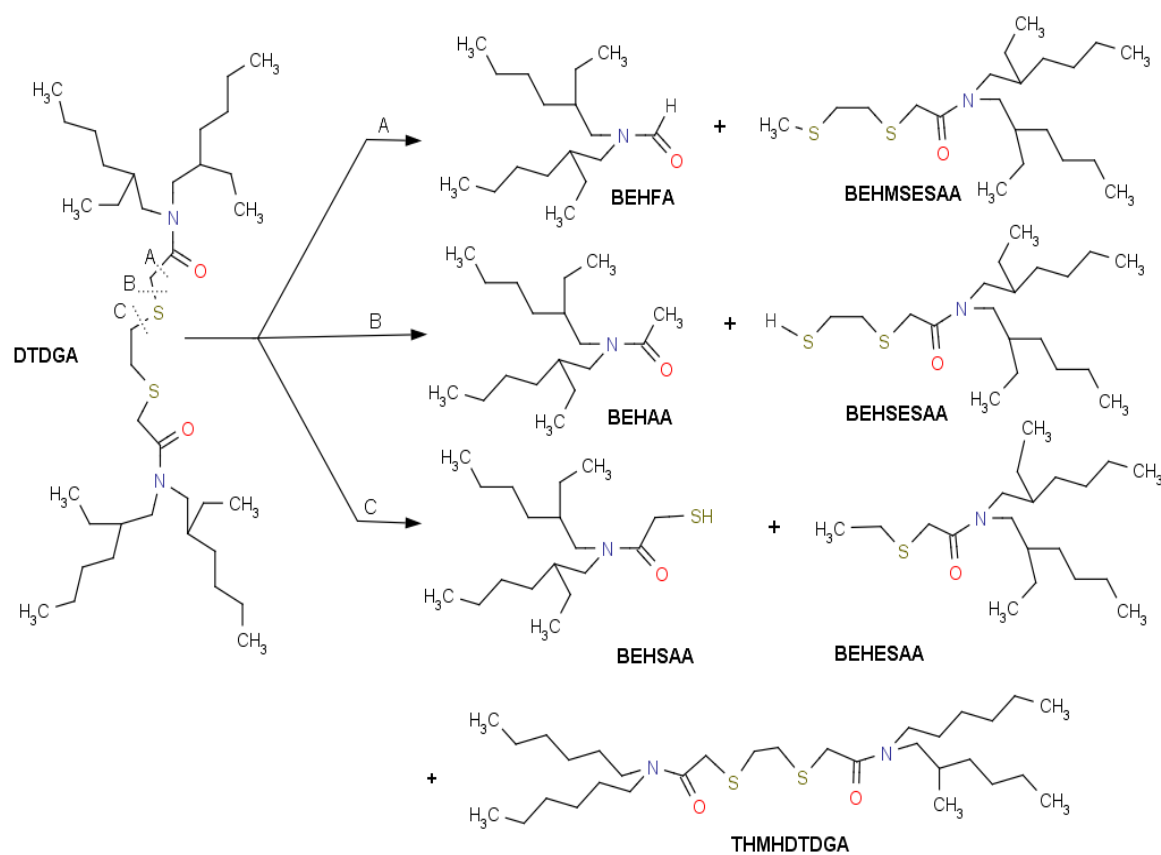


Fig. 4.16. Radiolytic degradation paths of DTDGA

4.13.3. Radiolytic stability of DTDGA solvent system

Three sets of samples, namely, (i) pure DTDGA, (ii) 0.025 M - 0.1 M DTDGA/n-dodecane and (iii) 0.025 M - 0.05 M DTDGA /n-dodecane in contact with 3.0 M HNO₃ were irradiated with ‘ γ ’ radiations. Figure 4.17 shows the residual concentration of DTDGA after irradiation represented as [DTDGA]_{irr} against the absorbed dose. From the figure it is evident that degradation of neat DTDGA is considerably less in case of neat solvent as compared to DTDGA in n-dodecane. The degree of degradation relates to the amount of absorbed dose by the following equation defined by Mincher and Cury

$$C = C_0 \cdot \exp(-k \cdot D) \quad (1)$$

Where C is the concentration of DTDGA (in mol/L) after irradiation, C₀ is the initial concentration of DTDGA before irradiation, D is the dose absorbed by the sample and k is the dose constant. The absolute value of dose constant indicates the degree of degradation by radiation and is obtained by slopes of the plots of Fig. 4.17. From the plot it is evident that slope for DTDGA/n-dodecane is greater than neat DTDGA indicating that the presence of n-dodecane have sensitization effect on degradation of DTDGA. This is in agreement with the earlier reported works where n-dodecane was found to sensitize the degradation of extractant molecule via charge transfer reactions, already discussed in the previous chapter. This observation is further corroborated when, on decreasing the concentration of DTDGA from 0.1 M to 0.025 M (which means increasing the dodecane content), the degradation rate increases. Further, the degradation curve of 0.025 M DTDGA/n-dodecane in contact with 3.0 M nitric acid was found to be similar to that of 0.025 M DTDGA/n-dodecane indicating that nitric acid has less effect on the extent of radiolysis. The plot also indicates that up to an absorbed dose of 0.2 MGy, the loss of DTDGA is less than 10%, above which the degradation rate was found to increase.

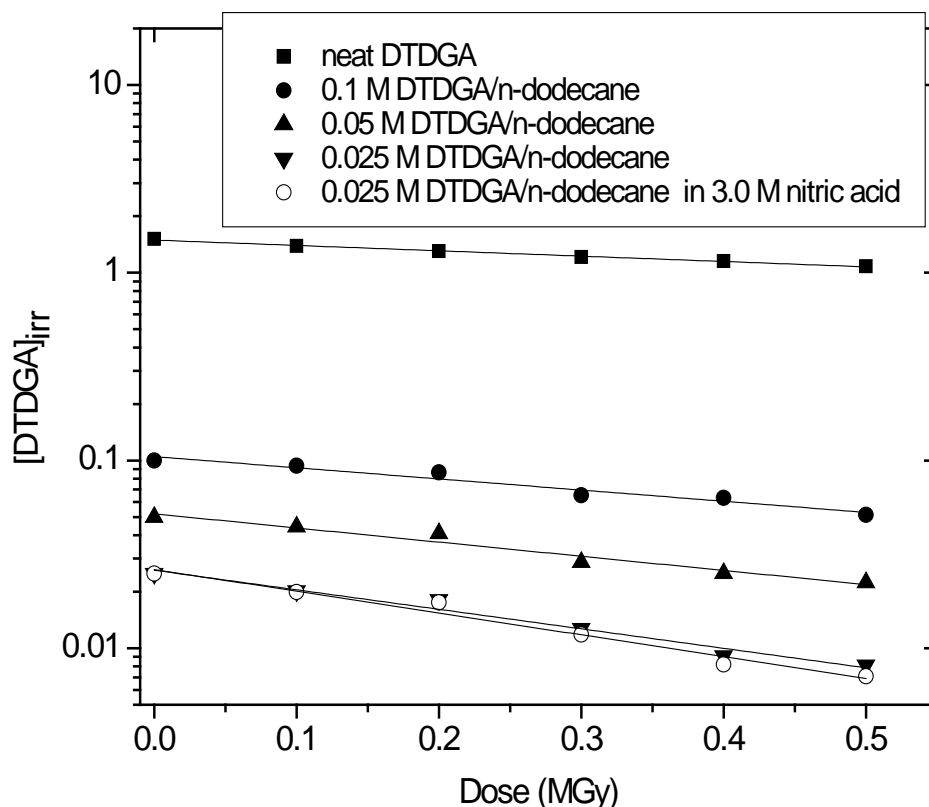


Fig. 4.17. Degradation curve of DTDGA as a function of absorbed dose.

The radiation chemical yield 'G' defined as the number of DTDGA molecules decreased by absorption of 100 eV energy, is calculated by using the following equation:

$$C = C_0 \cdot \exp(-1.04 \times 10^{-10} \text{ GMD}) \quad (2)$$

where, M is the molecular weight of DTDGA and D is the absorbed dose (Gy). By rearranging the above equation and taking logarithm of both the sides of the equation we get,

$$\ln(C/C_0) = -1.04 \times 10^{-10} \text{ GMD} \quad (3)$$

A plot of $\ln(C/C_0)$ vs. D gives a straight line with slope equal to 1.04×10^{-10} GM. From the slope, 'G' value for neat DTDGA was determined to be 9.64 ± 0.3 (Fig. 4.18). The 'G'

value of DTDGA is comparable with other extractants used for processing of HLLW for various applications. This indicates good radiolytic stability of DTDGA for use in the separation of Pd from HLLW.

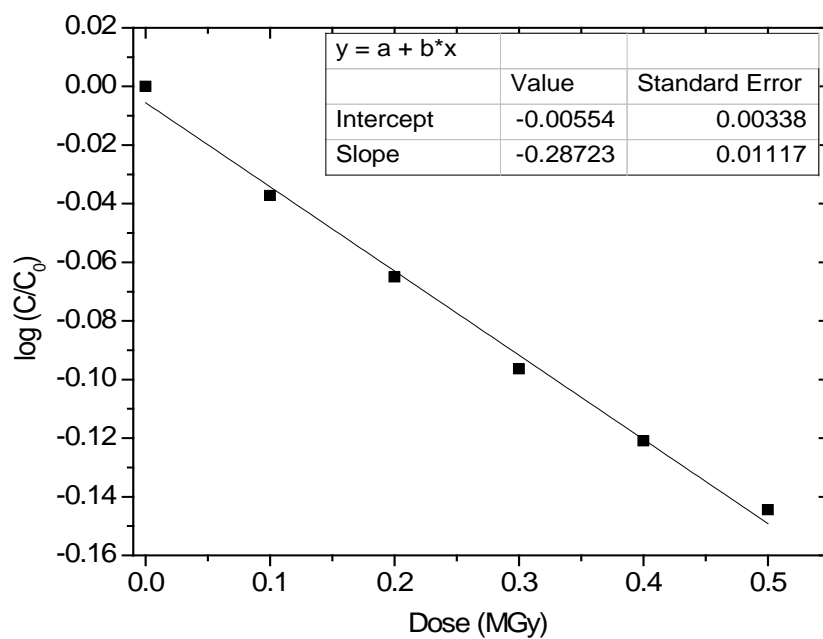


Fig. 4.18. Plot of $\log C/C_0$ vs. Dose (MGy).

4.13.4. Effect of radiolysis of solvent on extraction properties of SHLW Elements

Variation of D_{Pd} as a function of absorbed dose by the irradiated solvent is as shown in Fig. 4.19. The solvents used were 0.025 M DTDGA/n-dodecane and 0.05 M DTDGA/n-dodecane, which were irradiated in contact with 3.0 M nitric acid. From figure it is evident that D_{Pd} decreases with increase in absorbed dose. Though, the distribution ratio decreases with increase in absorbed dose, the high extraction (% E) of palladium was maintained even up to 0.2 MGy. It was also observed that D_{Pd} is less affected up to an absorbed dose of 0.2 MGy, after which the decrease is more significant for 0.025 M DTDGA/n-dodecane compared to that for 0.05 M DTDGA/n-dodecane. This behavior could be attributed to the sensitization effect of n-dodecane discussed earlier. The significant decrease in D_{Pd} at

higher gamma doses could be due to the formation of water soluble degradation products of DTDGA which might complex Pd and thereby retain it in the aqueous phase.

Except Mo, the distribution ratios for other elements present in SHLW were found to be very small ($D_M \leq 10^{-3}$) and remained so even with increase in absorbed dose. This shows that the extractant retained its remarkable selectivity for palladium over other metal ions even under high radiation environments.

Earlier it was found that 0.01 M thiourea in 0.1 M HNO₃ is sufficient to quantitatively back extract palladium from loaded organic phase, it was therefore of interest to study the stripping behavior under radiation environment. For this purpose, irradiated solvent at different absorbed doses was contacted with SHLW solutions and then the loaded palladium was back extracted using 0.01 M thiourea in 0.1 M nitric acid medium. It was found that the back extraction efficiency with non-irradiated and irradiated solvent were nearly the same regardless the extent of radiation exposure. This suggests the efficient recovery of palladium using thiourea as stripping agent.

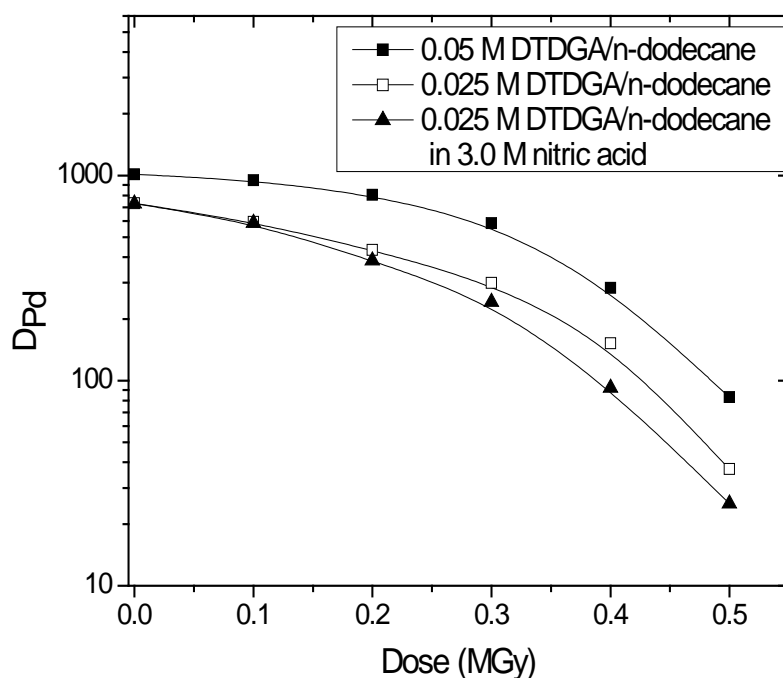


Fig. 4.19. Extraction of metal ion as a function of absorbed dose. Aq. phase: 1×10^{-3} M Pd in 3.0M HNO₃.

These studies suggest that the solvent is fairly stable and retains its extraction and stripping properties up to gamma radiation dose of 0.2 MGy and it is therefore suitable for use in palladium separation from high level liquid waste.

4.14. Structural investigation studies of Pd-ligand complex

4.14.1. Pd(II)-aquo complex

(a) EXAFS

Figure 4.20 shows the k^2 -weighted EXAFS data for the Pd(II) in 1.0 M HNO₃ and the corresponding R -space plots of the Fourier-Transformed EXAFS data. The metric parameters obtained after the fitting of the EXAFS data using IFEFFIT software package are given in table 1. The results show the presence of four oxygen atoms forming the first coordination shell around the Pd²⁺ ion at a distance of 2.00 Å with a Debye Waller

factor (DF) equal to 0.0024 \AA^2 . These data are in agreement with those reported in literature [77]. The analysis also shows the presence of two more oxygen atoms in the second shell at 2.84 \AA with a DF equal to 0.01 \AA^2 , indicating a diffused second shell due to secondary hydration sphere in conformity with the literature reports [77, 150].

(b) DFT

DFT calculations predict the square planar geometry of the $\text{Pd}(\text{H}_2\text{O})_4^{2+}$ complex with the four water molecules in the equatorial plane (figure 4.21), thereby supporting the EXAFS results. The perfect square planar geometry is further reflected by the bond angles made by the four water molecules around Pd(II) at angles close to 90° as shown in table 4.5. These observations validate the methodology for the analysis of the EXAFS data of Pd(II)-thio-di-glycolamide complexes reported below.

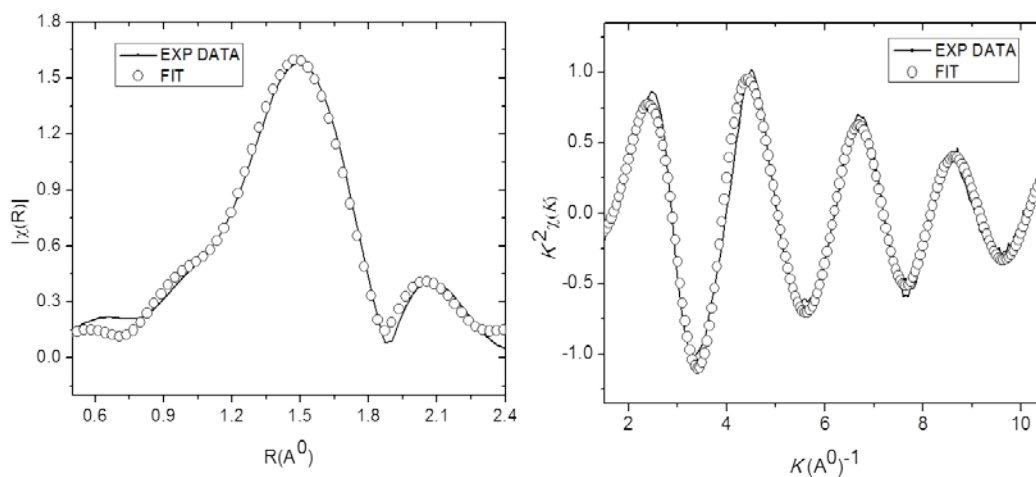


Fig. 4.20. k^2 -weighted EXAFS spectra of Pd(II) aqua ion and comparison of the corresponding Fourier transforms of the experimental data (solid line) with those of the theoretical signal (circles).

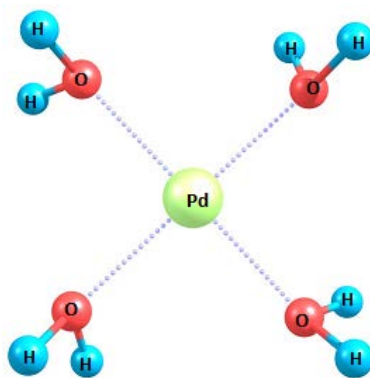


Fig. 4.21. Optimized geometry of Pd(II)-aqua complex

Table 4.5 Summary of curve fitting and DFT optimized results for $\text{Pd}(\text{H}_2\text{O})_4^{2+}$.

EXAFS Curve Fitting						
Shell	Atom	Coordination Number	Distance (R/Å)	ΔE (eV)	$\sigma^2/(\text{Å})^2$	
First	Oxygen	4	2.00	1.36	0.0024	
Second	Oxygen	2	2.84	0.73	0.0101	
DFT Optimized Structures				Angles $\theta(\text{O-Pd-O})$		
	Oxygen	4	2.05	90.0, 89.9, 90.0, 89.9		

4.14.2. Pd(II)-T(2EH)TDGA Complex

(a) EXAFS

Figure 4.22 shows the k^2 -weighted $\chi(k)$ data and the corresponding R -space plots, obtained by Fourier Transformation of $\chi(k)$ for T(2EH)TDGA-Pd(II) complex. The results of the quantitative fit of the EXAFS data are given in Table 4.6. The analysis shows two close scattering shells due to two oxygen atoms and two sulphur atoms placed at the distances of 2.04 Å and 2.24 Å respectively from Pd^{2+} , thereby confirming the 4 coordination number of Pd(II) in the complex. This confirmed the formation of 1:2 complex between Pd(II) and T(2EH)TDGA in agreement with the experimental results obtained from slope method, discussed in section 1. Hence no attempt was made to fit the

data for higher order shells. Considering the predominant square planar geometry of the Pd(II) complexes, it can be inferred that the T(2EH)TDGA-Pd(II) complex may also be formed with similar geometry. However, there is a possibility of two structures with contribution of one sulphur and one carbonyl oxygen from each T(2EH)TDGA molecule. The two structures involve ligation of palladium with sulphur and oxygen atoms in diagonally opposite sides (Trans) and same side (Cis) configuration as shown in the figures 4.23 A and 4.23 B respectively.

(b) DFT

In order to predict the configuration of the Pd(II)-T(2EH)TDGA complex, DFT calculations were performed. In all DFT calculations, to reduce the computational time, the bulkier alkyl group (2-ethylhexyl) has been replaced by smaller alkyl group (isobutyl), which would have little effect on overall optimized geometry of the complex. The major structural parameters for the corresponding geometries are given in table 4.6, which shows negligible difference in the bond length of Pd-S and Pd-O in the two optimized geometries. However, the bond angles for the trans configuration are different from that for cis configuration. The calculated thermodynamic parameters for the optimized geometries of two possible structures in gaseous phase are given in table 4.8, which indicates that the cis form is energetically more stable than the trans form. This could be due to the less steric hindrance in the cis form to achieve the square planar geometry of the complex.

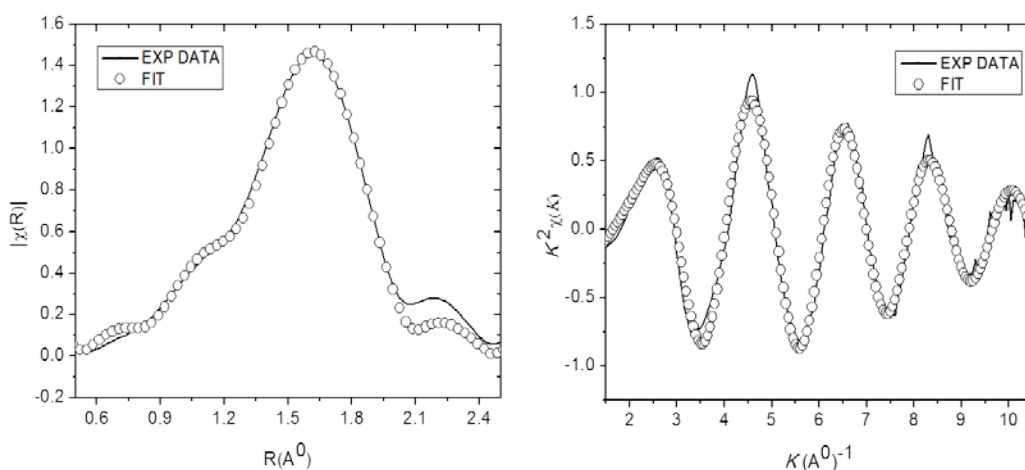


Figure 4.22 k^2 -weighted $\chi(k)$ spectra of the extraction complexes (Pd(II)-T(2EH)TDGA) and comparison of the corresponding Fourier transforms of the experimental data (solid line) with those of the theoretical signal (circles).

Table 4.6 Summary of EXAFS curve fitting and DFT optimization results for Pd(II)-T(2EH)TDGA.

EXAFS Curve Fitting						
Shell	Atom	Coordination Number	Distance (R/Å)	ΔE (eV)	$\sigma^2/(\text{Å})^2$	
First	Oxygen	2	2.04	0.53	0.0058	
Second	Sulphur	2	2.24	0.30	0.0043	
DFT Optimized Structures						
(A) Trans	Oxygen	2	2.04	Angles $\theta(\text{S-Pd-O})$		
	Sulphur	2	2.34	98.4, 96.1, 82.7, 82.6		
(B) Cis	Oxygen	2	2.06	$\theta(\text{S-Pd-S}): 100.2,$		
	Sulphur	2	2.31	$\theta(\text{S-Pd-O}): 83.6$ and $83.1,$ $\theta(\text{O-Pd-O}): 92.8,$		

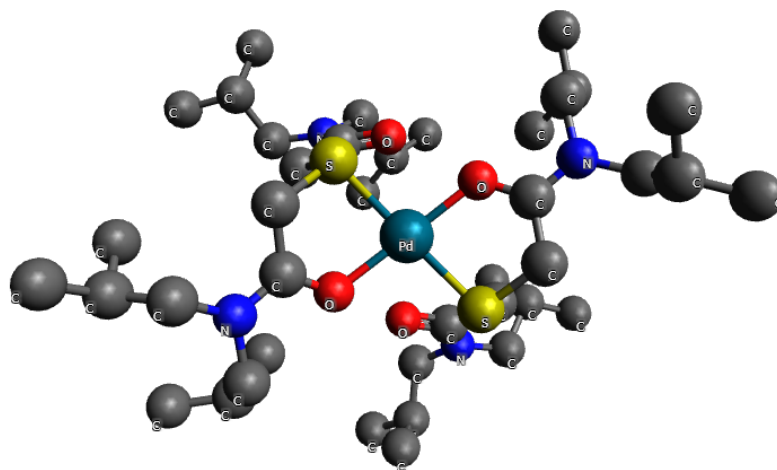


Figure 4.23 A. Optimized geometry of Pd(II)-TIBTDGA complex (Diagonally placed ‘S’ and ‘O’ donor atoms) (DPDA).

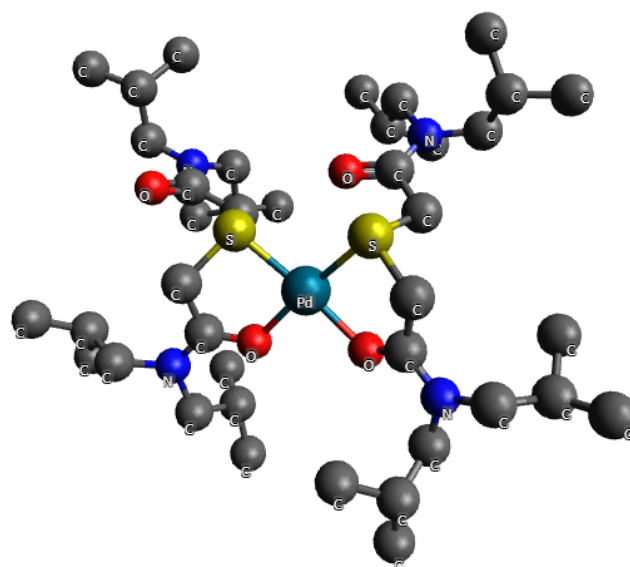


Figure 4.23 B. Optimized geometry of Pd(II)-TIBTDGA complex (Symmetrically placed ‘S’ and ‘O’ donor atoms) (SPDA).

4.13.3. Pd(II)-DTDGA complex

(a) EXAFS

Figure 4.24 shows the k^2 -weighted $\chi(k)$ spectra and the corresponding Fourier Transformed (FT) $\chi(R)$ spectra of DTDGA-Pd (II) complex. The corresponding structural

parameters obtained by fitting of these spectra are given in table 4.7. The results show the two equidistant thioetheric sulphur atoms and two oxygen atoms placed at a distance of 2.29 Å and 2.05 Å respectively. The associated values of ΔE and σ^2 for this fit are well within the acceptable limits. Analogous to the Pd(II)-T(2EH)TDGA complex (1:2 stoichiometry), Pd(II)-DTDGA complex also attains square planar geometry, except that the two sulphur and two oxygen atoms that participate in complex formation come from single DTDGA molecule. This is further confirmed by DFT studies, wherein, to reduce the computational time, 2-ethylhexyl (EH) groups of the amidic moieties have been replaced by isobutyl (IB) groups. Figure 4.25 shows the optimized structure of Pd(II)-DTDGA complex. It can be inferred that the complex attains square planar arrangement with slight distortion having dihedral angles as shown in the table 4.7. This could be attributed to (i) the presence of the ethylene bridge between the two 'S' atoms which constrains the latter to align perfectly in square planar arrangement and (ii) the bulkier alkyl group of amidic moieties which may restrict the perfect alignment. Major structural parameters obtained from the optimized structure are given in table 4.7. The steric strain is expected to be more in the case of Pd(II) complex with DTDGA than that with T(2EH)TDGA as the single ligand molecule satisfies the coordination number of the metal ion in the former complex, which is also evident from greater Pd-S bond lengths in the former complex. However, the greater degree of chelation might overcompensate for the steric hindrance which is also supported by the theoretical calculations as discussed below.

(b) DFT

While comparable bond lengths are observed for Pd-S and Pd-O bonds for both the Pd(II)-T(2EH)TDGA and Pd(II)-DTDGA complexes, the latter complex will be more energetically stable owing to higher degree of chelation, discussed in section. To confirm

this, hessian calculations were carried out in gaseous phase. The corresponding thermodynamic parameters of Pd(II)-DTDGA complex are as given in the table 4.8. The higher stability of the Pd(II) complex with DTDGA than that with T(2EH)TDGA is favored by both the enthalpy and entropy components of the free energy, owing to higher soft-soft interaction (2Pd-S bonds per metal ion compared to 1 Pd-S bonds per metal ion) as well as the greater degree of chelation in the former complex. These observations corroborate the experimental results of higher D_{Pd} values in case of DTDGA than that in case of T(2EH)TDGA.

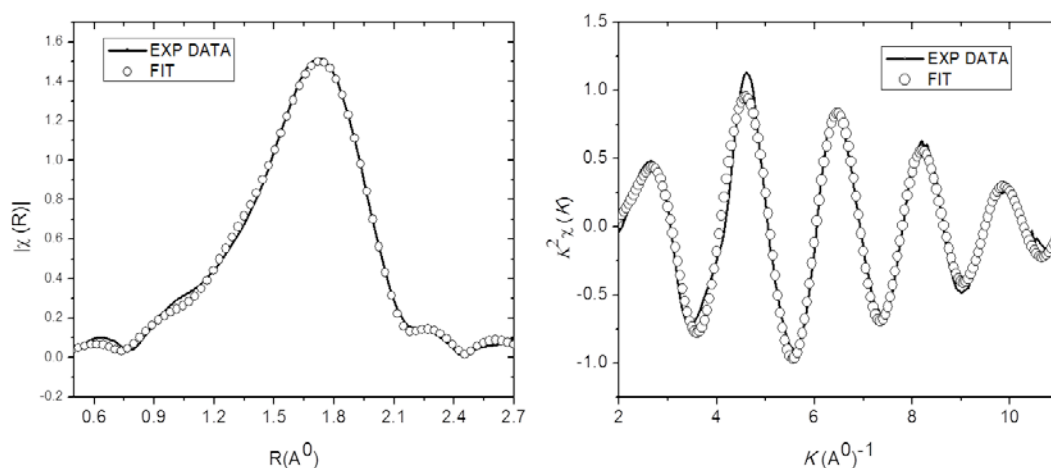


Figure 4.24. k^2 -weighted $\chi(k)$ spectra of the extraction complexes (Pd(II)-DTDGA)) and comparison of the corresponding Fourier transforms of the experimental data (solid line) with those of the theoretical signal (circles).

Table 4.7 Summary of EXAFS curve fitting and DFT optimization results for Pd(II)-DTDGA complex

EXAFS Curve Fitting					
Shell	Atom	Coordination Number	Distance (R/Å ⁰)	Δ E (eV)	σ ² / (Å ⁰) ²
First	Oxygen	2	2.05	1.5602	0.0054
Second	Sulphur	2	2.29	4.9948	0.0035
DFT Optimized Structures				Angles	
	Oxygen	2	2.04	θ(S-Pd-S): 90.4, θ(S-Pd-O): 85.4 and 83.8,	
	Sulphur	2	2.28	θ(O-Pd-O): 98.9	

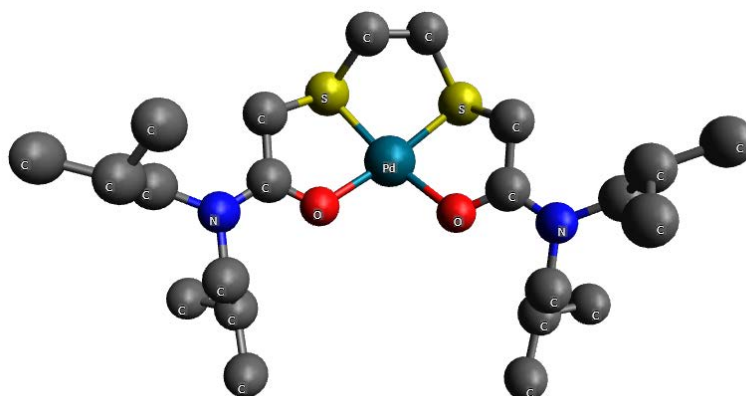


Figure 4.25. Optimized geometry of Pd(II)-TIBDTDGA complex

Table 4.8. Thermodynamic parameters for Pd(II) thiodiglycolamide complexes



Pd-ligand complex	ΔH (KJmol ⁻¹)	-TΔS (KJmol ⁻¹)	ΔG (KJmol ⁻¹)
Pd(II)-TIBDTDGA	-180.06	-108.78	-289.23
Pd(II)-TIBTDGA (Cis)	-175.44	-37.09	-212.54
Pd(II)-TIBTDGA (Trans)	-163.69	-40.01	-203.70

The above observations suggests that T(2EH)TDGA forms 1:2 complex with Pd(II) with the tetra coordination of Pd(II) being satisfied by one 'S' and one carbonyl 'O' atom from each of the two T(2EH)TDGA molecules. On the other hand, in the case of DTDGA, 1:1 complex formation between the metal ion and the ligand satisfies the tetra coordination of Pd(II). The square planar geometry of the complexes have been confirmed following the DFT calculations which also helped in identifying the more stable configuration out of the cis and trans isomers of Pd(II)-T(2EH)TDGA complex. The high selectivity of these ligands for Pd over other fission products can be explained in terms of the formation of strong metal ligand complexes due to soft-soft interaction between Pd(II) and the 'S' atoms of the ligands as well as the ability of the ligands to sterically orient around the metal ion to give a square planar geometry to the complexes.

Conclusions

A novel neutral multidentate ligand, namely, *N,N,N',N'*-tetra-(2-ethylhexyl)dithiodiglycolamide (DTDGA) was evaluated for Pd extraction from HLLW. The extraction equilibrium was achieved in less than 5 min. The stoichiometry of extracted species into the organic phase was found to be Pd(NO₃)₂.DTDGA. A very high distribution ratio of palladium was obtained with DTDGA as compared to other previously known extractants thus making it one of the highly efficient extractants for the same purpose. The separation factor (D_{Pd}/D_M) of the order of $\geq 10^5$ for palladium over other HLLW elements makes this extractant very promising for use on plant scale.

The conditional acid uptake constant (K'_H) of the DTDGA molecule was found to be 0.60. The basicity of DTDGA is comparable to that of T(2EH)TDGA. Batch-extraction studies with SHLW suggested the possible utilization of the extractant for the selective extraction of Pd(II) over other metal ions. Reusability of the extractant was demonstrated

and the quantitative recovery of palladium from the stripping solution was attained. Two extraction stages will be required for complete extraction of 100 mg/L Palladium in 3.0 M nitric acid solution using 0.0025 M DTDGA/n-dodecane solvent system. The results reflect the possible application of the extractant for the recovery of palladium from the HLLW.

DTDGA is found to be hydrolytically stable under ambient conditions, 'S' atom being stable towards oxidation by strong nitric acid. DTDGA/n-dodecane solvent system retains its extraction and stripping properties up to a high gamma radiation dose of 0.2 MGy. However, n-dodecane was found to sensitize the degradation. Majority of degradation products were formed through cleavage of thioetheric and amidic linkages of DTDGA. The radiation chemical yield (G) of DTDGA was determined to be 9.6 which is comparable to that of other extractants proposed for reprocessing of HLLW for different applications. Solvent extraction studies with SHLW elements revealed the possible application of extractant for selective separation and recovery of palladium from high level liquid waste.

The results of EXAFS and DFT studies illustrate that the structures of the extraction complexes of Pd(II)-T(2EH)TDGA and Pd(II)-DTDGA are square planar with slight distortion owing to the bulkier alkyl groups of the amidic moieties. Among the two possible structures for Pd(II)-T(2EH)TDGA, the structure that involves the ligation of similar donor atoms in cis configuration is found to be more energetically feasible than with similar donor atoms in trans configuration. Further, the stability of the Pd(II)-DTDGA was found to be more than that of Pd(II)-T(2EH)TDGA, owing to higher degree of chelation.

CHAPTER 5

Evaluation of Ligand Grafted Resins for Pd(II) Separation from HLLW

In the previous chapters we have evaluated two novel ligands for liquid-liquid extraction of palladium from HLLW. To overcome various problems associated with liquid-liquid extraction systems, like third phase formation, compatibility issues with the diluent and the corresponding hydrodynamics related problems, solid phase extraction becomes one of the most sought after methods for separation and recovery of palladium from HLLW solution. Several type of solid phase extraction resins have been developed depending on the type of palladium species present in the solution, which usually depends on the aqueous phase acidity. Thus, anion exchange resins, namely 4-(*N,N*-dimethyl benzimidazole) phenyl (AR-01) gives very high distribution ratio of palladium [78]. However, the exchange is so slow that equilibrium is attained only after 20 hours of contact at 60°C. For other anion exchangers like tertiary Amberlite IRA-93ZU and quaternary Amberlite IRA-900, Amberlite IRN-78, Dowex 1X8-400 and Dowex 2X8-400, sorption equilibrium of palladium is achieved after 1 hour at 60°C [78]. The strongly basic resin AV-17X8 gives distribution ratio of 64, 56 and 200 for Pd(II) at acidities of 0.5, 3.0 and 8.0 M HNO₃ respectively [78]. Similarly, a strongly basic pyridinium anion exchanger (VP-1AP) gives, for the same acidities, D_{Pd} values of 64, 77 and 35 respectively at corresponding acidities mentioned above [78]. A stronger affinity to Pd (II) is exhibited by a weakly basic anion exchanger (AN-104), which yields $D_{Pd} = 475$, 350 and 120, respectively, and especially, by a strongly basic phosphonium anion exchanger (KhFO) with D_{Pd} values 900, 500 and 200, respectively [78]. On the other hand, some of the cation exchangers proposed for palladium sorption include sulfonic acid resin KU-2X8 and phosphoric acid resin KRF-20t-60, the latter giving $D_{Pd} = 9$ at 3.0 M nitric acid [79]. Another extractant, namely, imidazolium nitrate immobilized on

polystyrene-divinylbenzene resin matrix shows appreciable sorption of palladium ($D_{Pd} \sim 140$) at 3.0 M nitric acid, the equilibrium was attained within 2 hours [80]. Also, macroporous silica based anion exchangers containing either pyridine or methyl pyridine functional group have been reported to have efficient uptake of palladium ($D_{Pd} \sim 10^2$) at 6.0 M nitric acid concentration [81]. Recently, Tertiary amine grafted cedar wood powder have been found to give almost complete sorption of palladium from 0.1 M nitric acid medium, with the D value decreasing gradually with increase in nitric acid concentration [83]. However, dissolution of parts of the absorbent in highly active HLW may create problems during further processing. Bis-(2,4,4-trimethylpentyl)-monothiosphonic acid (Cyanex-302) encapsulated in microcapsules of Ca alginate gel shows high D_{Pd} of the order of $10^4 \text{ cm}^3/\text{g}$ from 0.2 to 0.5 M HNO_3 [84]. Appreciable separation factors ($\geq 10^2$) are achieved with respect to other platinum group metals. However, the kinetics of extraction is so slow that the equilibrium is attained only after 3 days. Similarly, triisobutyl phosphine sulphide (Cyanex-471X) impregnated on chromosorb-102 gives D_{Pd} of the order of 10^3 within 45 minutes, the complete back extraction being carried out by thiourea [85]. In view of the slow kinetics of sorption and low D_{Pd} values in the case of different types of resins it is necessary to synthesize and evaluate new resins.

In the present work, Amberlite XAD-16 resin functionalized with 2-acetyl pyridine group (AP-XAD 16) and 2-acetyl amide group (ACAM-XAD 16), have been synthesized and evaluated for the extraction of palladium (II) from nitric acid medium. The two resins would differ in mode of ligation to palladium as AP-XAD 16 has one soft donor 'N' atom of pyridine moiety and one hard donor 'O' atom of carbonyl moiety while ACAM-XAD 16 has two hard donor 'O' atoms of carbonyl moieties. The effect of donor atom participation in complex formation with palladium vis-à-vis other metal ions present in SHLW solution has been investigated. The effect of various parameters such as, time of

equilibration, concentration of nitric acid and palladium ion, on extraction of palladium by the resin has been reported.

The synthesis and characterization of AP-XAD 16 and ACAM-XAD 16 resins have been described in chapter 2. In this chapter the evaluation of resins for the extraction of Pd(II) vis- à-vis other metal ions present in SHLW solution have been discussed.

5.0. Evaluation of AP-XAD 16 and ACAM-XAD 16

5.1. Sorption kinetics

The details of the experimental methodologies for separation studies are given in chapter 2 (Section 2.4.5). The sorption of Pd by AP-XAD 16 and ACAM-XAD 16 resin as a function of time is shown in fig. 5.1 and fig. 5.2, respectively. It is evident that the sorption of Pd on to the resins is fast, the equilibrium being attained within 30 to 45 minutes for AP-XAD 16 and 45 to 60 minutes for ACAM-XAD 16 respectively.

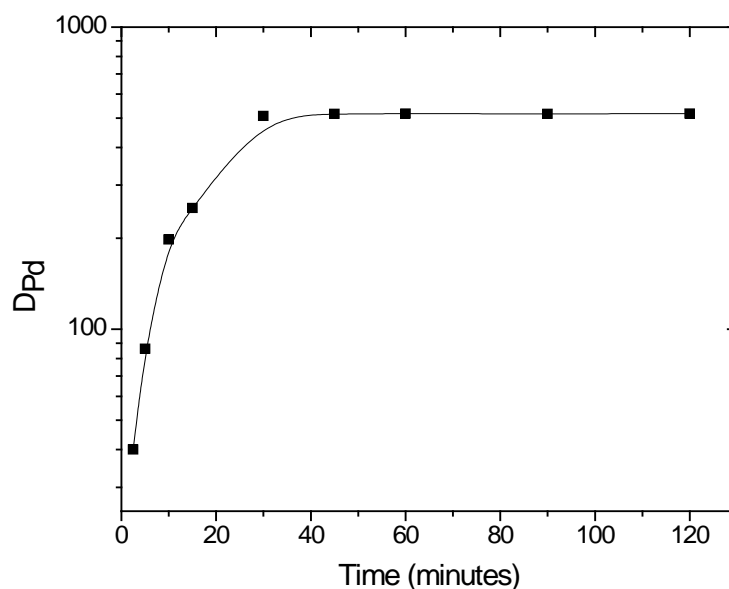


Fig. 5.1. Kinetics of sorption of palladium on AP-XAD 16 resin as a function of time.

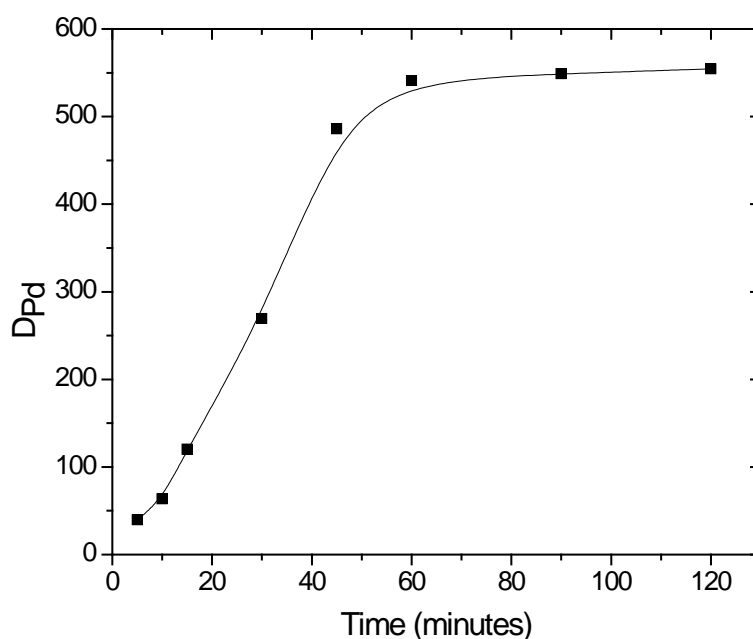


Fig. 5.2. Kinetics of sorption of palladium on ACAM-XAD 16 resin.

In order to investigate the mechanism of Pd sorption onto the resins and rate-controlling steps, the experimental data have been fitted using pseudo-first and pseudo-second-order kinetic models (cf. 2.5.7.2). The pseudo first order rate constant (k_f) and capacity (q_e) for the sorption of Pd by the two resins were calculated from the slope and intercept of the plots of $\log (q_e - q_t)$ against t (Fig. 5.3 and Fig. 5.5). The initial sorption rate (h), the equilibrium sorption capacity (q_e) and the pseudo-second-order rate constant (k_s) were obtained from the slope and intercept of the plots of t/q_t against t (Fig. 5.4 and Fig. 5.6). For both the resins, the correlation coefficient was found to be closer to unity for pseudo-second order kinetics model than that for pseudo-first-order kinetic model. This suggests that the sorption data follows pseudo-second-order kinetic model for both the polymeric resins.

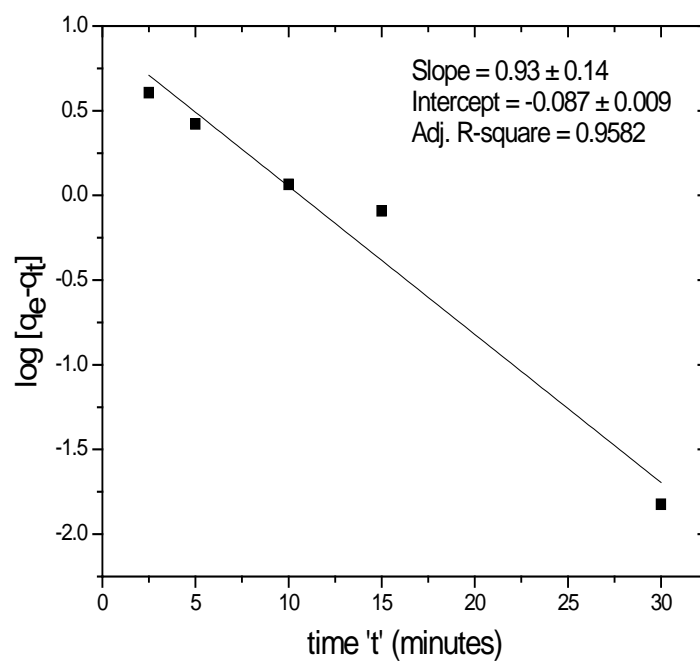


Fig. 5.3. Pseudo-first-order plot of palladium sorption onto AP-XAD16.

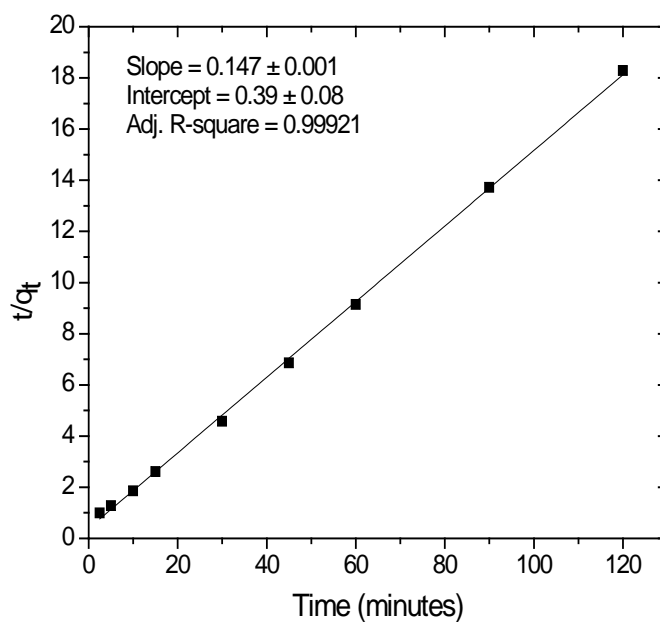


Fig. 5.4. Pseudo-second-order plot of palladium sorption onto AP-XAD 16.

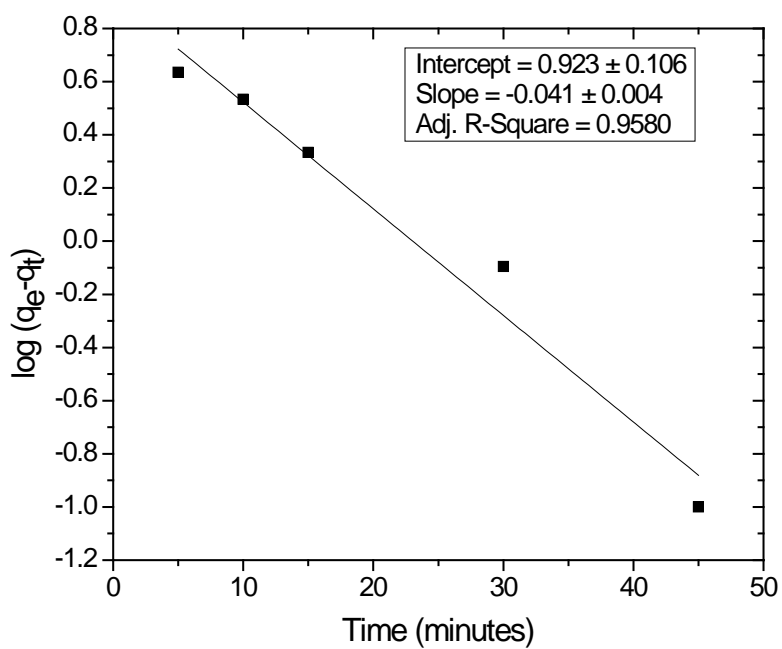


Fig. 5.5. Pseudo-first-order plot of palladium sorption onto ACAM-XAD16.

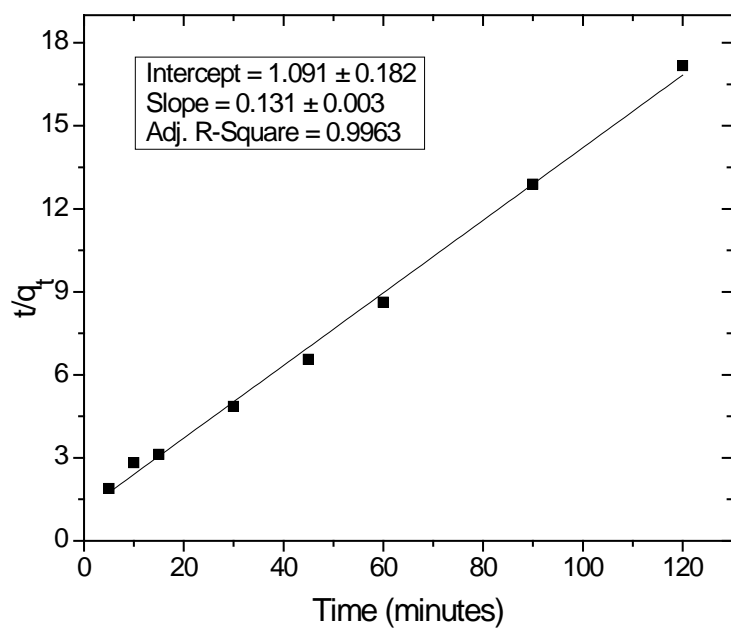


Fig. 5.6. Pseudo-second-order plot of palladium sorption onto ACAM-XAD16.

5.2. Effect of Acidity

The presence of pyridine moiety and the carbonyl group in AP-XAD 16 resin suggests that the sorption of palladium on this resin would be dependent on the acidity of aqueous feed solution. Fig. 5.7 shows the uptake of Pd by AP-XAD 16 resin as a function of acidity. It is observed that at lower acidity, the uptake is maximum, which decreases gradually with increase in acidity. However, D_{Pd} remains almost constant over the range of 2.0 to 3.8 M HNO_3 , with significant decrease at higher acidities.

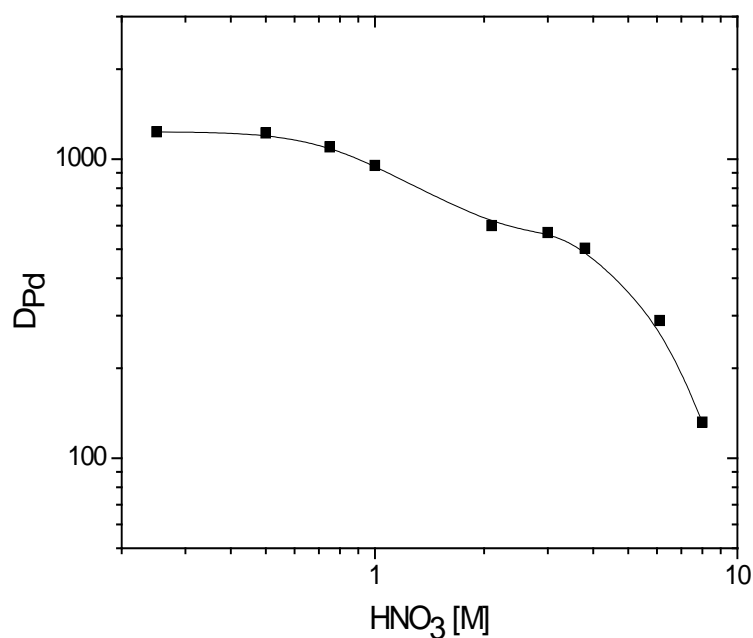


Fig. 5.7. Sorption of palladium on AP-XAD 16 resin as a function of initial nitric acid concentration.

The above acid dependence can be attributed to the fact that at lower acidity, 'N' atom of pyridine moiety and the 'C=O' group of acetyl moiety, both participate in the complex formation, resulting in higher D_{Pd} . With increase of acidity, 'N' atom gets protonated and consequently there is a decrease in D_{Pd} . Between 2.0 and 3.8 M nitric acid concentration, observed constancy of D_{Pd} values could be attributed to the participation of protonated 'N' atom in complex formation, albeit through anion exchange mechanism. This could be

due to the existence of palladium in the form of either $\text{Pd}(\text{NO}_3)_2$ or $\text{Pd}(\text{NO}_3)_3^-$ in this region, with the former species dominating at lower acidities. Finally, the significant decrease in D_{Pd} at higher acidity may be due to protonation of 'C=O' group at higher acidities which further prevents complex formation with palladium, and the uptake of Pd if any, will be solely because of anion exchange mechanism.

Figure 5.8 shows the uptake of Pd(II) onto ACAM-XAD 16 resin as a function of acidity. It is observed that with the increase in feed acidity D_{Pd} increases initially, reaches a maximum around 3.0 M and then finally decreases gradually.

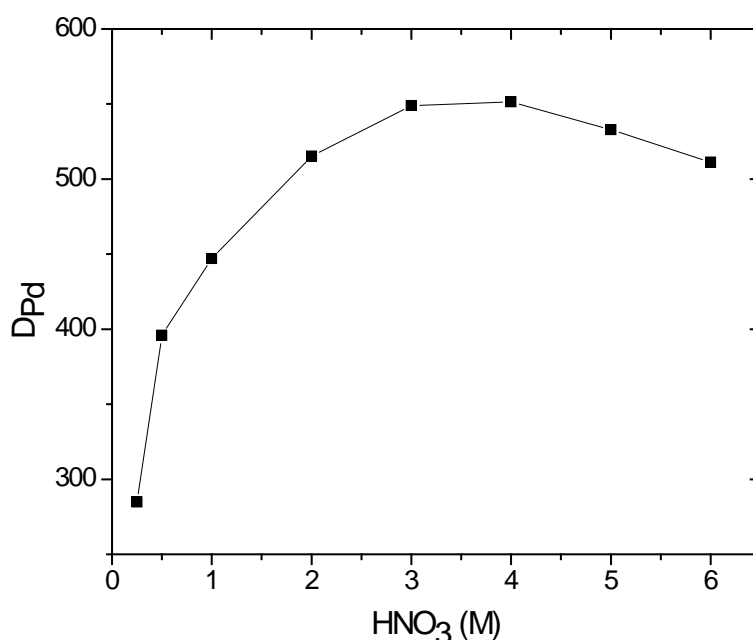


Fig. 5.8. Sorption of palladium on ACAM-XAD 16 resin as a function of initial nitric acid concentration.

At lower acidities, the increase in D_{Pd} with increase in feed acidity is due to the increase in the activity of nitrate ions which facilitates the extraction reaction in forward direction. The gradual decrease in D_{Pd} at higher acidity can be explained in terms of the protonation of 'C=O' group thereby hindering complex formation with palladium.

5.3. FTIR studies

Detailed FT-IR studies have been carried out to elucidate the mode of linkage between palladium and donor atoms anchored on to the resins. Fig. 5.9 shows the FT-IR spectra of neat AP-XAD 16 resin, AP-XAD resin in contact with 3.0 M HNO₃ and AP-XAD 16 resin contacted with Pd in 3.0 M HNO₃.

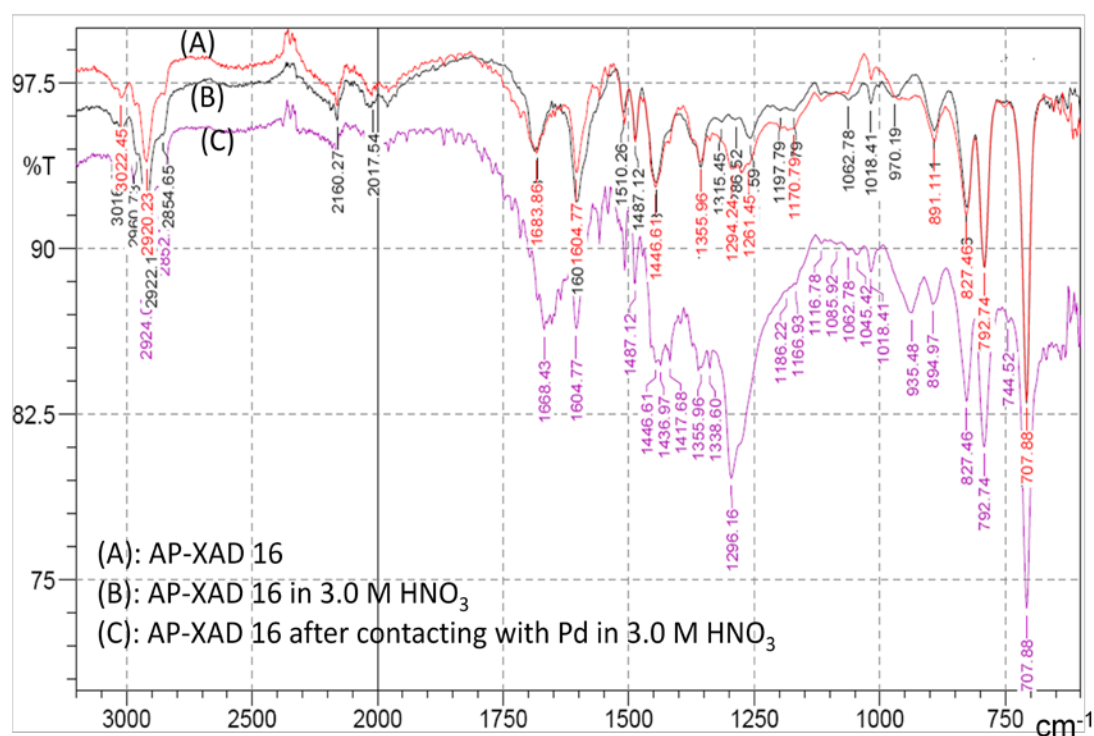


Fig. 5.9. FT-IR spectra of AP-XAD 16 resin

In the case of neat AP-XAD 16 and the resin in contact with 3.0 M nitric acid, the spectra are similar except that there is small downward shift in 'C=O' stretching frequency from 1682.4 to 1680.1 cm⁻¹ and slight shift in modes relating to pyridine moiety. However, for resin in contact with Pd (II) in 3.0 HNO₃, comparatively larger shift is observed from 1682.4 to 1668.3 cm⁻¹ for C=O' stretching mode. For pyridine moiety, while some of the peaks are shifted downward (viz., 970 to 935 cm⁻¹), others are shifted upwards (viz., 891.1 to 894.9 cm⁻¹). The downward shift in the C=O stretching frequency and that of some of the pyridine moiety suggest complexation of Pd with the ligand anchored on to the resin. The upward shifts could be due to the occurrence of different resonant forms of

pyridine. Also, some new peak appears, more remarkably at 1296 cm^{-1} which corresponds to the nitrate ions in the sorbed metal complex. Likewise, while almost similar spectra were obtained for neat ACAM-XAD 16 and the resin in contact with 3.0 M nitric acid, there is small downward shift in 'C=O' stretching frequency from 1682.4 to 1680.1 cm^{-1} . However, for resin in contact with Pd(II) in 3.0 HNO₃, comparatively larger shift is observed from 1682.4 to 1673.3 cm^{-1} for C=O' stretching mode. The downward shift corroborates with the binding of carbonyl moiety either with proton or the metal ion. Further, the peak at 1296 cm^{-1} corresponds to the nitrate ions in the sorbed metal complex.

5.4. Sorption studies

Sorption isotherm experiments were carried out with different initial total concentrations of palladium in the range of 25–120 mg/L in 3.0 M HNO₃ (as shown in Fig. 5.10 and Fig. 5.11). The equilibrium sorption capacity (q_e) of AP-XAD 16 and ACAM-XAD 16 resins increase with the increase of initial total concentration of palladium.

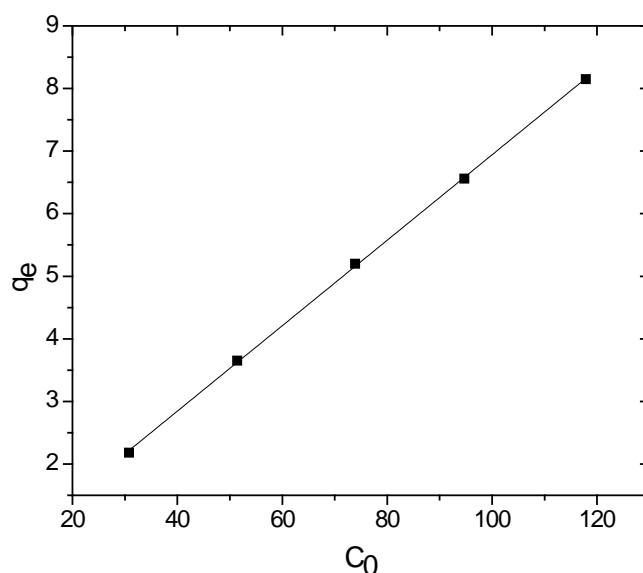


Fig. 5.10. Equilibrium sorption isotherms for palladium on AP-XAD 16.

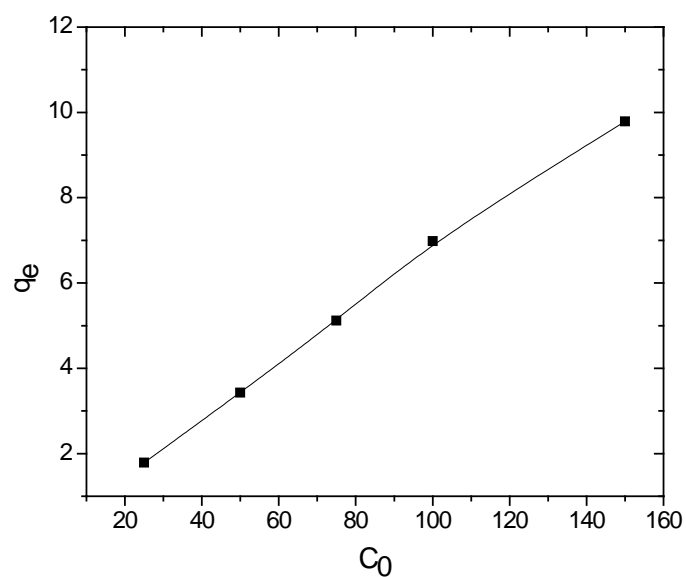


Fig. 5.11. Equilibrium sorption isotherms for palladium on ACAM-XAD 16.

The sorption isotherm data were fitted using the equations representing the Langmuir and the Freundlich isotherms (Section 2.5.7.3). Figures 5.12 and 5.13 show the respective isotherms for AP-XAD 16 along with the corresponding regression coefficients. Similarly figures 5.14 and 5.15 show the isotherms for ACAM-XAD 16. It is evident that the experimental data fit well with both the Langmuir as well as the Freundlich isotherm, which could be attributed to single to multilayer sorption of the metal ion in the given experimental conditions.

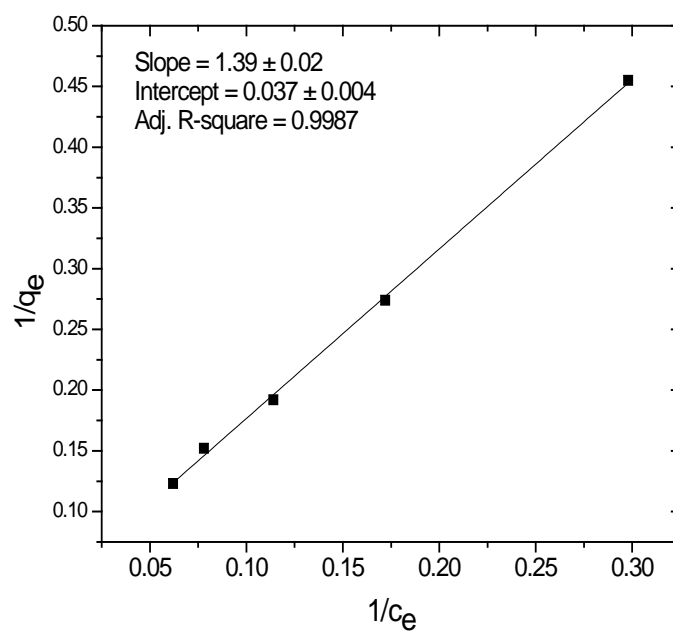


Fig. 5.12. Langmuir plot for the sorption of palladium onto AP-XAD 16 resin.

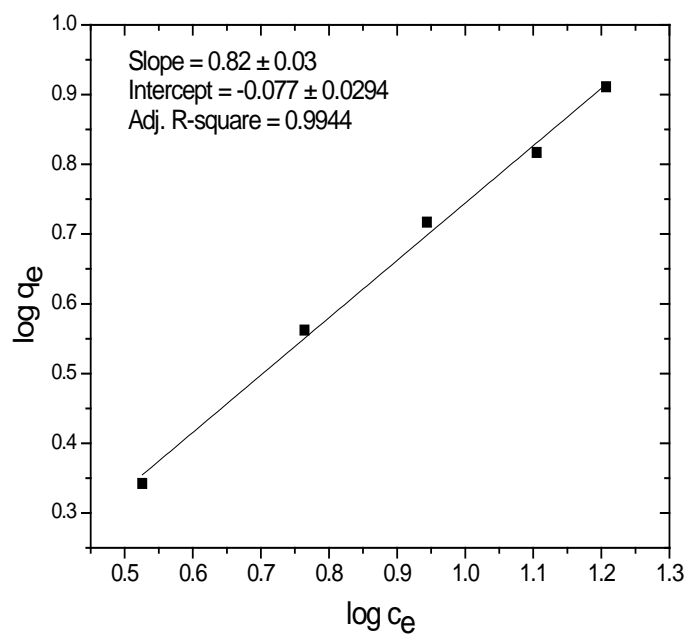


Fig. 5.13. Freundlich plot for the sorption of palladium onto AP-XAD 16 resin

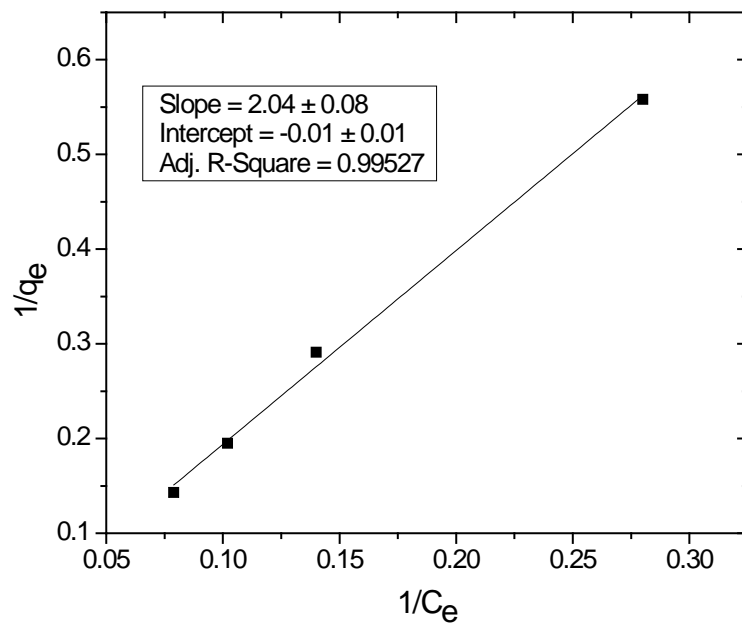


Fig. 5.14. Langmuir plot for the sorption of palladium onto ACAM-XAD 16 resin.

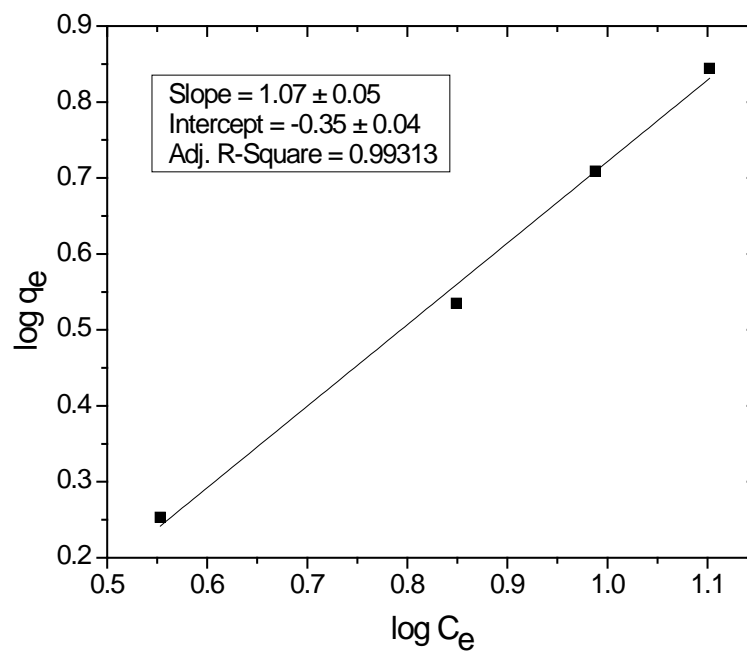


Fig. 5.15 Freundlich plot for the sorption of palladium onto ACAM-XAD 16 resin.

5.5. Maximum loading capacity

The maximum palladium sorption capacity for AP-XAD 16 and ACAM-XAD 16 resins were determined using 100 mg of resin beads, which were equilibrated with excess amounts of metal ion solution (10 ml, 100 µg/ml) for 1 hour. These resin beads were then repeatedly contacted with the above solution to the point where no further uptake was observed. It was found that maximum of 804 µg of palladium could be sorbed onto 100 mg of AP-XAD 16 resin, thus giving the maximum sorption capacity of ~ 8 mg/g of resin. For ACAM-XAD 16 resin, the maximum sorption capacity was found to be of ~ 9 mg/g of resin.

5.6. Back extraction studies

Back extraction of palladium from loaded AP-XAD 16 and ACAM-XAD 16 resins have been carried out with various reagents and the results are discussed below.

For loaded AP-XAD 16 resin it was found that deionized water at pH 7, 0.1 M HNO₃ or 0.05 M ammonium carbonate + 0.05 M ammonium nitrate, are not suitable for back extraction of palladium as only about 5-10% back extraction could be achieved in single step using these reagents. However with 0.01 M thiourea in 0.1 M nitric acid solution, almost quantitative back extraction was achieved in two steps.

For loaded ACAM-XAD 16 resin the back extraction of palladium with deionized water at pH 7 and 0.1 M HNO₃ was not suitable, as only about 5-10 % elution could be achieved in single step. With 0.1 M HEDTA in 0.1 M HNO₃, about 30-40 % of Pd can be back extracted. However with 0.01 M thiourea in 0.1 M nitric acid solution, almost quantitative elution was achieved in two steps.

5.17. Sorption studies with simulated high level waste solution (SHLW)

From above discussion it is evident that AP-XAD 16 and ACAM-XAD 16 resins can be used to separate and recover palladium from nitric acid medium. However, HLLW

arising from the PUREX process stream would contain stable/radioactive fission products along with the actinides in appreciable quantities. Therefore, to evaluate the efficacy of both the resins in separation and recovery of palladium from HLLW, sorption studies were carried out with SHLW solution which represents the composition of the HLLW generated during the reprocessing of a pressurized heavy water reactor spent fuel. Fig. 5.16 shows D_M and the % sorption of various elements present in SHLW, when contacted with AP-XAD. From the figure it is observed that almost 85% of palladium ($D_{Pd} \sim 500$) is sorbed along with Mo ($D_{Mo} \sim 2$, % sorption ~ 2) and Mn ($D_{Mn} \sim 1$, % sorption ~ 1) albeit in lesser amounts. Mo and Mn having fairly low D values than that of Pd, can be easily scrubbed from the resin phase using 3.0 M nitric acid, while other metal ions are hardly extracted on to the resin. Therefore, separation and recovery of palladium from SHLW solution could be achieved using the present resin.

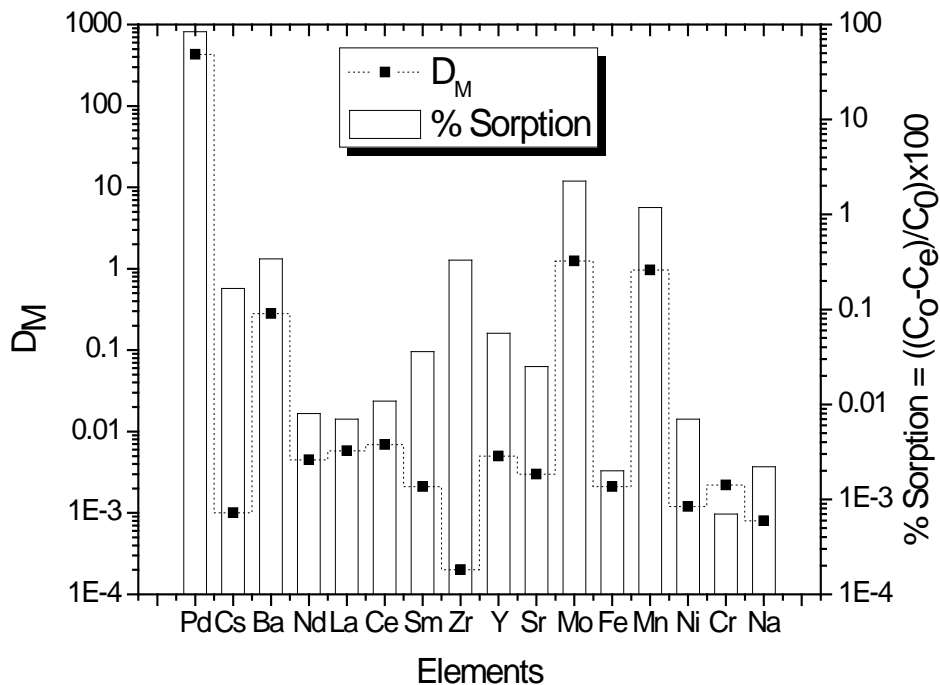


Fig. 5.16. Distribution ratio and % sorption of SHLW elements for AP-XAD16.

Preliminary sorption studies of ACAM-XAD 16 have shown appreciable uptake of lanthanides (10-20% sorption) along with palladium, which necessitates the separation of trivalent lanthanides prior to sorption of Pd. Earlier it has been reported that during actinide partitioning from HLLW, trivalent lanthanides are recovered along with trivalent actinides [151]. Therefore, the SHLW was contacted with 0.2 M TEHDGA/ 30% isodecyl alcohol/n-dodecane prior to use for sorption of Pd. Fig. 5.17 shows the D_M of various elements present in SHLW when contacted with ACAM-XAD 16 resin. From the figure it is evident that palladium ($D_{Pd} \sim 510$) is sorbed along with other elements namely, Ba, Sr, Mo, etc., having fairly lower D than that of Pd, which can be easily scrubbed from the resin phase using 3.0 M nitric acid leaving only Pd sorbed onto the resin.

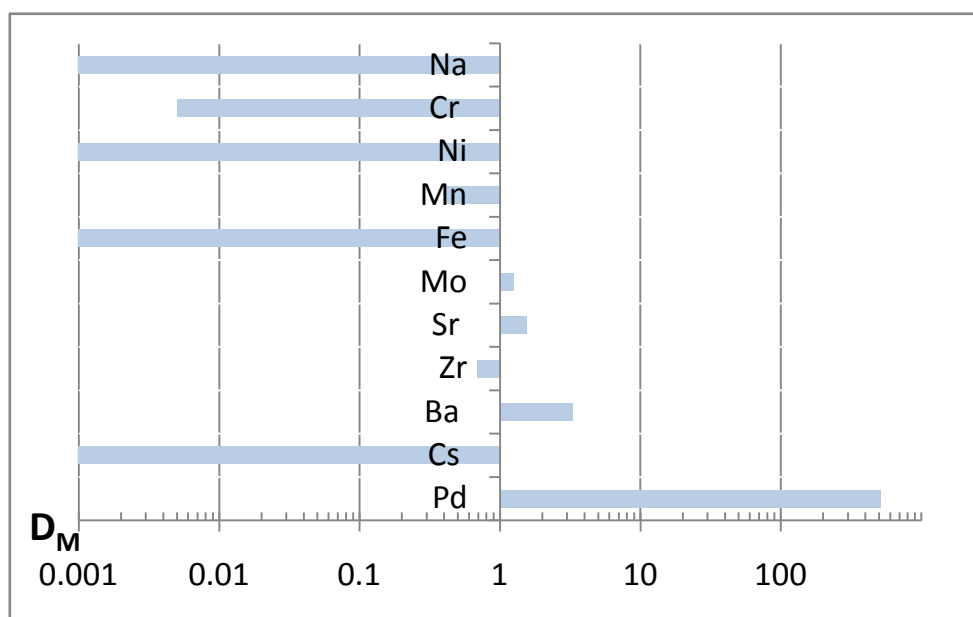


Fig. 5.17. Distribution ratio of SHLW elements with ACAM-XAD16.

Conclusions

Novel sorbents, namely, AP-XAD 16 and ACAM-XAD 16 were evaluated for the separation and recovery of Pd from SHLW solution by batch sorption technique. Pd sorption on to both the resins was found to follow a pseudo-second-order kinetics. The adsorption isotherm data for both the resins fit well to both the Langmuir and Freundlich isotherm models. Maximum loading capacity for Pd was determined to be 8 and 9 mg/g for AP-XAD 16 and ACAM-XAD 16 respectively. FT-IR studied revealed the mode of ligation of Pd onto AP-XAD 16 and ACAM-XAD 16 resin. Satisfactory results were obtained for the separation and recovery of Pd from SHLW solution. Thus, AP-XAD 16 can be used directly for the separation and recovery of Pd from SHLW solutions, whereas ACAM-XAD can only be used after actinide partitioning. The sorbents can be effectively regenerated by treating with 0.01 M thiourea in 0.1 M HNO₃.

Chapter 6

Summary and conclusions

Separation and recovery of palladium from high level waste HLLW originating from reprocessing of spent nuclear fuel is necessary from the viewpoint of various problems encountered during vitrification as well as the conceptualization of the process where HLLW can be treated as a secondary source of this valuable metal. In the present thesis efforts have been made towards the synthesis and evaluation of novel class of reagents for separation and recovery of palladium from HLLW.

The work reported in this thesis can be summarized as follows:

(i) A novel neutral multidentate ligand, namely, *N,N,N',N'*-tetra-(2-ethylhexyl)-thiodiglycolamide (T(2EH)TDGA) was synthesized and evaluated for the extraction of palladium from nitric acid medium. Extraction equilibrium studies showed that almost complete extraction of palladium was obtained within 5 min. The influence of nitric acid, nitrate ion and T(2EH)TDGA concentration on the distribution of palladium has been investigated. With the increase in nitric acid/nitrate ion concentration, increase in extraction of palladium was observed. Stoichiometry of the extracted species was found to be $\text{Pd}(\text{NO}_3)_2 \cdot 2\text{T}(2\text{EH})\text{TDGA}$ by slope analysis method. Loading studies with 10^{-3} M T(2EH)TDGA/*n*-dodecane showed maximum uptake of 5.44×10^{-4} M palladium thus conforming to above stoichiometry of metal to ligand. Acid uptake studies have shown that 1:1 stoichiometry exists between T(2EH)TDGA and HNO_3 at nitric acid concentration above 3.5 M. The acid uptake constant (K_H) was found to be 0.62 which could be due to the presence of two carbonyl groups of amidic moiety. The effect of

various diluents on the extraction of palladium showed quantitative uptake irrespective of the nature of diluents. More than 99% of palladium was back extracted in single contact using 0.01 M thiourea in 0.1 M nitric acid. Reusability studies of the extractant indicate that D_{Pd} remained almost constant even after five successive cycles of extraction and stripping. Palladium was quantitatively recovered from thiourea strip solution by treating it with ammonia and filtering the precipitate of palladium sulphide. T(2EH)TDGA has shown very high selectivity for Pd (II) over other metal ions present in SHLW solution. Extraction studies with HLLW elements showed negligible uptake of U, Am, Eu, Sr, Cs and Ru. The separation factor (SF) for Pd (II) over other metal ions was found to be more than 10^5 .

To account for very high extractability of palladium with T(2EH)TDGA over other 'S' donor extractants, namely Bis-(2-ethylhexyl) sulphoxide (BESO), FT-IR, as well as Raman studies were carried out, which suggested the ligation through carbonyl as well as the thio-ether group. Conditional extraction constants ($\log K_{ex}^0$) were determined and the thermodynamic parameters were calculated from the dependence of the $\log K_{ex}^0$ on temperature. ΔG_{ex} , ΔH_{ex} , and ΔS_{ex} values were $-41.78 \text{ kJ mol}^{-1}$, $-55.12 \text{ kJ mol}^{-1}$ and $-44.04 \text{ JK}^{-1} \text{ mol}^{-1}$ respectively. The extraction process was found to be enthalpy driven with the entropy factor counteracting it.

Hydrolytic and radiolytic stability of T(2EH)TDGA solvent system has been investigated to establish its application in separation and recovery of palladium from HLLW. Hydrolysis of T(2EH)TDGA solvent system with nitric acid was not observed. Moreover, unlike other "S" donor extractants used for the said purpose, the oxidation of thioetheric sulphur to sulphoxide or sulphones was also not observed. However, radiolytic degradation was notably observed and found to increase with increase in absorbed dose. *n*-dodecane was found to sensitize the degradation of T(2EH)TDGA. Up to a gamma

radiation dose of 0.2 MGy, no significant loss of T(2EH)TDGA was observed. The degradation products were identified by GC-MS. The major products were found to be formed by cleavage of thioetheric and amidic bonds of T(2EH)TDGA molecule. The extraction studies of palladium with irradiated solvent indicate that with 0.025 M T(2EH)TDGA/*n*-dodecane, there was no significant change in D_{Pd} up to an absorbed dose of 0.2 MGy above which it decreases significantly. However, with 0.05 M T(2EH)TDGA/*n*-dodecane, there was gradual decrease in D_{Pd} with increase of absorbed dose. Further, the radiolysis does not affect the stripping behavior of palladium. Extraction studies of Pd(II) and other fission products from SHLW solutions to irradiated solvent system showed that, except palladium, none of the other elements is extracted significantly, thus retaining its remarkable selectivity.

A precise, sensitive and selective method for the spectrophotometric determination of palladium (II) using T(2EH)TDGA as an extractant has been developed. Pd(II) forms a yellow colored complex with T(2EH)TDGA which exhibits an absorption maximum at ~ 300 nm and obeys Beer's law in the concentration range $1.0\text{--}15.0 \mu\text{g ml}^{-1}$ of palladium with a molar absorptivity of $1.29 \times 10^5 \text{ M}^{-1} \text{ cm}^{-1}$. The effects of various experimental parameters have been studied to establish the optimum conditions for the extraction and determination of palladium. The precision of the method has been evaluated and the relative standard deviation has been found to be less than 0.5%. The method has been successfully applied to the determination of palladium in SHLW solution.

(ii) Another novel multidentate ligand, namely, *N,N,N',N'*-tetra-(2-ethylhexyl) dithiodiglycolamide (DTDGA) has been synthesized and studied for its extraction behavior towards Pd and other elements present in HLLW. Extraction of Pd was found to increase with increase in nitric acid concentration up to 3.0 M, above which the extraction remains almost constant. Acid uptake studies showed 1:1 stoichiometry

between DTDGA and HNO_3 at nitric acid concentration above 3.0 M. The acid uptake constant (K_H) was found to be 0.60 which could be due to the presence of two carbonyl groups of amidic moiety. DTDGA has shown very high extractability and selectivity for Pd over other metal ions present in SHLW. The SF for Pd over other metal ions was found to be more than 10^4 . Almost complete back extraction of palladium from organic phase was achieved with 0.01 M thiourea in 0.1 M nitric acid. Reusability studies of the extractant indicate that D_{Pd} remained almost constant even after five successive cycles of extraction and stripping. Two extraction stages will be required for complete extraction of 100 mg/L palladium in 3.0 M nitric acid solution using 0.0025 M DTDGA/n-dodecane solvent system. The extractant showed remarkable extractability and selectivity for palladium over other metal ions present in HLLW. The distribution ratios as well as the separation factor for palladium were found to be the highest reported so far thus making this extractant the most promising candidate for effective separation of palladium from HLLW.

DTDGA solvent system was evaluated for hydrolytic and radiolytic stability to ascertain its application in separation and recovery of palladium from HLLW solutions. Hydrolysis of DTDGA solvent system was not observed up to a contact time of two weeks with 3.0 M nitric acid solution. Moreover, contrary to other 'S' donor extractants used for the said purpose, the oxidation of thioetheric sulphur to sulphoxide or sulphones was also not observed. On the other hand, radiolysis of DTDGA solvent system was notably observed, which was found to increase with increase in absorbed dose. Up to a gamma radiation dose of 0.2 MGy, no significant loss of DTDGA was observed. Aliphatic diluent namely n-dodecane was found to have sensitization effect on degradation of DTDGA. The degradation products were identified by GC-MS, the major ones were found to be formed by cleavage of thioetheric and amidic bonds of DTDGA molecule. The liquid - liquid

extraction studies of palladium with irradiated solvent indicate that there was no significant change in D_{Pd} up to an absorbed dose of 0.2 MGy above which it decreases gradually. Further, the radiolysis does not affect the stripping behavior of palladium. Extraction studies of SHLW elements with irradiated solvent system showed that, except palladium, none of the other elements is extracted significantly thus retaining its remarkable selectivity.

The structure of the extraction complexes of palladium (II) with novel ligands, namely, T(2EH)TDGA and DTDGA have been determined by EXAFS in conjunction with theoretical calculation (DFT). T(2EH)TDGA, having one thioetheric 'S' atom forms square planar complex with Pd (II) ion, exhibiting 2:1 stoichiometry, with one sulphur atom and one carbonyl oxygen atom from each T(2EH)TDGA molecule interacting with Pd(II) at distances of 2.24 and 2.04 Å respectively. On the other hand, DTDGA having two 'S' atoms in addition to two carbonyl groups, forms square planar complex with Pd(II), exhibiting 1:1 stoichiometry, wherein both the sulphur atoms and the carbonyl oxygen of DTDGA interact with Pd(II) at distances of 2.29 and 2.05 Å respectively. The slight distortion from the perfect square planar geometry could be attributed to the steric hindrance imposed by the bulky alkyl group of the amidic moieties. DFT calculations for the Pd-ligand complexes show that Pd(II)-DTDGA complex with 1:1 stoichiometry is energetically more stable than Pd(II)-T(2EH)TDGA complex with 1:2 stoichiometry. Among the two possible Pd(II)-T(2EH)TDGA complex geometries, the symmetric ligation appears more feasible.

(iii) Amberlite XAD-16 has been functionalized with 2-acetyl pyridine by coupling it with 2-chloro pyridine after acetylation. The resulting functionalized resin (AP-XAD 16) has been characterized by various techniques like FT-IR, TGA, elemental analysis, etc., and has been evaluated for the solid phase extraction of palladium and other metal ions

present in HLLW. Sorption equilibrium was attained within 30 to 45 minutes. The pseudo-second order kinetics model yielded the best fit for the experimental data of sorption kinetics. Pd sorption was found to decrease gradually with increase in aqueous phase acidity. The sorption process involves the complex formation between Pd(II) and the functional groups, viz., the carbonyl group and soft 'N' atom of pyridine moiety with lone pair of electrons. The loaded palladium can be effectively back extracted using acidic thiourea solutions. The adsorption isotherm data fitted well with Langmuir as well as Freundlich models. The maximum sorption capacity of the resin was found to be 8 mg/g which is in agreement with the equilibrium sorption capacity. Sorption studies carried out with SHLW solution have shown very high uptake of palladium as compared to the other elements, thus showing the potential for possible use of the resin for efficient separation and recovery of palladium from HLLW.

(iv) Acetyl Amide grafted XAD-16 (ACAM –XAD 16) resin has been synthesized by acetylating Amberlite XAD-16 resin followed by coupling it with *N,N'*-diisobutyl-2-chloro acetamide. Various instrumental techniques like FT-IR, TGA, elemental analysis, etc., were used to characterize ACAM-XAD 16 resin. The resin has been evaluated for the solid phase extraction of palladium and other metal ions present in HLLW. The sorption kinetics of Pd onto the resin was found to be fast, the equilibrium being attained within 45 to 60 minutes. The pseudo-second order kinetics model fit well with the experimental data of sorption kinetics. With the increase in aqueous phase acidity, Pd sorption increases initially, reaches a maximum around 3.0 M and then decreases. The sorption process involves the complex formation between Pd(II) and the functional groups, viz., the carbonyl groups from the acetyl and the amidic moieties. The loaded palladium can be effectively eluted using acidic thiourea solutions and HEDTA solutions. Both the Langmuir and the Freundlich models fits well with the isothermal adsorption

data with maximum sorption capacity equal to 9 mg/g which corroborates well with the equilibrium sorption capacity. Sorption studies carried out with SHLW have shown very high uptake of palladium, and with less but finite co-extraction of lanthanides.

The conclusions drawn from the present studies can be listed as:

1. Novel ligands, namely, *N,N,N',N'*-tetra-(2-ethylhexyl)thiodiglycolamide (T(2EH)TDGA) and *N,N,N',N'*-tetra-(2-ethylhexyl)dithiodiglycolamide (DTDGA), have shown very high extractability and selectivity for Pd over other metal ions present in HLLW. Both the ligands have shown fair radiolytic and hydrolytic stability, and therefore have shown potential for their direct use in separation and recovery of Pd from HLLW solutions.
2. Novel ligand grafted resins, namely, AP-XAD16 and ACAM-XAD16, have shown high extractability for Pd. AP-XAD16, showing adequate selectivity for Pd can be used directly for HLLW solutions, whereas ACAM-XAD16 showing co-extraction of lanthanides along with Pd, can only be used after actinide partitioning.

List of Publications

1. *N,N,N',N'*-tetra-(2-Ethylhexyl) Thiodiglycolamide T(2EH)TDGA: A Novel Ligand for Separation and Recovery of Palladium from High Level Liquid Waste (HLLW) Solutions. R. Ruhela, J.N. Sharma, B.S. Tomar, S. Panja, S.C. Tripathi, R.C. Hubli, A.K. Suri. **Radiochimica Acta**, 2010, 98, 209-214.
2. *N,N,N',N'*-tetra-(2-Ethylhexyl)Thiodiglycolamide (T(2EH)TDGA): A Promising Ligand for Separation and Recovery of Palladium from High Level Liquid Waste (HLLW) Solutions. R. Ruhela, J.N. Sharma, B.S. Tomar, V.C. Adya, T.K. Sheshgiri, R.C. Hubli, A.K. Suri. **Separation Science & Technology**, 2011, 46, 1-7.
3. Extractive spectrophotometric determination of palladium with *N,N,N',N'*-tetra-(2-ethylhexyl)-thiodiglycolamide T(2EH)TDGA. R. Ruhela, J.N. Sharma, B.S. Tomar, R.C. Hubli, A.K. Suri. **Talanta**, 2011, 85 (2), 117-1220.
4. Dithiodiglycolamide: Novel ligand with highest selectivity and extractability for palladium. R. Ruhela, J.N. Sharma, B.S. Tomar, M.S. Murali, R.C. Hubli, A.K. Suri. **Tetrahedron Letters**, 2011, 52, 30, 3929-3932.
5. Studies on hydrolysis and radiolysis of *N,N,N',N'*-tetra-(2-ethylhexyl)thiodiglycolamide T(2EH)TDGA. R. Ruhela, J.N. Sharma, B.S. Tomar, K.K. Singh, M. Kumar, R.C. Hubli, A.K. Suri. **Radiochimica Acta**, 2012, 100, 37-44.
6. Studies on Separation and Recovery of palladium from Simulated High Level Liquid Waste (SHLW) Solution with novel extractant *N,N,N',N'*-tetra-(2-ethylhexyl)-dithiodiglycolamide DTDGA. R. Ruhela, B.S. Tomar, J.N. Sharma, T.K. Sheshgiri, V.C. Adya, R.C. Hubli, A.K. Suri. **Separation Science & Technology**, 2012, (DOI: 10.1080/01496395.2012. 724 140).

7. Stability Studies of *N,N,N',N'*-tetra-(2-ethylhexyl) dithiodiglycolamide (DTDGA). R. Ruhela, B.S. Tomar, K.K. Singh, J.N. Sharma, M. Kumar, P.N. Bajaj, V.C. Adya, T.K. Seshagiri, R.C. Hubli, A.K. Suri. **Radiochimica Acta**, **2012** (DOI: 10.1524/ract.2013.2008).
8. Amberlite XAD-16 functionalized with 2-acetyl pyridine group for the solid phase extraction and recovery of palladium from High Level Waste (HLW). R. Ruhela, K.K. Singh, B.S. Tomar, J.N. Sharma, M. Kumar, R.C. Hubli and A.K. Suri. **Separation and Purification Technology**, 2012, 99, 36–43.
9. Separation and Recovery of Palladium from Spent Nuclear Fuel – a Review. R. Ruhela, B.S. Tomar, J.N. Sharma, R.C. Hubli, A.K. Suri. Communicated.
10. Amberlite XAD-16 functionalized with 2-Acetyl Amide group for the solid phase extraction and recovery of palladium from High Level Waste (HLW). R. Ruhela, K.K. Singh, B.S. Tomar, T.K. Seshagiri, M. Kumar, R.C. Hubli, A.K. Suri. Communicated.
11. Investigation of the Extraction Complexes of Palladium (II) with Novel Ligands Thiodiglycolamide and Dithiodiglycolamide by EXAFS and Computational Methods. R. Ruhela, B.S. Tomar, A.K. Singh, R.C. Hubli, A.K. Suri. Communicated.

References

1. G.M. Forker, Norbert Adolph Lange, The Handbook of Chemistry, Handbook Publishers, 1952.
2. C.R. Hammond, The Elements, in Handbook of Chemistry and Physics 81st edition. CRC Press, 2004.
3. C.C. Allen. The platinum metals. Mineral report Canada, No. 3 (1960).
4. Jr. J.B. Mertre, The good news platinum deposits, Alaska, Geol, Survey bull., 918 (1940).
5. R.E. Kirk, D.F. Othmer, Encyclopedia of chemical technology, willey, 3rd Edition, vol. 18, (1973) 228.
6. F.D Manchester, A. San-Martin, J.M. Pitre, Journal of Phase Equilibria, 15 (1994) 62.
7. F.J. McQuillin, Platinum Met. Rev., 37, 2 (1993) 71.
8. A.F. Gusovius, T.C. Watling, R. Prins, Appl. Catal. A., 188, 1-2 (1999) 187.
9. A. Pifer, T. Hogan, B. Snedeker, J. Am. Chem. Soc., 121 (1999) 7488.
10. B. Orel, Sens. Actuators B: Chem., 50, 3 (1998) 234.
11. B. Orel, Sens. Actuators B: Phys., 62, 1-3 (1997) 621.
12. R.B. Schwarz, Y. He, Mater. Sci. Forum, 1 (1997) 231.
13. N. Nishiyama, A. Inoue, Acta Mater., 47, 5 (1999) 1487.
14. L. Yernandes., Sol. Energy Mater. Sol. Cells, 44, 4 (1996) 367.

15. Y. Ijiri., F.J. DiSalvo, Phys. Rev. B: Condensed Matter, 55, 3 (1997) 1283.
16. B.J. Klemme, M.J. Adriaans, P.K. Day, D.A. Sergatskov, T.L. Aselage, R.V. Duncan, J. Low Temp. Phys., 116, 1-2 (1999) 133.
17. G. bar., Elektrike, 52, 10-12 (1998) 353.
18. I.J. Ferrer, P. Diaz-Chao, A. Pascual, C. Sanchez, 515 (2007) 5783.
19. G. Friedlander, J.W. Kennedy, E.S. Macias, J.M. Miller, Nuclear and Radiochemistry, 3rd Edition, 1981.
20. S. Glasstone, Source book of Atomic Energy, US Atomic Energy Commission, 1967.
21. K. Raj, K.K. Prasad, N.K. Bansal, Nuclear Engineering and Design, 236, 7, 8 (2006) 914.
22. N.S. Sunder Rajan, IAEA BULLETIN, SPRING 1986.
23. K. Nishihara, S. Nakayama, Y. Morita, H. Oigawa, T. Iwasaki, Journal of Nucl. Sci. and Tech., 45, 1 (2008) 84.
24. T. Todd, INL, Nuclear Regulatory Commission Seminar, Rockville, MD 2008.
25. A. Dakshinamoorthy, PhD Thesis, Mumbai, 2008.
26. H.J. Ache, L.H. Baetsle, R.P. Bush, A.F. Nechaev, U.P. Popik, Yu. Ying, IAEA Technical Report Series (1989).
27. F.P. Roberts, BNWL-1693 (1972).
28. J.C. Shippard, BNWL-1308-6 (1971).

29. A. Sawatzky, G.A. Ledoux, Proc. 2nd Int. Congr. Pergamon Press, New York, Vol. 1, 1977, Paper 1C8.
30. C.L. Stokes, R.E. Buxbaum, Nucl. Technol., 98 (1992) 207.
31. U. S. Patent (1992) 5,135, 709.
32. U. S. Patent (1978) 4,097, 402.
33. G.A. Eloff, C.J. Greyling, P.E. Viljoen, J. Nucl. Mater., 202 (1993) 239.
34. T.V. Rao, R.W. Vook, W. Meyer, C. Wittwer, J. Vac. Sci. Technol., A5, 4 (1987) 2701.
35. P. Schlossmacher, Mater. Lett., 31 (1997) 119.
36. D. Golberg, Ya Xu, Y. Murakami, K. Otsuka, T. Ueki, H. Horikawa, Mater. Lett., 22 (1995) 241.
37. U. S. Patent (1979) 4,178,350.
38. Yu. A. Sakharovskii, M.B. Rozenkevich, B.M. Andreev, E.P. Magomedbekov, Yu. S. Pak, D.M. Nikitin, I.Z. Khairullin, V.V. Uborskii, At. Energiya, 85, 1 (1998) 35.
39. U. S. Patent (1983) 4, 376, 066.
40. Japan Patent Appl. (1973) 49-002,000.
41. K. Fischer, Nucl. Technol., 112 (1995) 58.
42. T. Kanzleiter, M. Seidler, Atomwirtschaft, 40, 6 (1995) 392.
43. R.G. Clemmer, E.M. Larsen, L.J. Wittenberg., Nucl. Eng. Des., 39 (1976) 85.

44. R.E. Buxbaum, *Sep. Sci. Technol.*, 18, 12-13 (1983) 1251.
45. J.R. Young, *Rev. Sci. Instrum.*, 34, 4 (1963) 374.
46. R.E. Buxbaum, P.C. Hsu, *J. Nucl. Mater.*, 189 (1992) 183.
47. F. Botter, J. Menes, S. Tistchenko, G. Dirian, *Bull. Soc. Chim. Fr.*, 11 (1965) 3374.
48. J.H. Scogin, A.S. Poore, *Fusion Technol.*, 28 (1995) 736.
49. A. Omoto, H. Karasawa, *Nucl. Eng. Des.*, 197, 3 (2000) 192.
50. A. Michaelis, S. Kudelka, J.W. Schultze, *Electrochim. Acta*, 43, 1-2 (1998) 119.
51. A. Yu. Pokhitonov, WM'08 Conference, 2008, Phoenix, AZ.
52. S.K. Sundaram, J.M. Perez Jr., PNNL-13347, Pacific Northwest National Laboratory, Richland, WA (2000).
53. Z. Kolarik, E.V. Renard, *Platin. Metal Rev.* 47 (2003) 74.
54. Z. Kolarik, E.V. Renard, *Platin. Metal Rev.* 47 (2003) 123.
55. Yu. A. Pokhitonov, V.N. Romanovskii, *Radiochemistry*, 47, 1 (2005) 1.
56. H. Kleykamp, J.O. Paschoal, R. Pejsa, F. Thummler, *J. Nucl. Mater.*, 130 (1985) 426.
57. H. Kleykamp, *Nucl. Mater.*, 131 (1985) 221.
58. T. Muromura, T. Adachi, H. Takeishi, *J. Nucl. Mater.*, 174 (1990) 60.
59. A.F. Voigt, A.H. Daane, E.H. Dewell, R.G. Clark, J.E. Gonser, K.L. Malaby, *AIChE. Journal*, 2 (1956) 169.

60. S.M. Stroller, R.B. Richards, Reactor Hand Book, Vol. II, Fuel Reprocessing, 1961, 2nd edition Interscience publishers Inc., New York
61. F.J. Smith, Journal of the Less-Common Metals, 35 (1974) 147.
62. L.M. Ferris, J.C. Mailen, J.J., Lawrence, F.J. Smith, E.D. Nogueira, Jour. of Inorg. & Nucl. Chem., 32, 6 (1970) 2019.
63. F.J. Smith, H.F. McDuffie, Sep. Sci. & Tech., 16, 9 (1981) 1071.
64. H.F. McDuffie, ORNL/TM-6654, (Jan 1979).
65. C.A. Rohrmann, O.J. Wick (1983) United States Patent 4, 395,367.
66. K. Naito, T. Matsui, Y. Tanaka, J. Nucl. Sci. Technol., 23 (1986) 540.
67. G.R.B. Elliot, R.U. Sweezer, ANL-5633, 1956, ANL-5668, 1956, ANL-5730, 1957.
68. C. Wu, Y. Lin, L. Jiang, Nucl. Radiochim., 8, 3 (1986) 147.
69. D.O. Campbell, S.R. Buxton, (1981) U. S. Patent 4,290,967.
70. Y. Asano, T. Yamamura, K. Mizumachi, Y. Wada, (1994) (SPECTRUM-94), Atlanta, Georgia (USA), August 14-18, 2, 836.
71. A. Dakshinamoorthy, P.S. Dhami, P. W. Naik, S.K. Dudwadkar, S.K. Munshi, P.K. Dey, V. Venugopal, Desalination, 232 (2008) 26.
72. V.B. Gevirtz, L.A. Zelentsova, A.E. Kozlov, Yu. A. Pokhitonov, Radiochemistry, 47, 4 (2005) 378.

73. M. Yoneya, Y. Hanamoto, K. Kawamura, H. Igarashi, Y. Miyamoto, Proc. Int. Conf. Future Nucl. Systems: Challenge towards 2nd Nucl. Era Advanced Fuel Cycles (Global'97), 5-10 Oct., Yokohama, Japan, 1501.
74. K. Koizumi, M. Ozawa, R. J. Kawata, J. Nucl. Sci. Technol. 30 (1993) 1195.
75. M. Jayakumar, K.A. Venkatesan, T.G. Srinivasan, P.R. Vasudeva Rao, Electrochim. Acta, 54 (2009) 1083.
76. M. Jayakumar, K.A. Venkatesan, T.G. Srinivasan, P.R. Vasudeva Rao, J. Appl. Electrochem. 39, 10 (2009) 1955.
77. (a) E.C. Frias, H.K. Ly, J. Pitsch, C. Poitrenaud, Talanta, 42 (1995) 1675.
(b) J. Purans, B. Fourest, C. Cannes, V. Sladkov, F. David, L. Venault, M. Lecomte, J. Phys. Chem. B, 109 (2005) 11074.
78. S.H. Lee, H. Chung, J. Nucl. Sci. Technol., 37, 3 (2000) 281.
79. V.V. Milyutin, S.B. Peshkischev, V.M. Gelis, Radiokhimiya, 36, 1 (1994), 25;
Sov. Radiochem., 36, 1 (1994) 26
80. A.K. Venkatesan, B. Robert Selvan, M.P. Antony, T.G. Srinivasan, P.R. Vasudeva Rao, Hydrometallurgy, 86 (3-4) (2007) 221.
81. A. Zhang, Y. Wei, T. Arai, M. Kumagai, Solv. Extr. Ion Exch., 24 (2006) 447.
82. (a) M. Kubota, Radiochim. Acta, 63 (1993) 91.
(b) Y. Yamagishi, M. Kubota, J. Nucl. Sci. Technol., 30, 7 (1993) 717.
83. D. Parajuli, K. Hirota, N. Seko, J. Radioanal. Nucl. Chem., 288 (2011) 53.
84. H. Mimura, H. Ohta, K. Akiba, Y.J. Onodera, Nucl. Sci. Tech., 38, 5 (2001) 342.

85. A. Dakshinamoorthy, T. Kumar, K.K. Nandy, R.H. Iyer, J.N. Mathur, S.B. Manohar, *Jour. of Radioanal. & Nucl. Chem.*, 245, 3 (2000) 595.
86. K.A. Venkatesan, B. Selvan Robert, M.P. Antony, T.G. Srinivasan, P.R. Vasudeva Rao, *J. Radioanal. Nucl. Chem.*, 266 (2005) 431.
87. K.P. Lunichkina, E.V. Renard, V.B. Shevchenko, *Zh. Neorg. Khim.*, 19, 1 (1974) 205; *J. Inorg. Chem.*, 1 (1974) 205.
88. B.N. Zaitsev, E.N. Invoka, *Radiochemistry*, 23 (1981) 817; V.S. Shmidt and N. A. Shorokhov, *At. Energy*, 64, 2 (1988) 103.
89. V.S. Shmidt, N.A. Shorokov, S.S. Novikova, E.G. Teterin, A.N. Penteeleva, *Sov. Radiochem.*, 252 (1983) 189.
90. B.N. Zaitsev, I.B. Kvasnitskii, V.A. Korolev, V.A. Babain, Yu. A. Pokhitonov, *Radiochemistry*, 47, 4 (2005) 374.
91. (a) I.V. Smirnov, M.D. Karavan, T.I. Efremora, V.A. Babain, S.I. Miroshnichenko, S.A. Cherenok, V.I. Kalchenko. *Radiochemistry*, 49 (2007) 482.
- (b) I.V. Smirnov, M.D. Karavan, V.A. Babain, I. Kvasnitskii, E. Stoyanov, S.I. Miroshnichenko, *Radiochim. Acta*, 95 (2007) 97.
92. O. Courson, M. Lebrun, R. Malmbeck, G. Pagliosa, K. Romer, B. Satmark, J.P. Glatz, *Radiochim. Acta*, 88 (2000) 857.
93. Z. Zhu, Y. Sasaki, H. Suzuki, S. Suzuki, T. Kimura, *Anal. Chim. Acta*, 527 (2004) 163.
94. Y. Sasaki, Y. Morita, Y. Kitatsuji, T. Kimura, *Solv. Extr. & Ion Exch.*, 28 (2010) 335.

95. N.T. Hung, M. Watanabe, T. Kimura, *Solv. Extr. Ion. Exch.*, 25 (2007) 407.
96. M. Mohan Raj, A. Dharmaraja, Panchanatheswaran, A.K. Venkatesan, T.G. Srinivasan, P.R. Vasudeva Rao, *Hydrometallurgy*, 84 (2006) 118.
97. E.A. Mezhov, A.V. Kuchmunov, V.V. Druzhenkov, *Radiochemistry*, 44, 2 (2002) 135.
98. E.A. Mezhov, V.V. Druzhenkov, A.N. Sirotnin, *Radiochemistry*, 44, 2 (2002) 146.
99. E.A. Mezhov, I.A. Kulikov, E.G. Teterin, *Radiochemistry*, 44, 2 (2002) 141.
100. A. Dakshinamoorthy, P.S. Dhama, P.W. Naik, S.K. Dudwadkar, S.K. Munshi, P.K. Dey, V. Venugopal, *Desalination*, 232 (2008) 26.
101. Y. Sasaki, M. Ozawa, T. Kimura, K. Ohashi, *Solv. Extr. & Ion Exch.*, 27 (2009) 378.
102. M. Yu. Alyapyshev, V.A. Babain, L.I. Tkachenko, I.I. Eliseev, A.V. Didenko, M.L. Petrov, *Solv. Extr. & Ion Exch.*, 29 (2011) 619.
103. G.H. Rizvi, J.N. Mathur, M.S. Murali, R.H. Iyer, *Sep. Sci. Tech.*, 31 (1996) 1805.
104. (a) K. Kirishima, H. Shibayama, H. Nakahira, H. Shimauchi, M. Myochin, Y. Wada, K. Kawase, Kishimoto, (1993) *Proc. Int. Conf. Nucl. Waste Management Environ. Remed.*, 5-11, Sept., Prague, Czech Rep., ASME, New York, NY, U.S.A., 1, 667.
- (b) S.J. Al-Bazi, H. Freiser, *Solv. Extr. Ion Exch.*, 5 (1987) 265.

105. V. Guyon, A. Guy, J. Foos, R. Chomel, T. Moutarde, G. Lebuzyte, M.J. Lemaire, *Radioanal. Nucl. Lett.*, 187, 1 (1994) 19.
106. J.P. Shukla, R.K. Singh, S.R. Sawant, N. Varadarajan. *Anal. Chim. Acta*, 276 (1993) 181.
107. (a) V.G. Torogov, V.V. Tatarchuk, I.A. Druzhinina, T.M. Korda, A.N. Tatarchuk, E. V. Renard, *At. Energiya*, 76, 6 (1994) 478; *Sov. At. Energy*, 76, 6 (1994) 442.
- (b) L.V. Arsenkov, B.S. Zakharkin, K.P. Lunichkina, E.V. Renard, V. Yu. Rogozhkin, N.A. Shorokhov, *At. Energiya*, 72, 5 (1992) 462; *Sov. At. Energy*, 72, 5 (1992), 411.
108. A.J. Daoud, S.A. El-Reefy, H.F.J. Aly. *Radioanal. Nucl. Chem. Lett.*, 166, 5 (1992) 441.
109. M. Draye, A.R. Favre, G. Le. Buzit, J. Foos, M. Lemaire, A.J. Guy. *Radioanal. Nucl Chem.*, 220, 1 (1997) 105.
110. R.C. Gatrone, L. Kaplan, E.P. Horwitz, *Solv. Extr. Ion Exch.*, 5 (1987) 1075.
111. P. Metilda, K. Sanghamitra, J.M. Gladis, G.R.K. Naidu, T. Prasada Rao, *Talanta*, 65 (2005) 192.
112. A. Dakshinamoorthy, Ph.D. Thesis, University of Mumbai, India (2008).
113. M. Abe, J. Takahashi, *J. Radioanal. Nucl. Chem.*, 90 (1985), 247.
114. B. Spencer, R. Counce, B. Zane Egan, *Alche. J.* 43 (1997) 555.
115. B.J. Mincher, G. Modolo, P.S. Mezyk, *Solv. Extr. & Ion Exch.*, 27 (2009) 1.

116. B.J. Mincher, G. Modolo, P.S. Mezyk, *Solv. Extr. & Ion Exch.* **27** (2009) 331.
117. W. Davis, (W.W. Schulz, J. D. Navratil, A.E. Talbot, Eds.) CRC Press, Florida (1984) 221.
118. K.L. Nash, R.C. Gatron, G.A. Clark, P.G. Rickert, E.P. Horwitz, *Sep. Sci. Technol.*, 23 (12 & 13) (1988) 1335.
119. G. Modolo, S. Seekamp, *Solv. Extr. & Ion Exch.*, 20 (2002) 195.
120. Y. Sugo, Y. Sasaki, S. Tachimori, *Radiochim. Acta*, 90 (2002) 161.
121. J.N. Sharma, R. Ruhela, K.K. Singh, M. Kumar, C. Janardhanan, P.V. Achutan, S. Manohar, P.K. Wattal and A.K. Suri, *Radiochimica Acta*, 98(2010) 485.
122. A.V. Bellido, M.N. Rubenich, *Radiochim. Acta.*, 36 (1984) 61.
123. Y. Sugo, Y. Izumi, Y. Yoshida, S. Nishijima, Y. Sasaki, T. Kimura, T. Sekine, H. Kudo, *Radiat. Phys. Chem.* 76 (2007) 794.
124. R. Prins, D.E. Koningsberger, *X-ray Absorption, Principles, Applications, Techniques for EXAFS, SEXAFS, and XANEX*; Wiley-Interscience, New York, 1988.
125. B.K. Teo, *EXAFS: Basic Principles and Data-analysis*; Springer, New York, 1986.
126. Alex A. Granovsky, Firefly version 7.1.G, www. <http://classic.chem.msu.su/gran/firefly/index.html>.
127. (a) The Stuttgart RSC 1997 ECP basis set for Pd and 6-31G** basis set for H, C, N, O, and S were obtained from the Extensible Computational Chemistry

Environment Basis Set Database, Version 1.2.2, as developed and distributed by the Molecular Science Computing Facility, Environmental and Molecular Sciences Laboratory which is part of the Pacific Northwest Laboratory, P.O. Box 999, Richland, Washington 99352, U.S.A., and funded by the U.S. Department of Energy.

(b) D. J. Feller, *Comp. Chem.*, 17, 13 (1996) 1571.

(c) K.L. Schuchardt, B.T. Didier, T. Elsethagen, L. Sun, V. Gurumoorthi, J. Chase, J. Li, T.L. Windus, *J. Chem. Inf. Model.*, 47, 3 (2007) 1045.

128. H. Narita, M. Tanaka, K. Morisaku, T. Abe, *Chemistry letters*, 33 (2004) 1144.

129. Y. Uzumasa, T. Okura, *Bull. Of the Chem. Soc. of Japan*, 23, 5 (1950) 163.

130. A. David Huebner, U. S. Patent 5,485,808.

131. W. Songping, G. Guobang, *Journal of University of Science and Technology Beijing, Mineral, Metallurgy, Material*, 14 (2007) 107.

132. Y.E. Nikitin, Y.I. Murinov, A.M. Rozen, *Russian Chemical Reviews*, 45 (1976)

133. H. Ramsis, E.R. Perez, J. Roger, J.L. Delarbre, L. Maury, *Journal of Raman Spectroscopy*, 27 (1996) 637.

134. C. Yuan, H. Ma, J. Cao, L. Zhou, R. Luo, *Solvent Extr. Ion Exch.*, 6 (1988) 739.

135. B.J. Mincher, R.D. Curry, *Appl. Radiat. Isot.* 52 (2000) 189.

136. T.L. White, R.A. Peterson, W.R. Wilmarth, M.A. Norato, S.L. Crump, L.H. Delmau, *Sep. Sci. Technol.* 36 (5–6) (2001) 743.

137. T. Kanetake, M. Otomo, *Anal. Sci.*, 4 (1988) 411.

138. S.H. Sinha, A.D. Sawant, *Bull. Chem. Soc. Jpn.*, 65 (1992) 1622.

139. T. Nakanishi, M. Otomo, *Anal. Sci.*, 1 (1985) 161.
140. B.J. Desai, V.M. Shinde, Z. Fresenius, *Anal. Chem*, 295 (1979) 412.
141. S.K. Majumdar, P. Chattopadhyay, P.K. Paria, *J. Ind. Chem. Soc.* 62 (1985) 540.
142. A. Kumar, M. Gautam, B.K. Puri, *Microchem. J.* 33 (1986) 256.
143. F. Kamil, R.S. Chawla, S.K. Sindhvani, *J. Ind. Chem. Soc.* 65 (1988) 790.
144. C. Bandyopadhyay, B.C. Roy, M.B. Saha, *J. Ind. Chem. Soc.* 63 (1986) 707.
145. L.S. Sarma, J.R. Kumar, K.J. Reddy, A.K. Kumar, A.V. Reddy, *Anal. Sci.* 18 (2002) 1257.
146. S.L. Narayana, K.J. Reddy, S.A.N. Reddy, J.R. Kumar, A.V. Reddy, *J. Chin. Chem. Soc.* 54 (2007) 1233.
147. K.J. Reddy, J.R. Kumar, C. Ramachandraiah, A.V. Reddy, *Environ. Monit. Assess.* 136 (2008) 337.
148. A. Dakshinamoorthy, R.K. Singh, R.H. Iyer, *J. Radioanal. Nucl. Chem.* 177 (1994) 327.
149. P. Giridhar, K.A. Venkatesan, T.G. Srinivasan, P.R. Vasudeva Rao, *Hydrometallurgy* 81 (2006) 30.
150. D.T. Bowron, E.C. Beret, E. Martin-Zamora, A.K. Soper, E.S. Marcos, *J. Am. Chem. Soc.*, 134 (2012) 962.
151. S. Manohar, J.N. Sharma, B.V. Shah, P.K. Wattal, *Nucl. Sci. Eng.*, 156 (2007) 96.